Regulation of epinephrine biosynthesis by intermittent and continuous hypoxia

by

Rebecca Bourdon

A thesis submitted in partial fulfillment
of the requirements for the degree of
Master of Science (MSc) in Biology

The Faculty of Graduate Studies
Laurentian University
Sudbury, Ontario, Canada

THESIS DEFENCE COMMITTEE/COMITÉ DE SOUTENANCE DE THÈSE
Laurentian Université/Université Laurentienne
Faculty of Graduate Studies/Faculté des études supérieures

Title of Thesis Titre de la thèse	Regulation of epinephrine biosynthesis by intermittent and continuous hypoxia
Name of Candidate Nom du candidat	Bourdon, Rebecca Brigitte
Degree Diplôme	Master of Science
Department/Program Département/Programme	Biology
Date of Defence Date de la soutenance	August 05, 2020

APPROVED/APPROUVÉ

Thesis Examiners/Examinateurs de thèse:

Dr. TC Tai
(Co-Supervisor/Co-directeur(trice) de thèse)

Dr. Aseem Kumar
(Co-Supervisor/Co-directeur(trice) de thèse)

Dr. Kabwe Nkongolo
(Committee member/Membre du comité)

Approved for the Faculty of Graduate Studies
Approuvé pour la Faculté des études supérieures
Dr. David Lesbarrères
Monsieur David Lesbarrères
Dean, Faculty of Graduate Studies
Doyen, Faculté des études supérieures

Dr. William Durante
(External Examiner/Examinateur externe)

ACCESSIBILITY CLAUSE AND PERMISSION TO USE

Abstract

Phenylethanolamine N-methyltransferase (PNMT) synthesizes the catecholamine (CA), epinephrine (Epi), and is increased in hypertensive patients. Patients with obstructive sleep apnea (OSA) experience oxidative stress, which is associated with elevated blood pressure (BP) and CAs, and consequently, hypertension (HTN). Studies have demonstrated PNMT regulation by continuous hypoxia (CH) and intermittent hypoxia (IH). In the present study, the role of Epi synthesis by both forms of hypoxia are compared in O_2-sensitive PC12 cells. RT-PCR and Western analysis demonstrated a robust induction in CA biosynthesis enzymes by IH, compared to CH, especially following the sustained duration of exposure. Further, mechanisms involved in this IH-mediated induction include a potent increase in transcription factors that regulate the PNMT gene. This led to an enhanced activation of the PNMT promoter by IH, compared to that resulting from CH exposure, as shown by the luciferase reporter assay. Additionally, IH, but not CH, contributed to increased reactive oxygen species (ROS), which appeared to play a prominent role in the induction of CA biosynthesis enzymes. Prior treatment with a synthetic antioxidant and selected polyphenols were able to abolish these IH-mediated inductions. In summary, these findings demonstrate the role of IH-induced oxidative stress in PNMT gene regulation. This study furthers our understanding of how IH, associated with OSA, contributes to the development of secondary HTN.

Keywords

Phenylethanolamine N-methyltransferase, intermittent hypoxia, continuous hypoxia, reactive oxygen species, oxidative stress, obstructive sleep apnea, hypertension, epinephrine, hypoxia-inducible factor 1α, tyrosine hydroxylase, dopamine β-hydroxylase, catecholamine, polyphenol.

Acknowledgements

I would like to express my gratitude to several individuals for their guidance during my graduate studies. Firstly, to my supervisor, Dr. T.C. Tai, for providing me with the opportunity to pursue research in his lab, and for teaching me the power of critical thinking and perseverance. Secondly, I would like to thank Dr. A. Kumar and Dr. K. Nkongolo for their insight and confidence towards my thesis. Further, I wish to convey my sincere appreciation to research associate, Dr. S. Khurana, for the endless hours spent teaching me the art of science, and always making the time to answer questions, provide technical training, assist in troubleshooting, and decode seemingly inexplicable results. Finally, I would like to acknowledge all the members of Dr. Tai's lab, and all of my family and friends for their camaraderie, assistance, and support throughout my studies.

Dedication

I would like to dedicate this thesis to my parents, Kaija and Claude Mailloux, and my husband, Alexander Bourdon, for their love, support, and encouragement throughout my education and life, as well as to 'Baby Bourdon,' who helped defend my thesis presentation while I was pregnant with them.

Table of Contents

Abbreviations

AC	Adenylate cyclase
ACh	Acetylcholine
AChR	Acetylcholine receptor
ACTH	Adrenocorticotropic hormone
AdoMET	S-adenosylmethionine
AMP	Adenosine monophosphate
ANOVA	Analysis of variance
ANS	Autonomic nervous system
AP	Activator protein
APS	Ammonium persulfate
ARNT	Aryl hydrocarbon receptor nuclear transporter
ATF	Activating transcription factor
ATP	Adenosine triphosphate
BBE	Bicoid-type binding element
BCS	Bovine calf serum
BH_4	Tetrahydrobiopterin
bHLH	Basic helix-loop-helix
BP	Blood pressure
BSA	Bovine serum albumin
CA	Catecholamine
CAD	C-terminal activation domain
CaMK	Calcium/calmodulin-dependent protein kinase
cAMP	Cyclic adenosine monophosphate
CBP	CREB-binding protein
cDNA	Complimentary deoxyribonucleic acid
CDTA	1,2-Cyclohexylenedinitrilotetraacetic acid
CH	Continuous hypoxia
CH1	Cysteine/histidine-rich 1
CMV	Cytomegalovirus
CNS	Central nervous system
$CoCl_2$	Cobalt chloride
CRE	Cyclic adenosine monophosphate response element
CREB	Cyclic adenosine monophosphate response element-binding protein
CRH	Corticotropin-releasing hormone
CSA	Central sleep apnea
CTM	Charcoal-treated media
D/2	Dyad/2 motif
DAPI	4’6-Diamidino-2-phenylindole
DB1	Multifunctional genetic regulatory element
DBH	Dopamine β-hydroxylase
DCF	Dichlorofluorescein
DCFH-DA	2’7’-Dichlorofluorescin diacetate
Dex	Dexamethasone

DEPC	Diethylpyrocarbonate
DH5α	Douglas Hanahan 5α cells
DI	Deionized
DMEM	Dulbecco's modified Eagle's medium
DNA	Deoxyribonucleic acid
DNase	Deoxyribonuclease
dNTP	Deoxynucleoside triphosphate
DOPA	L-3,4-Dihydroxyphenylalanine
DTT	Dithiothreitol
E box	Enhancer box
ECL	Enhanced chemiluminescence
E. coli	*Escherichia coli*
EDTA	Ethylenediaminetetraacetic acid
EGCG	Epigallocatechin gallate
Egr1	Early growth response protein 1
Em	Maximum emission
Epi	Epinephrine
ERE	Estrogen response element
$ERK_{1/2}$	Extracellular signal-regulated kinase
ES	Equine serum
Ex	Maximum excitation
FIH1	Factor-inhibiting hypoxia-inducible factor 1
GAPDH	Glyceraldehyde 3-phosphate dehydrogenase
GC	Glucocorticoid
GCM_1	Glial cell missing transcription factor
GFP	Green fluorescent protein
GR	Glucocorticoid receptor
GRE	Glucocorticoid response element
GS	Gentamycin sulphate
GSH	Glutathione
GTP	Guanosine triphosphate
HBSS	Hank's buffered salt solution
HD	Homeodomain
Hept	Heptamer
HIF	Hypoxia-inducible factor
HPA	Hypothalamic-pituitary-adrenal
HRE	Hypoxia-response element
HRP	Horseradish peroxidase
HSP90	Heat shock protein 90
HTN	Hypertension
IH	Intermittent hypoxia
IgG	Immunoglobulin G
IP_3	Inositol 1,4,5-triphosphate
JNK	c-Jun N-terminal kinase
K_m	Michaelis-Menten constant
LB	Lysogeny broth

MAPK	Mitogen-activated protein kinase
MAZ	Myc-associated zinc finger protein
MG	Methyl gallate
MnTMPyP	Manganese (III) tetrakis porphyrin pentachloride
mRNA	Messenger ribonucleic acid
mTOR	Mammalian target of rapamycin
Mu-MLV	Murine leukemia virus
NAC	N-acetylcysteine
NAD	N-terminal activation domain
NBRE	Nerve growth factor responsive element
NE	Norepinephrine
NFκB	Nuclear factor κ-light-chain-enhancer of activated B cells
NOX	Nicotinamide adenine dinucleotide phosphate oxidase
Oct	Octamer
ODD	O_2-dependent degradation domain
OSA	Obstructive sleep apnea
PAC1	Pituitary adenylate cyclase 1 receptor
PACAP	Pituitary adenylate cyclase-activating peptide
PAGE	Polyacrylamide gel electrophoresis
PAS	Period circadian protein-aryl hydrocarbon receptor nuclear transporter-single-minded protein
PBS	Phosphate buffered saline
PC12	Rat pheochromocytoma cell line
PCNA	Proliferating cell nuclear antigen
PEI	Polyethylenimine
pGL3RP893	Rat phenylethanolamine N-methyltransferase reporter-promoter gene construct
PHD	Prolyl 4-hydroxylase domain protein
phox	Phagocytic oxidase
PI3K	Phosphoinositide 3-kinase
PKA	Protein kinase A
PKC	Protein kinase C
PLC	Phospholipase C
PMA	Phorbol-12-myristate-13 acetate
PMSF	Phenylmethylsulfonyl fluoride
PNMT	Phenylethanolamine N-methyltransferase
PO_2	Partial pressure of O_2
PP	Protein phosphatase
Pre-POMC	Pre-pro-opiomelanocortin
PVDF	Polyvinylidene difluoride
q	Studentized range distribution
RAAS	Renin-angiotensin-aldosterone system
RNA	Ribonucleic acid
RNase	Ribonuclease
RNS	Reactive nitrogen species
ROS	Reactive oxygen species
rRNA	Ribosomal ribonucleic acid

RT	Reverse transcriptase
RT-PCR	Reverse transcription-polymerase chain reaction
SA	Sympathoadrenal
SDB	Sleep-disordered breathing
SDS	Sodium dodecyl sulfate
SEM	Standard error mean
siRNA	Small interfering RNA
SNS	Sympathetic nervous system
SOC	Super optimal broth with catabolite repression
SOD	Superoxide dismutase
Sp1	Specificity protein 1
SRE	Serum responsive element
TAD	Transcriptional activation domain
TBARS	Thiobarbituric acid reactive substances
TBE	Tris base, boric acid and ethylenediaminetetraacetic acid
TBS-T	Tris-buffered saline and Tween 20
TEMED	Tetramethylethylenediamine
TH	Tyrosine hydroxylase
TP	Tempol
USR	Negative regulatory element
VHL	Von Hippel-Lindau
XO	Xanthine oxidase
YY1	Yin yang 1

List of Tables

List of Figures

List of Appendices

Chapter 1: Introduction

1.1 Overview

Phenylethanolamine N-methyltransferase (PNMT) is the terminal enzyme in the catecholamine (CA) biosynthesis pathway, and catalyzes the transfer of a methyl group from S-adenosylmethionine (AdoMET) to norepinephrine (NE), producing epinephrine (Epi)[1]. This enzyme is abundant in adrenal medullary chromaffin cells, the major source of circulating Epi in the body[1]. Epi is a stress hormone that maintains cardiovascular homeostasis in the body[1]. Epi is released as part of the fight-or-flight response, a physiological reaction that occurs in response to a perceived stress on the body[2]. PNMT is a critical determinant in Epi production during adverse physiological, psychological, and environmental stressors, which can ultimately contribute to the pathophysiology of many diseases, including hypertension (HTN)[3]. PNMT, as well as other CA biosynthesis enzymes, are stress responsive; however, their responses are stressor-specific, and are dependent on stress intensity, duration, and number of exposures[4].

Our lab has previously shown that continuous hypoxia (CH) is among the variety of stressors that can regulate and elevate PNMT[5]. CH, as experienced by high-altitude dwellers, leads to adaptations at the physiological and molecular level[6]. For example, residents of Tibetan highlands, where the partial pressure of oxygen (PO_2) is 110 mmHg, compared to residents at sea level (PO_2 = 150 mmHg), have normal pulmonary arterial pressure, hemoglobin levels, and aerobic tissue metabolism, despite CH[7]. At the molecular level, previous studies have shown that there is a genetic selection in Tibetan highlanders at the locus encoding hypoxia-inducible factor (HIF) 2α, prolyl 4-hydroxylase domain protein (PHD) 2, factor-inhibiting HIF1 (FIH1), and HIF target

genes, producing a net effect that alters the balance between HIF2α and HIF1α, transcription factors that mediate vascular/erythropoietic and metabolic/vascular responses to hypoxia, respectively[8]. Although these responses to CH have been appreciated for a long time, the role of intermittent hypoxia (IH) in Epi biosynthesis, as experienced in patients with obstructive sleep apnea (OSA), has been considerably less examined. Generally, the study of IH suggests that the influence of reactive oxygen species (ROS) during the periods of reoxygenation results in an altered, and perhaps enhanced, cellular response to that elicited by CH[9].

OSA is the most common form of sleep-disordered breathing (SDB), and it is characterized by episodes of brief, but recurrent, complete or partial upper airway closures during sleep[10]. These patients experience IH, leading to excessive generation of ROS and reactive nitrogen species (RNS) by the mitochondria[11]. The generation of ROS/RNS is referred to as oxidative stress, a condition in which the balance between their production and clearance is altered[12]. Oxidative stress may trigger molecular pathways that could lead to fixed functional effects, including increased cardiac output, vascular remodeling, and changes in vascular tone, that ultimately cause disease development and progression[13]. Previous studies have shown that OSA and IH promote a sustained increase in blood pressure (BP), elevated CAs, and consequently, has been identified as a secondary cause of HTN[14]. Although epidemiological studies have revealed a strong correlation between OSA and HTN, as well as the linkage of OSA in the pathogenesis of HTN, the cellular mechanisms defining this association are not clearly established[15].

The purpose of this study was to understand the role of oxidative stress in IH exposure on PNMT gene regulation, the transcriptional machinery involved, and compare these responses to an equivalent duration of CH exposure. This, in turn, will allow for a better understanding of the role of Epi production via PNMT in patients with OSA and concomitant HTN.

The present study shows that subjecting O_2-sensitive rat pheochromocytoma-derived PC12 cells to IH and CH may increase CAs by regulating CA biosynthesis enzymes, and their transcription factors. Reverse transcription-polymerase chain reaction (RT-PCR) analysis revealed an increase in the gene expression of CA biosynthesis enzymes, including tyrosine hydroxylase (TH), dopamine β-hydroxylase (DBH), and intron-retaining PNMT after 1 and 8 h of IH and CH exposure. In addition, Western analysis revealed that both forms of hypoxia exposure (8 h duration) resulted in elevated cytosolic protein expression levels of CA biosynthesis enzymes, compared to normoxic cells. Moreover, IH and CH exposure increased PNMT transcription factor gene expression, including HIF1α, early growth response protein 1 (Egr1), specificity protein 1 (Sp1), as well as their nuclear protein expression levels following 8 h of hypoxic exposure. Interestingly, only IH exposure, and not CH, increased mRNA and *de novo* protein synthesis of cytosolic glucocorticoid receptor (GR), another known transcription factor of PNMT. Protein levels of nuclear GR were unaffected by both IH and CH exposure. Furthermore, PNMT promoter-driven luciferase activity was elevated following 8 h of IH and CH exposure in pGL3RP893 transfected cells, which is indicative of increased PNMT promoter activation following hypoxic exposure. Importantly, exposure of cells to IH was more potent in elevating cytosolic TH, PNMT, and GR, and nuclear HIF1α, Egr1, and Sp1 protein, as well as PNMT promoter-driven luciferase activity, than an equivalent duration of CH exposure. Furthermore, intracellular ROS levels were augmented more significantly by 8 h of IH exposure, than by 8 h of CH exposure. Polyphenols, including epigallocatechin gallate (EGCG), methyl gallate (MG), and tempol (TP), effectively attenuated this IH-induced ROS elevation. Finally, the ROS scavenger and potent antioxidant, N-acetylcysteine (NAC), was administered to determine the role of oxidative stress in the gene regulation of PNMT following IH and CH exposure. NAC effectively reduced IH-induced

elevations in TH, DBH, PNMT, HIF1α, Egr1, and Sp1 protein, in addition to IH-induced PNMT promoter activity and ROS levels. In contrast, pretreatment with NAC prior to CH exposure did not alter protein responses in comparison to CH alone, with the exception of PNMT protein levels, which was comparably affected by both forms of hypoxia with NAC pretreatment.

These results demonstrate that IH elicits a robust production of intracellular ROS in PC12 cells, and this enhanced oxidative stress promotes PNMT gene transcription via increased gene and protein expression of transcription factors, and via elevated PNMT promoter activity. Additionally, IH is more potent than CH in elevating ROS and intron-retaining PNMT transcripts; whereas a different duration of CH may be required to produce the same elevated effect. Unlike IH, CH may regulate and elevate PNMT via other mechanisms other than via ROS, especially at the longer exposure durations. These findings will help further the understanding by which the PNMT gene is regulated by two different forms of hypoxia. Furthermore, it will help elucidate the molecular mechanism by which IH in OSA patients regulates CA biosynthesis, and will help explain how this syndrome, characterized by intermittent O_2 deficiency, is linked to the pathophysiology of HTN.

1.2 Hypertension

HTN is defined as having persistently elevated BP, ≥135/85[16]. BP is the force exerted by the blood against the walls of the blood vessels, and the magnitude of this force is dependent on cardiac output[17].

HTN is classified as either primary (essential) HTN, occurring in 90% of cases, in which no discernable etiology is found, or secondary (non-essential) HTN, occurring in 10% of cases, in which the cause of HTN is identified[18]. Although the etiology of primary HTN is incompletely

understood, it is likely triggered by one or more environmental factors, such as advancing age, low birth weight, low socioeconomic status, or sedentary lifestyle, occurring in an already genetically susceptible individual[16]. The pathophysiological mechanisms involved with primary HTN may also be attributed to (1) increased sympathetic nervous system (SNS) output from the medulla oblongata, leading to increased vasomotor tone and BP (possibly due to lower than expected baroreceptor activity for a given BP); (2) activation of the renin-angiotensin-aldosterone system (RAAS), which promotes both vasoconstriction via angiotensin II and Na^+/H_2O retention via aldosterone; and (3) increased blood volume due to high salt intake[16]. As opposed to primary HTN, secondary HTN is due to a specific and distinguishable cause. The most common cause of secondary HTN is chronic kidney disease, while the combination of renovascular disease, a variety of endocrine disorders, and medications accounts for most of the remaining cases[16].

1.3 Obstructive sleep apnea

Recently, OSA has been identified as a secondary cause of HTN[14]. Sleep apnea is a common disorder in which the patient has intermittent, cyclical cessations in breathing while sleeping[19]. There are two major forms of sleep apnea: central sleep apnea (CSA) and OSA.

OSA is characterized by episodes of brief, but recurrent complete upper airway closures (apnea) or partial closures (hypopnea) during sleep, usually occurring at the level of the nasopharynx or oropharynx, and that are terminated by arousals[10]. Unlike CSA, patients with OSA demonstrate ongoing respiratory efforts, and the apneas/hypopneas are caused by narrowing of respiratory passages, rather than a reduction or cessation of brainstem output[20]. Episodes of breathing cessation in OSA typically last 20-30 seconds, with an occurrence of at least five episodes per h of sleep[21]. These patients experience IH, portrayed as intervals of normoxia (in the

range of 10-21% O_2) followed by hypoxia (O_2 tensions between 1-5%)[22]. These episodes usually occur during sleep stages 1 and 2, rarely occur during stages 3 and 4, and are most prevalent and can solely occur during rapid eye movement sleep[23].

1.4 Stress response

Homeostasis is the tendency toward a relatively stable equilibrium. Unremittingly, the body has several processes to regulate its internal environment despite changes in the external environment. Nevertheless, the body encounters many stressors, and has developed numerous physiological and behavioural mechanisms to restore homeostasis, a process termed allostasis[24]. To a greater or lesser extent, stress affects everyone on a daily basis, and luckily, the human body has many ways of coping with these stressors. The fight-or-flight response is an acute physiological reaction that occurs in response to a perceived threat to survival, triggering the sympathetic division of the autonomic nervous system (ANS), and secreting CAs, especially NE and Epi[25]. This is commonly called an 'adrenaline rush', when a massive surge of CAs enter the bloodstream, causing the heart to increase its rate, and BP to rise. Many of the enzymes that synthesize CAs are stressor-specific, dependent on stress intensity, duration, and number of exposures[4]. Regardless of the type of stressor, the ultimate goal is to return the body to its resting norm; however, if a stressor persists, it can often lead to adverse effects including cardiovascular disease, immune dysfunction, and psychiatric disorders[26].

1.4.1 Physiological mechanisms involved in response to stress

When the body senses a stressor, whether this occurs consciously or not, it sends signals about that stressor to the hypothalamus, a portion of the brain that maintains the body's

homeostasis[27]. The hypothalamus contains a control center for many functions of the ANS, as it receives information from nearly all parts of the nervous system, and plays an important role in the endocrine system due to its complex interaction with the pituitary gland[27]. The hypothalamus is thought to be the link between these two regulatory systems, namely the hypothalamic-pituitary-adrenal (HPA) and sympathoadrenal (SA) axis[27]. Functioning as the command center, the hypothalamus controls several involuntary body functions via the ANS, including breathing, BP, heart rate, and the dilation and constriction of blood vessels and bronchioles[28]. The ANS is subdivided into the sympathetic branch, which triggers the fight-or-flight response and provides the body with energy to respond to the perceived threat, and the parasympathetic branch, which controls functions that promote the resting-and-digesting response that returns the body to a neutral state once the danger has passed[29]. The hypothalamus also produces releasing and inhibiting hormones, which initiate or inhibit the production of other hormones throughout the body[30]. Furthermore, the hypothalamus plays a pivotal role in sending signals to the adrenal medulla in response to long- and short-term stress via the HPA and SA axes, respectively[31].

1.4.2 Hypothalamic-pituitary-adrenal axis

The HPA axis is a set of direct effects and feedback interactions among three endocrine glands, namely the hypothalamus, the pituitary gland, and the adrenal gland. This axis is involved in release of glucocorticoids and regulation of CAs[32]. In response to stress, parvocellular neurosecretory cells of the paraventricular nucleus in the hypothalamus synthesize corticotropin-releasing hormone (CRH)[33]. CRH is released from the neurosecretory nerve terminals at the median eminence, an integral part of the hypophyseal portal system, connects the hypothalamus to the adenohypophysis, also known as the anterior pituitary gland[33]. Binding of CRH to its

receptor on pituitary corticotropes promotes the secretion of stored adrenocorticotropic hormone (ACTH), also known as corticotropin, from corticotrope cells in the adenohypophysis[33]. ACTH is synthesized from pre-pro-opiomelanocortin (pre-POMC), following the removal of a signal peptide, and post-translational modifications[34]. This pulse of ACTH begins within minutes of the HPA axis response, and lasts for a relatively short period of time. This response is dependent on stimulus duration, intensity, and feedback[35]. From there, ACTH travels via the systemic circulation to the parenchymal cells of the zona fasciculata, which is located in the adrenal cortex, the superficial layer of the adrenal gland[33]. ACTH stimulates the biosynthesis of glucocorticoids (GCs; a class of corticosteroids), such as cortisol. Cortisol is synthesized in a multi-step pathway from cholesterol[33]. Since GCs must undergo *de novo* production, the GC response lags in time, however, it lasts for an extended duration, and is dependent on active feedback signaling and passive GC degradation processes[35]. High concentrations of GCs travel via the intra-adrenal portal vascular system, and subsequently diffuse through the cell membrane into adrenal chromaffin cells in the adrenal medulla, the inner part of the adrenal gland[36]. GCs then bind to GRs in the cytoplasm of adrenomedullary cells, which allows the dissociation of heat shock protein 90 (HSP90) from GRs, and the translocation of GRs via active transport into the nucleus[37]. Once inside the nucleus, homodimerization of the receptor occurs, followed by binding to glucocorticoid response elements (GREs) in the promoter region of CA biosynthesis enzyme genes, promoting their transcription[37].

In summary, the HPA axis is an important physiological system involved in the stress response and the interaction between three endocrine glands, which ultimately upregulate CA biosynthesis and storage. Once in the systemic circulation, NE and Epi can positively feedback on the adenohypophysis to increase the synthesis of ACTH[38]. On the other hand, the release of cortisol can act via a negative feedback loop to inhibit the synthesis and release of CRH and ACTH from

the hypothalamus and adenohypophysis, respectively[39]. This balance between opposing forces will ultimately allow the body to cope with the stressor, and return to homeostasis.

1.4.3 Sympathoadrenal axis

The sympathoadrenal (SA) axis is part of the physiological stress response system that involves the interaction between the SNS and the adrenal gland. In this axis, electrical input is converted into a hormonal output. In comparison to the HPA axis, the SA axis has a short latency due to the direct innervations of the adrenal chromaffin cells from the SNS, and produces a relatively temporary effect[35]. When the body receives sensory information, primarily from limbic structures, the SNS sends signals by means of preganglionic nerve fibers that emerge from the intermediolateral cell column of the thoracolumbar spinal cord, and extend to the adrenal medulla through thoracic splanchnic nerves[31]. At the level of the adrenal gland, neurotransmitters and neuropeptides are released from the splanchnic nerve terminals, which synapse on neuroendocrine adrenal medullary chromaffin cells[4]. Activation upon binding of these ligands to plasma membrane receptors on chromaffin cells, which act as postganglionic nerve fibers, leads to synthesis and release of CAs into the blood[4]. In addition, CA secretion depends on local gap junction-mediated communication between neighbouring chromaffin cells that help propagate these electrochemical signals[40,41]. This CA discharge leads to a rapid increase in heart rate and force of contraction, peripheral vasoconstriction, and energy mobilization[31].

1.5 Catecholamines and catecholamine biosynthesis pathway

CAs are monoamines that are comprised of a catechol (benzene with two hydroxyl side groups at carbon 1 and 2) and a side-chain amine[42]. These compounds are derived from the

essential amino acid phenylalanine[4]. Included among CAs are dopamine, NE, and Epi. These CAs are also classified as both neurotransmitters and hormones, due to their dual effects in the central nervous system (CNS) and bloodstream[4].

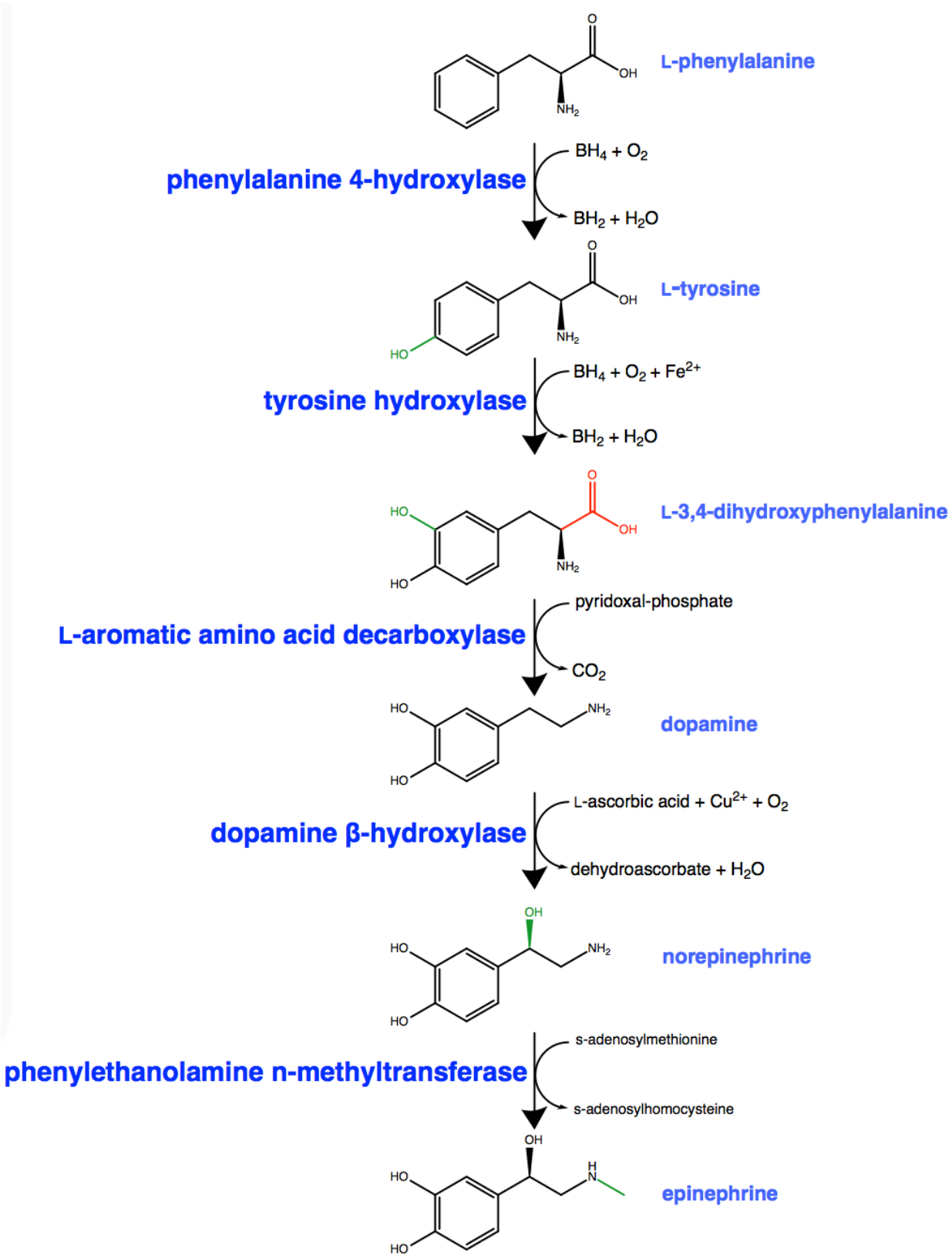

Figure 1: Catecholamine biosynthesis pathway (adapted from: Kvetnansky et al. 2009)[4].

The biosynthesis begins with L-phenylalanine, which is hydroxylated to L-tyrosine by phenylalanine 4-hydroxylase, and the cofactors, tetrahydrobiopterin (BH_4) and O_2 (Figure 1)[43]. Once L-tyrosine enters a chromaffin cell, a sympathetic or brain catecholaminergic nerve terminal, it is hydroxylated in the meta position to L-3,4-dihydroxyphenylalanine (DOPA) by the cytoplasmic enzyme TH, an Fe^{2+}-containing, biopterin-dependent amino acid hydroxylase[4]. The hydroxyl group is added onto the 6-carbon aromatic ring, ortho to the existing hydroxyl group[44]. DOPA is rapidly decarboxylated at the 2-chain aliphatic carbon moiety, and this reaction produces dopamine by the nonspecific enzyme, aromatic L-amino acid decarboxylase, and the cofactor pyridoxal phosphate[4]. Cytoplasmic dopamine is then taken up into storage vesicles. Dopamine is hydroxylated at the α-carbon adjacent to the aromatic ring, and produces NE by DBH and the cofactors L-ascorbic acid, Cu^{2+}, and O_2[4]. In the final step of the CA biosynthesis pathway, NE is methylated at the amino group substituted on the β-carbon of the aliphatic side chain, producing Epi by the soluble cytoplasmic enzyme PNMT using AdoMET as methyl donor and cofactor[4].

CAs in the adrenomedullary chromaffin cells are sequestered in storage vesicles, and released via Ca^{2+}-mediated exocytosis into the circulation. Epi is a CA, a hormone, and neurotransmitter that, once in the blood, circulates and promotes a number of physiological changes[45]. Heart rate and cardiac output increase in order to pump blood to the muscles, heart, and vital organs at a faster speed; as a result, BP increases, and pulse rate strengthens[46]. Other significant changes include blood vessel constriction, increased respiratory rate, dilation of bronchioles, release of glucose and adipose from temporary storage, and increased energy[46]. These functional effects are triggered by the binding of Epi to α and β adrenoceptors expressed in a variety of tissues[47].

Epi is primarily synthesized and released from the chromaffin cells of the adrenal medulla, although it is also released by certain neurons, and the heart[45]. In addition to the increased release of CAs in response to stressors, there is also an increase in the expression of genes that encode CA biosynthetic enzymes, notably, the Epi-synthesizing enzyme, PNMT, under stressful conditions[48,49]. Increased Epi has been shown to play a role in the development of HTN, and several studies have demonstrated that the PNMT gene is a candidate gene associated with the pathophysiology of this cardiovascular disease[50–54].

1.5.1 Tyrosine hydroxylase

Human TH is encoded by a single gene localized to chromosome 11, and it is comprised of 14 exons and 13 introns within 12.5 kbp[55]. This gene undergoes alternative splicing in humans; however, it is unclear whether this mechanism is pertinent during physiological manipulations[4]. In addition, rodent TH does not appear to undergo alternative splicing; therefore, it is not an important concern in experiments on stress[4]. The TH gene produces a protein that can be detected at 62 kDa using SDS-PAGE[56].

TH catalyzes the rate-limiting step in the synthesis of CAs[57]. Fe^{2+}, O_2, and BH_4 are the cofactors needed in this step[57]. BH_4 is present in subsaturating levels, therefore, TH activity depends on BH_4 availability, which is synthesized from dihydropterin by the enzyme, dihydropteridine reductase[58]. TH activity also depends on short-term regulation of enzyme activity by phosphorylation, feedback product inhibition, changes in the redox state of the Fe^{2+}, and allosteric regulation, as well as by medium- to long-term regulation of gene expression by enzyme stability, transcriptional activation resulting in *de novo* protein synthesis, RNA stability, alternative RNA splicing, translational regulation, cellular compartmentalization, and cofactor synthesis[59,60].

TH is a 240 kDa homotetramer that is present in the CNS, SNS, gastrointestinal system, retina, and the adrenal medulla[59,61]. Each subunit of this tetramer contains three domains, including the C-terminal tetramerization domain, the catalytic domain that binds Fe^{2+}, and the N-terminal regulatory domain[59]. The rat subunits each have a molar mass of 55,903 Da, and these subunits form dimers via salt bridges, and tetramers via leucine zippers[43,62]. The N-terminal regulatory domain in the rat enzyme contains four serine residues, including serine-8, serine-19, serine-31, and serine-40[57,63]. These residues are phosphorylated by a variety of protein kinases, which increase the activity of TH, and are dephosphorylated by protein phosphatases (PPs)[57]. Phosphorylation of TH is the primary mechanism responsible for maintaining CA levels in tissues after CA secretion, and seems to influence both short- and long-term regulation of TH[43,57]. Phosphorylation of TH alters the V_{max} (maximum rate that the reaction can proceed at) and Michaelis-Menten constant (K_m, substrate concentration that is required for the reaction to occur at $½V_{max}$), resulting in a more active enzyme[57].

Dopamine, NE, and Epi regulate TH activity by feedback inhibition[64]. This occurs when the Fe^{2+} bound to the active site of TH is oxidized to Fe^{3+} by O_2[57]. This ferric form of TH irreversibly binds CAs that inactivate the enzyme by inhibiting cofactor BH_4 interaction[57]. This inhibition acts as a sensor of local concentrations of CAs[57]. The phosphorylation of serine-40 relieves feedback inhibition by altering TH's conformation, producing an enzyme that can now be reversibly bound to CAs[65]. Since CAs are now liberated from the enzyme, BH_4 is able to reduce Fe^{3+} and return the enzyme to an active state[57].

The TH proximal promoter contains several putative regulatory elements (Figure 2). The perfect consensus cyclic adenosine monophosphate (cAMP) response element (CRE) at -45 bp, and the noncanonical activator protein (Ap)1 element at -205 bp are important for basal expression

of TH, and are stimulated by cAMP, hypoxia, and intracellular Ca^{2+}[4,66]. The CRE motif can bind both cAMP response element-binding protein (CREB) homodimers and CREB heterodimers containing activating transcription factor (ATF) members[67]. This element also overlaps with an imperfect estrogen response element (ERE) in the TH promoter, potentially causing sex differences in TH transcription in response to stress[68]. An Sp1/Egr1 motif is also localized in the TH promoter, spanning -138 bp to -104 bp, and is involved in the response to stressful stimuli[69]. The Sp1/Egr1 motif can interact with the Ap1 motif, and increase TH transcriptional response[69,70]. The TH promoter also contains two Ap2 motifs, a hypoxia-response element (HRE), an enhancer box (E box), octamer (Oct)/heptamer (Hept) sites, a bicoid-type binding element (BBE), a nerve growth factor responsive element (NBRE), and a dyad/2 motif (D/2)[4]. Finally, GCs can increase the transcription of TH by binding to a GRE located within 2.5 kbp upstream of the transcription start site[71]. A second GRE is located at approximately -5.7 kbp, which closely resembles the consensus Ap1 binding site[72].

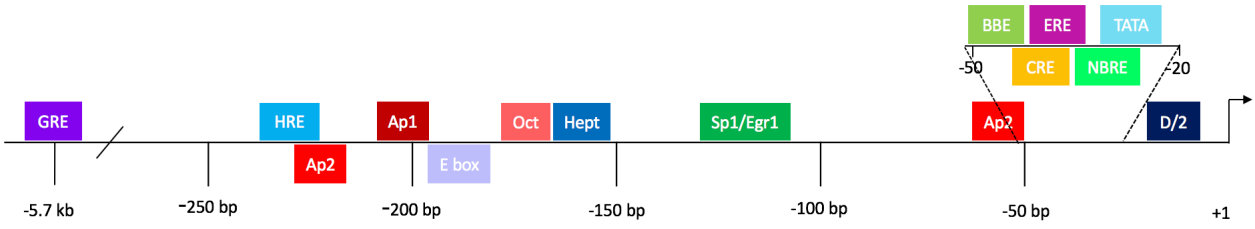

Figure 2: Tyrosine hydroxylase promoter containing multiple regulatory elements (adapted from: Kvetnansky et al. 2009)[4].

1.5.2 Dopamine β-hydroxylase

Human DBH is encoded by a single gene present on chromosome 9q34, and contains 12 exons within 23 kbp[73]. This gene undergoes a number of polymorphisms, one of which is a C to T

transition 1021 bp upstream of the transcription start codon, which likely diminishes gene transcription, and is strongly associated with very low DBH plasma activity[74]. Alternative use of two polyadenylation sites in the 3'-untranslated region from a single DBH gene generates two different mRNAs, in which one form contains a 3'-extension of 300 bp in humans, and 200 bp in rats[75,76]. The cDNAs encode the same amino acid sequence, and produce a protein of 69,883 Da[76]. DBH is a tetrameric glycosylated protein, composed of two dimers linked by disulfide bridges[77].

DBH is an enzyme found in soluble, and membrane-bound forms within storage vesicles[78]. Both forms are derived from the same mRNA and produce sufficient enzyme activity[77,78]. Their difference lies in the nonremoval of a signal sequence, resulting in a membrane-bound DBH[77,78]. DBH is expressed in noradrenergic nerve terminals of the CNS, and peripheral nervous system, as well as localized in adrenomedullary chromaffin cells[79]. Because of its function in vesicles, DBH may be released by exocytosis with NE and Epi, and consequently, DBH may also be found in blood serum and plasma, as well as in cerebrospinal fluid[80,81].

The DBH proximal promoter contains several accepted regulatory elements involved in the basal, suppressed, and induced regulation of DBH expression (Figure 3). The Egr1 motif located at -227 bp/-224 bp is involved in the inhibitory role of Egr1 on DBH promoter activity, and reduces endogenous DBH mRNA[82]. In addition, a negative regulatory element, termed USR, located between -282 bp and -232 bp, represses DBH gene transcription in noncatecholaminergic cells[83]. An Sp1 motif, located between -59 bp to -40 bp, interacts with the transcription factor Sp1, independent of cell type specificity[84]. The transcription factor Ap2 regulates the expression of DBH by binding to an Ap2 binding site between -129 bp and -120 bp of the DBH promoter[85]. Binding of Ap2 to this site is important in maintaining basal levels of DBH transcription[85]. Ap2 prominently interacts with its response element in the DBH promoter in noradrenergic cells[86]. This

transcription factor may also contribute to the neurotransmitter phenotype of noradrenergic and adrenergic cells that co-express TH and DBH[86].

A multifunctional genetic regulatory element, designated DB1, is located between -180 bp and -151 bp of the DBH gene[79]. This segment is responsive to stimulation by cAMP and phorbol ester second messenger pathways[79]. The DB1 enhancer consists of a CRE/Ap1 site located directly adjacent to two core homeodomain (HD) protein recognition sites, HD1 and HD2[87]. A third HD3, occurs downstream of the DB1 enhancer[88]. When Arix binds to either HD on the DB1 enhancer, it contributes to basal activity of the DBH promoter[89]. The regulation of DBH transcription in the presence of Arix requires the activation of the cAMP/protein kinase A (PKA) pathway; these transcription factors synergistically regulate DBH transcription[4,90]. The overlapping CRE/Ap1 motif can bind CREB and/or Ap1 family members, and overlaps with a yin yang 1 site (YY1)[91]. The CRE located within the DB1 enhancer is situated between -173 bp and -167 bp, while the CRE that is distal to this is located between -232 bp and -228 bp[79]. In addition, DBH can be regulated by GCs by binding to three core GR binding sequences (between -832 and -827 bp, -662 and -657, and -271 and -265) in the first 1 kbp of the upstream DBH gene[92]. The DBH promoter region also contains two putative E-box motifs (CAATTG and CAAATG)[93], but not an HRE for binding by HIFs[48].

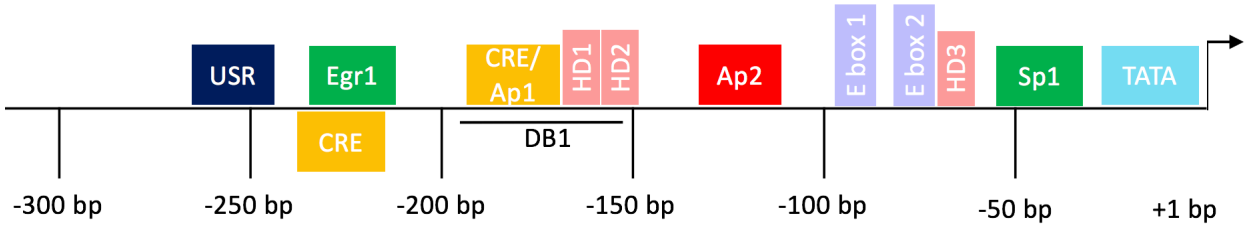

Figure 3: Dopamine β-hydroxylase promoter containing multiple regulatory elements (adapted from: Kvetnansky et al. 2009)[4].

1.6 Overview of phenylethanolamine N-methyltransferase

PNMT is the final enzyme in the CA biosynthesis pathway, and its enzymatic function is to methylate NE, producing Epi[4]. The essential cofactor, AdoMET, donates its methyl group to NE, and is itself converted into S-adenosylhomocysteine[4]. Binding of AdoMET to PNMT also protects the enzyme from proteolytic degradation[94]. PNMT is a soluble cytoplasmic enzyme localized in adrenergic chromaffin cells in the adrenal medulla, the main organ for Epi biosynthesis[4]. In smaller amounts, PNMT is also localized to sympathetically innervated organs, and adrenergic neurons of the medulla oblongata and the hypothalamus in the brain, as well as in non-neuronal cells, such as the heart, skeletal muscle, and epidermis[95–97].

Human PNMT is encoded by a single gene present on chromosome 17q21-q22[98]. This gene contains only three exons within 2.5 kbp[4]. Rat PNMT is located on chromosome 10, in a region known to be syntenic to human chromosome 17[99]. This area shows a positive linkage to risk for HTN[99].

Since Epi must be replenished in order to sustain Epi-elicited behavioural and physiological responses during stress, PNMT expression and activity can be regulated by different forms of stress[100]. The sustained activation of PNMT by some stressors (i.e., immobilization and hypoxic stress) and not others (i.e., cold stress) suggests that multiple mechanisms are involved in the regulation of PNMT and is likely stressor-specific[4]. Once the stressor has ceased, homeostasis must be restored and Epi must return to basal expression[101]. Epi is an autoregulator of its own synthesizing enzyme[101]. Eventually, Epi will negatively feedback and inhibit PNMT, and consequently, Epi levels return to normal quantities[101].

1.6.1 Transcriptional regulation of the phenylethanolamine N-methyltransferase gene

The PNMT gene can be activated by several different transcription factors, which bind to their consensus binding element in the PNMT promoter, and promote gene transcription (Figure 4)[102]. The 5'-upstream region of the rat PNMT promoter extends distally by approximately 20 kbp from the transcription start site[103]. However, the more proximal region generally has a greater influence on transcriptional control due to its close proximity to the transcription initiation site, and as such, the proximal region is more extensively studied than the distal region of the promoter. Transcriptional control of the PNMT gene is predominantly orchestrated through the proximal 1 kbp region[103]. These transcriptional regulators include HIF1α, Egr1, Sp1, and GR, as well as Ap2, myc-associated zinc finger protein (MAZ), and glial cell missing transcription factor (GCM_1)[104–107]. These transcription factors play important roles in the hormonal and neural regulation of PNMT, by independently stimulating the PNMT gene, or interacting cooperatively to synergistically elevate PNMT mRNA and protein expression levels[102].

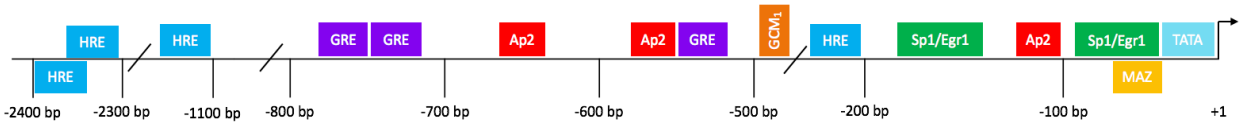

Figure 4: Phenylethanolamine N-methyltransferase promoter containing multiple regulatory elements (adapted from: Kvetnansky et al. 2009)[4].

1.6.1a Hypoxia-inducible factor

HIFs are critical regulators of gene expression under insufficient O_2 conditions[108]. HIFs bind specifically to a 5'-RCGTG-3' HRE in the promoter of hypoxia-inducible genes[109]. A putative, weak HRE within the proximal -893 bp PNMT promoter is found at -282 bp[100]. In a

greater expanse of the upstream PNMT promoter, there are three perfect match HREs present at -2398 bp, -2340 bp, and -1166 bp[100]. The -2398 bp HRE generates the highest levels of HIF1α protein/HRE binding complex formation[100].

HIF1 is a heterodimer, composed of a 120 kDa HIF1α subunit, and a 91-94 kDa HIF1β subunit[110]. This heterodimer belongs to the period circadian protein-aryl hydrocarbon receptor nuclear transporter-single-minded protein (PER-ARNT-SIM or PAS) subfamily of the basic helix-loop-helix (bHLH) family of transcription factors[109,110]. Both HIF1α and HIF1β contain three domains, which include an N-terminus containing the bHLH domain; a central region containing the PAS domain; and a C-terminus[109]. The basic domain is essential for DNA binding, whereas the bHLH domain and the N-terminal half of the PAS domain are necessary for DNA binding and heterodimerization[109]. The HIF1α subunit contains two transcriptional activation domains (TADs)[108]. One of these TADs is referred to as the N-terminal activation domain (NAD), and the other is the C-terminal activation domain (CAD)[108]. The α subunit also contains an O_2-dependent degradation domain (ODD) that controls protein stability, and this ODD overlaps with the NAD[108]. HIF1β is an aryl hydrocarbon receptor nuclear transporter (ARNT), and contains only one TAD at the C-terminus[108,109]. Other HIF isoforms exist, including HIF2 and HIF3; however, HIF1α is the predominant isoform found in adrenal medullary chromaffin cells[94].

HIFs are consistently activated by hypoxic stress, certain transition metals (Co^{2+}, Ni^{2+}, Mn^{2+}), Fe^{2+} chelation, certain growth factors, and cytokines[108]. Although both HIF1α and HIF1β mRNAs and proteins are constitutively expressed, only the α subunit responds to reducing intracellular O_2 tensions. However, HIF1β is still necessary for HIF activity[108]. HIF1α is recognized as the master regulator of hypoxic signaling; although its activity is limited by hydroxylation[111]. Under normoxic conditions, HIF1α is intrinsically unstable and is continuously

degraded through the ubiquitin-proteasome pathway[112,113]. This occurs when a family of PHDs catalyze the hydroxylation of two proline residues on HIF1α in the ODD[114]. PHDs belong to the 2-oxoglutarate-dependent oxygenase superfamily, and they depend on O_2, Fe^{2+}, and 2-oxoglutarate[114]. Hydroxylation occurs on HIF1α at proline-402 and proline-564 via recognition and specific binding by von Hippel-Lindau (VHL)[115]. VHL only contains a single, conserved hydroxyproline-binding pocket for HIF1α, thus VHL can only bind to a single proline at a time[116]. Mutation of either proline partially stabilizes HIF1α, whereas mutation of both prolines markedly increases HIF1α stability[116]. VHL is a component of the protein complex that includes elongin B, elongin C, and cullin-2, and possesses ubiquitin ligase E3 activity[117]. Ubiquitination by VHL marks HIF1α for proteolysis via the proteasome[113]. In addition to the two prolines, the leucine-574 is also essential for VHL-dependent HIF1α degradation[118]. Under normoxia, the half-life of HIF1α is less than 5 min[119]. In contrast, under hypoxic conditions, the destruction of HIF1α is slowed[108]. The enzymatic activity of the PHDs is inhibited by hypoxia, Fe^{2+} chelation, cobaltous ions, and the 2-oxoglutarate analog, N-oxalyl glycine[108]. Since the HIF1α-VHL interaction strictly requires hydroxylation, the inhibition of PHDs by hypoxia allows the ODD of HIF1α to be liberated from hydroxylation, and unable to be targeted for degradation by VHL[120].

As mentioned above, HIF1α contains two TADs; however, only the CAD is essential for transcriptional activation of HIF1α target genes[121]. The leucine-rich interface of the CAD on HIF1α interacts with the cysteine/histidine-rich 1 (CH1) domain of the co-activator, p300-CREB-binding protein (CBP)[122]. During normoxia, the hydroxylation of asparagine-803 in the CAD prevents the binding of HIF1α with its co-activator[108]. The asparaginyl hydroxylation is catalyzed by FIH1, an O_2- and Fe^{2+}-dependent enzyme that interacts with the C-terminal domain of HIF1α, and represses its transcriptional activity[123]. Under these conditions, the unbound CAD is

intrinsically disordered[124]. During hypoxia, the activity of FIH1 is inhibited, thereby permitting the interaction of p300-CBP with the CAD of HIF1α[108]. The CH1 domain of the hypoxia-induced co-activator p300-CBP, serves as a scaffold for the CAD of HIF1α through extensive hydrophobic and polar interactions[124]. Once HIF1α has evaded PHD and FIH1 inhibition, it can associate with its co-activator, as well as dimerize with HIF1β, and translocate into the nucleus where it can bind to an HRE in the promoter of hypoxia-regulated genes.

HIFs are consistently activated by hypoxic stress and they undergo a very broad spectrum of regulatory mechanisms[26]. These controls include transcriptional, post-transcriptional, translational, and post-translational processing, as well as nuclear trafficking and transactivation[26]. This finding is in contrast to earlier evidence, which suggested that the main mechanism by which hypoxia increased HIF1α was via HIF1α protein stabilization and prevention of proteolysis[125]. Our lab has previously demonstrated that CH (5% O_2) activates HIF1α by increasing its mRNA, nuclear protein, and nuclear protein/HRE binding complex formation in PC12 cells[100]. Specifically, there was a rapid, significant induction by 1 h, maximum stimulation by 6 h, and a decline towards basal levels by 24 h of hypoxic stress[100]. Further, HIF1α, truncated HIF1α (active portion of HIF1α), or HIF1β over-expression, increases PNMT promoter-driven luciferase activity, with the greatest induction by the direct expression of HIF1α and HIF1β proteins[100]. Similarly, the HIF1α construct transfected in PC12 cells for 24 h was able to induce endogenous, fully-processed PNMT mRNA and protein expression[100]. Moreover, hypoxia-mimetic agents and HIF1α-inducers, cobalt chloride ($CoCl_2$, 200 μM) or deferoxamine (100 μM) for 6 h significantly elevated PNMT promoter activity to the same extent as 6 h hypoxia treatment alone[100]. It has been demonstrated that HIF1α may predominantly affect PNMT promoter-driven gene expression indirectly via Egr1 and Sp1 induction, rather than directly through the HRE[100]. Lastly, hypoxia,

rather than HIF1α, limits PNMT promoter-driven gene expression. This was demonstrated by the fact that the highest relative concentrations of HIF1α were in hypoxia-treated cells, $HIF1\alpha_{5\%O2} \geq HIF1\alpha_{5\%O2+HIF1\alpha} \geq HIF1\alpha_{HIF1\alpha}$.

1.6.1b Early growth response protein 1

Egr1, an immediate early gene transcription factor, is a nuclear phosphoprotein with three zinc fingers of the Cys2His2 class[126]. The specific DNA-binding activity of Egr1 resides in these three zinc fingers[126]. Egr1 is expressed in the rat adrenal gland, and stimulates endogenous PNMT mRNA expression[127]. The activation potential of Egr1 is distributed over an extensive serine/threonine-rich N-terminal domain[126]. The DNA-binding domain, and basic flanking sequences of Egr1, specify the nuclear localization signal of Egr1[126]. The rat PNMT promoter contains two Egr1 response elements that are GC-rich[128]. A 9/9 perfect match consensus sequence (5'-CGCCCCCGC-3') is located at -165 bp, while an 8/9 consensus match sequence (5'-GCGGGGGGG-3') is located at -45 bp[128]. The Egr1 site at -165 bp appears to be more important for mediating the Egr1 response on the PNMT promoter[127]. However, both Egr1 sites are necessary for maximum luciferase reporter PNMT gene expression[127]. The Egr1 protein is post-translationally modified via phosphorylation[94]. The interaction of Egr1 with its consensus sites in gene promoters is independent of its state of phosphorylation; however, when Egr1 is phosphorylated and bound to a response element, this configuration does enhance the ability of Egr1 to induce transcription[94]. Furthermore, the TAD of Egr1 physically interacts with the N- and C-terminal domains of CBP, and direct protein-protein interactions have been demonstrated between p300-CBP and Egr1[129]. CBP and p300 act as transcriptional co-activators for Egr1-mediated gene transcription, as they interact with sequence-specific transcription factors of Egr1,

as well as components of the transcriptional apparatus to facilitate RNA polymerase II recruitment and transcriptional initiation[129].

Egr1 expression and activity can be regulated by a variety of stressors. Immobilization stress elevates PNMT mRNA, and this rise is preceded by induction of Egr1, accompanied by increases in Egr1 mRNA, protein, and Egr1/PNMT DNA binding complex formation[102]. Moreover, Egr1 mRNA and protein expression is induced by CH (5% O_2) in PC12 cells[5,94]. Egr1 mRNA rose rapidly and transiently, peaking at 1 h and declining to basal levels by 24 h[5]. Similarly, nuclear Egr1 protein increase is rapid, marked, and transient, with elevated 75 kDa-Egr1 protein levels apparent after only 30 min of hypoxic stress, a maximum elevation between 45-60 min, which was sustained by 6 h, and then a significantly rapid decline to basal levels by 24 h of hypoxia[94]. In addition, Egr1 participates in hypoxic transcriptional cis-activation of PNMT[5,94]. In response to CH, Egr1 protein/PNMT DNA binding complex formation increased rapidly and transiently, with peak induction at 1 h, and a decline to basal levels by 6 h[5]. Moreover, Egr1 regulation of PNMT under hypoxic stress is further evidenced by the inability of hypoxia to increase PNMT promoter-driven luciferase activity when the -165 bp and -45 bp Egr1 consensus sequence is inactivated by site-directed mutagenesis[5]. Similarly, co-transfection assays with wild-type construct pGL3RP893 and Egr1 siRNA, which caused Egr1 knock-down, prevented luciferase induction when PC12 cells were exposed to CH[5]. Lastly, as mentioned above, HIF1α, following hypoxic exposure, upregulates Egr1 (and Sp1) expression and thereby, the proximal -893 bp of the PNMT promoter[100]. Potential HRE consensus binding sequences have been found in the Egr1 (and Sp1) promoter region, which may mediate this indirect activation of PNMT via HIF1α[100].

Through neural stimulation, Egr1 is capable of activating PNMT gene expression[127]. This can occur via peptidergic stimulation by pituitary adenylate cyclase-activating peptide (PACAP), which mediates its effects primarily through the pituitary adenylate cyclase 1 receptors (PAC1s), and subsequently, though cAMP-PKA and Ca^{2+} signal transduction pathway[130]. In PC12 cells, 10 nM PACAP markedly activates the PNMT promoter-luciferase reporter gene construct, as well as Egr1; these inductions are both rapid and long-lasting (≥ 48 h)[130]. This neural induction can also occur via cholinergic stimulation by muscarine, nicotine, or carbachol, which mediate their effects via the acetylcholine receptor (AChR)[130]. These AChR agonists (100 μM) can induce a rapid increase in PNMT promoter activity, peaking at 6 h, and declining towards basal levels by 24 h[130]. Like peptidergic stimulation, cholinergic activation of the PNMT promoter involves a cAMP-PKA signaling pathway; however, this activation is much less than that caused by PACAP[130]. Forskolin activates adenylate cyclase (AC), increasing intracellular cAMP levels, and PKA signaling[104]. Forskolin (10 μM) treatment causes maximum induction of PNMT promoter activity at 3-6 h[104]. In addition, this treatment caused a rapid increase in the catalytic subunit of PKA, with a subsequent rise in nuclear Egr1 protein[104]. When the primary Egr1 consensus element was mutated, forskolin treatment was unable to increase PNMT promoter activity[104]. These findings lend support to the premise that PKA regulation is mediated via Egr1 binding to its consensus elements in the PNMT promoter[104]. To continue, simultaneous phorbol-12-myristate-13 acetate (PMA) treatment, an activator of protein kinase C (PKC), and forskolin, synergistically activate PNMT promoter activity in PC12 cells, whereas PMA alone had no effect[107]. The authors concluded that PKA stimulation precedes the PKC pathway[107]. These two pathways seem to mediate their effects via the binding of Egr1 to its consensus elements in the PNMT promoter[107]. This was evidenced by the fact that both forskolin and PMA treatment increased nuclear Egr1

protein, as well as phosphorylated Egr1 protein/PNMT DNA binding complex formation[107]. Furthermore, when the primary binding element of Egr1 was mutated, the combined treatment of forskolin and PMA were unable to evoke PNMT promoter activation[107]. The phospholipase C (PLC) signaling pathway also plays an important role in PNMT promoter induction[5]. With regards to hypoxic stress, these pathways (both PKA and PLC) mediate hypoxic activation of PNMT via Egr1[5]. When PC12 cells were treated with cAMP and PLC signaling inhibitors, hypoxia-induced elevations in PNMT mRNA, cytosolic PNMT protein, and PNMT promoter activity were abrogated[5]. This response also occurred in PKA- and PLC-deficient cell lines transfected with pGL3RP893[5]. Furthermore, inhibitors of cAMP, PLC, PKA, PKC, phosphoinositide 3-kinase (PI3K), extracellular signal-regulated kinase ($ERK_{1/2}$), and mitogen-activated protein kinase (MAPK), significantly decreased PNMT promoter activation by hypoxia[5]. Importantly, these inhibitors significantly decreased Egr1 mRNA, and nuclear protein induction, following hypoxic stress[5]. These hypoxia-activated kinases listed above may not only serve as gene activators, but also contribute to Egr1 phosphorylation, which can enhance Egr1 transcription of PNMT by facilitating consensus site binding[5]. Together, these findings suggest that Egr1 plays a key role in regulating PNMT expression by hypoxic stress, and may be mediated by PKA and PLC signaling mechanisms.

1.6.1c Specificity protein 1

Sp1 is a constitutively expressed, ubiquitous mammalian transcription phosphoprotein that regulates a variety of genes[131]. In housekeeping genes that lack TATA and CAAT boxes (e.g., insulin-like growth factor-binding protein-2), Sp1 initiates transcriptional activation[131]. The Sp1

transcription factor contains a zinc finger domain that binds directly to GC-rich motifs in the promoter of Sp1-regulated genes[131].

PNMT is one such Sp1-regulated gene[105]. The PNMT promoter contains an Sp1 motif (consensus=[G/T][G/A]GGC[G/T][G/A][G/A][G/T]) at -48 bp[105]. In the rat PNMT gene, a second Sp1 consensus element is located at -168 bp upstream of the transcription initiation site[132]. The Sp1 sites on genes overlap the binding elements of other transcription factors. It is suggested that this competitive binding between Sp1 and other factors for binding site occupancy is an important mechanism controlling gene expression[105]. One such transcription factor is MAZ, which overlaps the Sp1 motif by 1 bp and is located at -38 bp[105]. MAZ prevents the binding of Sp1 to its consensus sequence, due to the fact that MAZ has a higher affinity for its binding element[105]. Therefore, the ability of Sp1 to bind to its motif in the PNMT promoter depends on its binding affinity for its cognate target sequences, its intracellular concentration, as well as the concentration of its competing transcription factor, MAZ[105]. Although MAZ has a higher affinity for its response element, Sp1 is a more effective activator of PNMT transcription, and preferentially increases intronless mRNA[105]. Both Sp1 sites in the rat PNMT promoter overlap the 5' end by 6 bp with the binding elements for the transcription factor, Egr1[133]. Although both sites function as Sp1 or Egr1 response elements, the distal overlapping Sp1/Egr1 site (at -168 bp) may preferentially serve as a site for Egr1 induction, whereas the proximal site (at -48 bp) may preferentially function as a site for Sp1 induction[132]. This competitive binding between Sp1 and other transcription factors may contribute to the tissue-specific expression of the PNMT gene[132]. Similar to Egr1, the Sp1 sites depend on the concentration of Sp1 protein, especially those which have undergone post-translational phosphorylation[94]. However, unlike Egr1, phosphorylation of Sp1 is required for

binding of Sp1 to its consensus sequences in gene promoters[94]. In addition, this phosphorylation is also needed for Sp1 to induce gene transcription[94].

Although Sp1 is constitutively expressed, its expression and activity can be regulated by different forms of stress. Immobilization stress has been shown to evoke changes in Sp1 mRNA, protein, and Sp1/DNA binding complex formation, and this induction precedes the rise in PNMT mRNA[102]. The longer the duration of immobilization stress, the greater the rise in Sp1 protein; however, multiple, repeated exposures to this stressor appeared to blunt this induction[134]. Additionally, Sp1 mRNA and protein expression is upregulated by CH (5% O_2) in PC12 cells[5]. Sp1 mRNA elevation is rapid and sustained for at least 24 h of hypoxic stress, with increased Sp1 mRNA levels apparent by 1 h, and maximum increase at 6 h[5]. Similarly, Sp1 protein increase is rapid and sustained for 24 h, with elevated 95 kDa and 105 kDa Sp1 protein levels apparent after only 30 min of hypoxic stress[94]. In addition, Sp1 participates in hypoxic transcriptional cis-activation of PNMT[5,94]. In response to CH, Sp1 protein/PNMT DNA binding complex formation increased rapidly and was sustained, with peak induction at 6 h[5]. The Sp1 protein/PNMT DNA binding complex formation produced a more robust increase, compared to the relative rise in Sp1 protein induced by hypoxia[5]. Sp1 regulation of PNMT under hypoxic stress is further evidenced by the inability of hypoxia to increase PNMT promoter-driven luciferase activity when the -168 bp and -48 bp Sp1 consensus sequence is inactivated by site-directed mutagenesis[5]. Even when these sites were individually mutated, hypoxic stimulation of the PNMT promoter was completely abrogated[5]. Similarly, co-transfection assays with wild-type construct pGL3RP893 and Sp1 siRNA, fully prevented luciferase induction when PC12 cells were exposed to CH[5]. From this study, it was concluded that Sp1 and Egr1 transcription factors are essential for hypoxic regulation of PNMT, and they work cooperatively and synergistically[5]. In the absence of one or the other,

CH cannot activate the PNMT promoter[5]. Lastly, hypoxic stress leads to a more extensive phosphorylation of Sp1 protein, as evidenced by the increased expression of the 95 and 105 kDa phosphorylated forms[94]. The 105 kDa form is more abundant than the 95 kDa form of Sp1 following hypoxic stress, whereas both isoforms are equally abundant in response to immobilization stress[94]. Thus, this increased phosphorylation of Sp1 by hypoxic stress may be an important mechanism that preferentially controls PNMT expression.

Through neural stimulation, Sp1 is capable of activating PNMT gene expression. This may occur via PKA and PKC signaling mechanisms[107]. This was demonstrated by the treatment of PC12 cells with PMA (a PKC activator), or the combination of forskolin (a PKA activator) and PMA, which resulted in increased phosphorylated Sp1 protein/PNMT DNA binding complex formation, without altering nuclear Sp1 protein levels[107]. Phosphorylation of Sp1 is an important post-translational modification that is regulated by PKA and PKC activation[107]. When nuclear extracts were treated with calf intestinal phosphatase, the dephosphorylation of nuclear proteins prevented Sp1 from forming a complex with PNMT[107]. Moreover, when the Sp1 site at -48 bp in the PNMT promoter was mutated, forskolin and forskolin/PMA activation was decreased significantly[107]. In contrast, the mutation of the -168 bp Sp1 site had little to no effect on promoter activation by PKA and PKC signaling[107]. As mentioned earlier, the PLC signaling pathway also plays an important role in PNMT promoter induction[5]. With regards to hypoxic stress, these pathways (both PKA and PLC) mediate hypoxic activation of PNMT via Sp1[5]. When PC12 cells were treated with inhibitors of cAMP, PLC, PKA, PKC, PI3K, $ERK_{1/2}$, and MAPK, Sp1 mRNA, and nuclear Sp1 protein induction was abrogated, following hypoxic stress[5]. These hypoxia-activated kinases listed above may not only serve as gene activators, but may also contribute to Sp1 phosphorylation, which can enhance Sp1 protein/PNMT DNA complex formation, as well as

transcription of PNMT[5]. Together, these findings suggest that Sp1 plays a key role in regulating PNMT expression by hypoxic stress and may be mediated by PKA and PLC signaling mechanisms.

1.6.1d Glucocorticoid receptor

PNMT is inducible by newly synthesized GCs produced and released from the adrenal cortex following stimulation by ACTH; therefore, an intact HPA axis is crucial for PNMT induction and activity[49,135]. GCs released by the activation of the HPA axis can increase CA production by regulating PNMT, as evidenced by studies in which hypophysectomy decreased PNMT mRNA, as well as enzyme expression, and activity[136]. Furthermore, one of these studies showed that this PNMT activity could be restored by the administration of ACTH or GCs[137].

GRs are hormone-activated transcription factors, which bind with a very high affinity to GCs[138]. GCs can influence both adrenergic differentiation, as well as induce the expression of PNMT by binding and activating the GR[139]. GRs are inactive when unbound in the cytosol[138]. However, when the GC-GR complex is formed, it can translocate into the nucleus of chromaffin cells[140]. Within the nucleus, this complex then binds to GREs in the promoter of PNMT[140]. In the PNMT promoter, three functional GREs have been identified[106]. Of these three, it has been determined that the GREs at -759 bp and -773 bp, which overlap by 1 bp, are primarily responsible for GC sensitivity and contribute to maximum induction of the PNMT promoter in response to GCs[106]. These GREs contain the highly conserved 3'-hexanucleotide sequence TGTTCT in the 15 bp palindromic, 5'-AGAACANNNTCTTCT-3'[106]. In contrast to these two more recently identified GREs, based on PNMT promoter-reporter gene expression, as well as PNMT mRNA expression, the originally identified GRE at -533 bp, has both variable and weak responsiveness

to GC activation[106]. Instead, the GRE at -533 bp may limit GC responsiveness mediated by the other two GREs[106]. However, GRs bound to the -533 bp GRE can cooperatively interact with Ap2 transcription factors bound to their recognition sites (-653 bp, -571 bp, and -45 bp), and synergistically regulate PNMT[106]. Moreover, the GRE at -759 bp has a 2-fold greater affinity for GRs, compared to the GRE located at -773 bp, and therefore, may be a more functionally important GRE[106]. That being said, both GREs must be intact for maximum GC sensitivity of the PNMT promoter[106]. GRs bound to these two GREs can also interact with Egr1, and/or Ap2, to stimulate PNMT promoter activity[106].

In order to delineate the signaling mechanisms involved in mediating GR induction of the PNMT gene, studies have investigated the role of PKA and PKC signaling induction. Firstly, when rats are administered the synthetic GC, dexamethasone (Dex), or the GC agonist, RU28362, PNMT mRNA levels rise significantly[141]. Similarly, Dex also causes an increase in PNMT promoter activity[3]. However, the PKA inhibitor, H-89, reduces this Dex-mediated PNMT promoter activity in these cells[3]. Therefore, intracellular cAMP and PKA may be important regulators of GC, and thus GR-mediated induction of the PNMT promoter. PKC signaling may also be involved in GR-mediated PNMT transcriptional activity, as evidenced in a study involving Dex and PMA[3]. Considering PNMT contains GREs in its proximal promoter, and its expression can be regulated by hypoxic stress, GR expression levels were measured following CH (5% O_2)[5]. However, hypoxic stress did not alter GR mRNA, protein, or GR protein/PNMT DNA binding complex formation following 1, 6, or 24 h of CH[5]. The authors concluded that this transcription factor was not involved in PNMT induction by hypoxic stress[5].

1.6.2 Post-transcriptional and post-translational regulation of the phenylethanolamine N-methyltransferase gene

PNMT can also be regulated post-transcriptionally by an alternate splicing mechanism and intron retention or removal. This alternative splicing produces two different forms of PNMT mRNA, and these forms have been identified in PC12 cells, in the heart of mice, as well as in the heart and adrenal medulla of rats[142,143]. The PNMT nucleotide sequence consists of three exons and two introns, and spans about 2.8 kb in length[144]. The partially processed nascent precursor PNMT mRNA transcript is produced when one of the two introns is not removed during RNA splicing[94]. This error introduces a stop codon into the mRNA transcript[94]. Consequently, a truncated PNMT protein is synthesized when this long form of PNMT mRNA is used as a template for protein translation[94]. The intron-retaining PNMT produces a truncated PNMT protein that appears to be inactive[94]. In contrast, the fully processed pre-mRNA PNMT transcript is created when all introns are removed, and this form is 110 bp shorter compared to the intron-retaining variant[94,144]. This short form of mRNA, also termed intronless PNMT, produces a full length, functionally active PNMT enzyme following protein translation[94]. Although CH has been shown to elevate PNMT mRNA, post-transcriptional controls may limit the amount of fully processed PNMT transcript produced, and thus, the amount of functional PNMT enzyme generated[94]. In fact, hypoxia increases the proportion of intron-retaining PNMT mRNA relative to the intronless PNMT variant[49]. This indicates that post-transcriptional control of PNMT is an important regulatory mechanism for the PNMT gene, especially in the case of hypoxic stress[49].

GCs promote PNMT transcription by increasing the amount of intronless PNMT mRNA splice variant[145]. PC12 cells express a very low basal level of both PNMT mRNA variants, and consequently, very low basal PNMT enzymatic activity[145]. However, when the synthetic GC,

dexamethasone (Dex) was administered, there was a significant elevation in only the intronless PNMT mRNA, as well as an upregulation in PNMT enzymatic activity[145].

Moreover, PNMT can be controlled post-translationally via GC regulation of PNMT enzyme stability[146]. GCs increase PNMT protein activity and stability by sustaining endogenous concentrations of AdoMET, via its metabolic enzymes, S-adenosylmethionine synthetase and S-adenosylhomocysteine hydrolase[106,146]. Binding of the co-substrate and methyl donor, AdoMET, allows sufficient PNMT activity, and also protects PNMT against proteolysis[106]. S-adenosylhomocysteine, the demethylated product formed during transmethylation by PNMT, stabilizes PNMT[147]. When AdoMET is administered to hypophysectomized rats, PNMT levels are partially restored and stabilized[147].

1.7 Regulation of catecholamines by hypoxia

Humans can experience many forms of hypoxia, including acute (of short duration) or chronic (long-lasting), as well as continuous or intermittent. Continuous exposure to hypoxia can be experienced during high-altitude sojourns, whereas intermittent exposure to hypoxia can be observed in patients with OSA who repeatedly experience closures in their upper airway during sleep[60]. Interestingly, humans and animals physiologically adapt to the effects of CH, whereas the response to IH leads to autonomic abnormalities[60]. O_2 is required as a cofactor for CA enzymes, including TH and DBH, and O_2 also regulates HIF1α activity, an important transcription factor in the regulation of TH and PNMT. Due to the importance of O_2 in controlling enzymatic and transcription factor activity, several studies have examined the effects of hypoxia on CA biosynthesis enzyme expression and activity, in order to determine cellular mechanisms involved in CA synthesis and release.

1.7.1 Regulation of catecholamines by continuous hypoxia

High-altitude dwellers experience CH, and interestingly, this chronic, CH leads to phenotypic remodelling and adaptive responses at the physiological and molecular level. In contrast to people who experience IH, physiological systems adapt to CH, and there is no increased risk of HTN, myocardial infarction, or stroke[148]. In fact, living in CH may provide some protection, for example, death from coronary artery disease or stroke is less common among high-altitude residents in Switzerland than in the general population[149]. CH is also experienced in patients with chronic lung disease. Interestingly, cardiovascular risk is markedly increased in patients with IH, as in OSA, compared to patients with chronic lung disease[150]. To further demonstrate the protective effect of CH, residents of Tibetan highlands, where the PO_2 is 110 mmHg, compared to residents at sea level (PO_2 = 150 mmHg), have normal pulmonary arterial pressure, hemoglobin levels, and aerobic tissue metabolism, despite CH[7]. At the molecular level, previous studies have shown that there is a genetic selection in Tibetan highlanders at the locus encoding HIF2α, PHD2, FIH1, and HIF target genes, producing a net effect that alters the balance between HIF2α and HIF1α, transcription factors which mediate vascular/erythropoietic and metabolic/vascular responses to hypoxia, respectively[8]. Since IH leads to pathophysiological conditions, and CH does not, there must be different mechanisms that regulate these responses. These mechanisms may involve activation or inactivation of specific genes, and *de novo* protein synthesis[26]. It has been proposed that CH-induced cFos expression, in the immediately early gene family, contributes to Ap1 transcription factor activity, and stimulates Ap1-regulated downstream genes, and thus, constitutes one potential molecular mechanism that triggers adaptations to CH[151]. However, in a study by Yuan et al. (2004), where IH was compared to CH, IH resulted in only a modest decrease of PO_2 (~20 mmHg), whereas CH caused a more pronounced drop in PO_2 (~70 mmHg)[148]. Surprisingly,

IH produced a significant stimulation of cFos, while a comparable cumulative duration of CH failed to activate cFos[148]. Prabhakar et al. (2001) demonstrated that the feature that distinguishes IH from CH is the intervening periods of normoxia, in which ROS, especially $O_2\bullet^-$, are produced, as well as downregulation of aconitase enzymes and elevated H_2O_2[13]. Aconitase catalyzes a non-redox-active process involving the isomerization of citrate to isocitrate in the citric acid cycle, and is inhibited by $O_2\bullet^-$, thus this enzyme serves as an index of ROS generation. Furthermore, mice exposed to IH have increased protein oxidation in cortical regions, measured as thiobarbituric acid reactive substances (TBARS)[152]. ROS are produced due to inhibition of the mitochondrial complex I, as IH inhibits several proteins that contribute to the assembly of complex I in the electron transport chain[148]. Several cytosolic and membrane-bound oxidases also generate ROS[153]. In fact, the duration of the normoxic episode is more critical in determining the extent of cFos activation, than the absolute duration of the hypoxic episodes[148]. Whereas scavengers of ROS have prevented IH-induced gene activation, the pretreatment with ROS scavengers prior to CH exposure did not prevent the upregulation of genes[154]. It is suggested that with long exposures to CH (>6 h), mechanisms other than ROS may contribute to gene upregulation[155]. Some of these mechanisms may include the regulation of CA biosynthesis enzymes, their transcription, translation, enzyme activity, and transcription factors (Table 1).

Table 1: Studies published in the literature demonstrating the regulation of catecholamine biosynthesis enzymes by continuous hypoxia.

Study	Animal/Tissue	Parameters	Duration	Findings
Tyrosine hydroxylase				
Hanbauer, 1977[156]	Rat	?	Several days	**1.** ↑ TH activity in the carotid body
Czyzyk-Krzeska et al., 1992[157]	Adult rat	CH: 10% O_2 Normoxia: Room air	1-48 h	**1.** TH mRNA ↑ at all time points in carotid body type I cells, but not in cells of superior cervical ganglion or adrenal medulla **2.** TH mRNA ↑ did not require innervation of carotid body or intact adrenal glands

				3. Hypercapnia failed to induce an ↑ in TH mRNA in type I cells
Czyzyk-Krzeska et al., 1994[158]	PC12 cells	CH: 5% O_2 Normoxia: 21% O_2	1-24 h	**1.** TH mRNA ↑ within first h of exposure, reached a peak at 6 h, and remained ↑ for entire exposure to CH (24 h) **2.** cAMP is not the primary regulator of TH transcription during CH, since 10-200 μM forskolin (activator of AC) caused only a weak ↑ in transcription of TH mRNA **3.** Half-life/stability of TH mRNA is ↑ during CH
Millhorn et al., 1997[159]	PC12 cells or rat carotid body	CH: 5 or 10% O_2 Normoxia: 21% O_2	1-72 h	**1.** PC12 cells (like the carotid body) express O_2-sensitive K^+ channels; CH reversibly inhibited outward current, leading to membrane depolarization and an ↑ in free intracellular Ca^{2+} (that is not dependent on extracellular Ca^{2+}) **2.** ↑ in dopamine release following CH in PC12 cells **3.** CH (10% O_2) ↑ TH mRNA in rat carotid body after 1 h, and remained elevated during a 24 h exposure, with peak ↑ at 6 h **4.** TH mRNA unaffected in sympathetic ganglia **5.** TH mRNA not regulated by hypercapnia in carotid body **6.** Reduction in O_2 from 21% to 15% for 6 h caused ↑ in TH mRNA in PC12 cells, and more severe O_2 tensions (10 and 5% O_2) further ↑ TH mRNA **7.** CH (5% O_2) ↑ TH protein in PC12 cells for 24-72 h **8.** ↑ binding activity with nuclear extracts from PC12 cells exposed to 5% O_2 for 6 h with TH gene (-190 bp to -284 bp relative to transcription start site) **9.** Competition probes containing either Ap1 or HIF1 sequence partially blocked binding of nuclear extracts to the native TH gene fragment, indicating that TH contains Ap1 and HIF1 elements that are regulated by CH **10.** ↑ in CH-induced binding activity with Ap1 double-stranded oligonucleotide probe, but not the HIF1 probe **11.** Antibody against cFos and JunB produced super-shifted band only detectable with protein from PC12 cells exposed to 5% O_2, indicating that cFos and JunB binding to Ap1 site is ↑ by CH; but not cJun (a protein that often forms a heterodimer complex with cFos) **12.** Mutation of the Ap1 element in the TH gene prevented ↑ by CH **13.** PKA activity ↓ during CH, and TH mRNA regulated by CH in mutant PC12 cells deficient in PKA, indicating that cAMP-PKA pathway is not required for CH-mediated regulation of TH gene expression in PC12 cells
Kroll and Czyzyk-Krzeska, 1998[154]	PC12 cells	CH: 5% O_2 Normoxia: Room air	1-20 h	**1.** H_2O_2 concentration ↓ and this induced TH mRNA **2.** 5 mM NAC alone also ↓ H_2O_2 and induced TH mRNA

Höhler et al., 1999[155]	PC12 cells	CH: 1% and 5% O_2 Normoxia: 20% O_2	1 h	**1.** ↑ in ROS production measured by oxidation of dihydrorhodamine to rhodamine in PC12 cells exposed to CH for 1 h compared to normoxia **2.** Hypoxia-induced ↑ in signal is prevented by the scavenger manganese (III) tetrakis porphyrin pentachloride (MnTMPyP) **3.** 2-fold ↑ in TH mRNA after exposure to 5% O_2 for 6 h **4.** Neither extracellular (by superoxide dismutase [SOD]) nor intracellular $O_2^{\bullet-}$ scavenging (by MnTMPyP) suppressed ↑ in TH mRNA by 5% O_2
Hui et al., 2003[160]	Male Sprague-Dawley rats	CH: 10% O_2 Normoxia: Room air	1, 3, 7, 14, or 30 days	**1.** Rapid ↑ in TH protein, as well as phosphorylations on serine-19, serine-31, and serine-40, within day 1 of exposure, and remained ↑ till day 30 in carotid body **2.** Guanosine triphosphate (GTP) cyclohydrolase-1 protein ↑, beginning at day 1 and remaining ↑ for 30 days – GTP cyclohydrolase-1 is the rate-limiting enzyme in BH_4 biosynthesis **3.** Absence of major changes in TH protein, and ↓ in phosphorylated serine-19 and serine-40 in superior cervical ganglia **4.** Modest ↑ in TH protein at later time points; phosphorylation on serine-19 was somewhat ↑ following 30 days, whereas phosphorylated serine-31 and serine-40 were transiently ↑ at 3 and 7 days of exposure, in adrenal glands
Schnell et al., 2003[161]	PC12 cells	CH: 1% O_2 Normoxia: 21% O_2	16 h	**1.** Activity of -272 TH-CA construct ↑ when co-transfected with HIF1α or HIF2α expression vectors in normoxia and CH **2.** Mutation of HRE within -272 TH-CA construct abolished regulation of TH promoter by HIFs **3.** Five repeats of TH HRE cloned upstream from a luciferase reporter gene was ↑ **4.** HIF/TH HRE complex formation ↑ **5.** Co-expression of VHL and the RING-box protein 1 (Rbx1; a protein with E3 ligase activity associated with VHL complex), with the HIF2α expression vector, inhibited HIF2α-induced transactivation of the TH promoter **6.** HIF1α accumulation ↓ during hypoxia in cells overexpressing VHL
Gozal et al., 2005[162]	Adult male Sprague-Dawley rats	CH: 10% O_2 Normoxia: Room air	6 h, 1 day, 3 days, 7 days, and 14 days	**1.** TH activity (as measured by DOPA accumulation) ↑ in cerebral cortex **2.** TH activity ↓ in brainstem, and was unchanged in frontal cortex and in Cornu Ammonis (CA)1 and CA3 hippocampal regions **3.** TH mRNA ↑ beginning at 3 days and persisted until 14 days in cerebral cortex **4.** Total TH protein ↑ at 3 days in cerebral cortex (not significantly) **5.** TH phosphorylation at serine-40 ↑ at 7 days in cerebral cortex **6.** No change in serine-40 phosphorylation in brainstem

Kato et al., 2010[163]	Male Wistar rats (8-11 weeks old)	CH: 10% O_2 Normoxia: Untreated	2, 4, 8, 12, 18, or 24 h	**1.** TH immunoreactivity ↑ in cytoplasm of type I cells in carotid body at 4, 8, 12, 18 and 24 h CH **2.** TH fluorescence intensity ↑ at 12, 18, and 24 h
Wakai et al., 2010[164]	Rat	CH: 10% O_2 Normoxia: 20% O_2	2-24 h	**1.** TH mRNA ↑ in carotid body after 4 h (6.6-fold), 6 h (6.0-fold), and 8 h (7.8-fold) **2.** TH immunoreactivity ↑ in carotid body after 12 and 24 h **3.** TH mRNA and immunoreactivity unaltered in rats exposed to hypercapnia (10% CO_2) in carotid body
Kato et al., 2013[165]	Male Wistar rats (8-9 weeks old)	CH: 10% O_2 Normoxia: Untreated	6, 12, 18, and 24 h	**1.** Total TH protein ↑ after 12, 18, and 24 h of CH in carotid body **2.** Phosphorylated TH at serine-31 and serine-40 ↑ with all time-points of CH in carotid body **3.** Immunoreactive type I cells for phosphorylated TH at serine-31 and serine-40 ↑ at all time points of CH
Dopamine β-hydroxylase				
Hui et al., 2003[160]	Male Sprague-Dawley rats	CH: 10% O_2 Normoxia: Room air	1, 3, 7, 14, or 30 days	**1.** DBH protein ↑ transiently (1 and 3 days) in the superior cervical ganglia **2.** DBH protein ↑ in adrenal glands
Kato et al., 2013[166]	Male Wistar rates (8-9 weeks old)	CH: 10% O_2 Normoxia: Untreated	6, 12, 18, and 24 h	**1.** DBH protein ↑ after 12 h of CH in the carotid body **2.** DBH immunoreactivity ↑ after 12 h of CH in glomus cells
Phenylethanolamine N-methyltransferase				
Evinger et al., 2002[167]	MPC712 cells	Anoxia: 0% O_2 CH: 1-10% O_2 Normoxia: 21% O_2	1 min-16 h	**1.** Anoxia ↑ PNMT promoter luciferase expression within 15 min, with peak at 45 min, then subsiding to normoxic levels by 120 min **2.** Anoxia ↑ PNMT mRNA after 1 h, and ↑ up to 16 h **3.** Egr1 mRNA ↑ following hypoxia at 30 and 60 min **4.** HIF1α mRNA ↑ following hypoxia at 60 min
Hui et al., 2003[160]	Male Sprague-Dawley rats	CH: 10% O_2 Normoxia: Room air	1, 3, 7, 14, or 30 days	**1.** PNMT protein unchanged in adrenal glands **2.** No PNMT immunoreactivity was detected in carotid body extracts
Wong et al., 2004[49]	PC12 cells	CH: 5% O_2 Normoxia: 21% O_2	0-24 h	**1.** PNMT promoter-driven luciferase expression ↑ (using construct pGL3RP893), with maximum activity at 9.5 h **2.** Pretreatment of cells with PKA and PKC inhibitors attenuated the ↑ in hypoxia-induced luciferase activity **3.** Mutation of Egr1 binding site completely prevented PNMT promoter activation – Egr1 is essential to hypoxia-induced stress response **4.** Egr1 protein ↑, with maximum peak at 0.75 h **5.** PNMT mRNA ↑ after 6 h, with a shift to intron-retaining mRNA
Tai et al., 2009[100]	PC12 cells	CH: 5% O_2 Normoxia: 21% O_2	0-24 h	**1.** HIF1α mRNA, nuclear protein, and HIF1α-PNMT complex formation ↑, with peak stimulation at 6 h, followed by a decline towards basal values by 24 h **2.** PNMT promoter-driven luciferase activity ↑ following 6 h of hypoxia **3.** Overexpression of HIF1α ↑ Egr1 and Sp1 mRNA and nuclear protein, as well as PNMT mRNA and protein

				4. Overexpression of HIF1α in PC12 cells transfected with PNMT promoter-luciferase reporter gene constructs harbouring either mutated Egr1 or Sp1 binding elements did not ↑ luciferase reporter gene activity above basal levels – when hypoxic stress stimulates HIF1α, it in turn induces Egr1 and Sp1 expression, and thereby PNMT
Wong et al., 2010[44]	PC12 cells	CH: 5% O_2 Normoxia: 21% O_2	0-24 h	**1.** cAMP, PKA, PLC, PKC, PI3K, $ERK_{1/2}$ MAPK ↑ **2.** PNMT mRNA and cytosolic protein ↑ after 6 h
Tai et al., 2010[5]	PC12 cells	CH: 5% O_2 Normoxia: 21% O_2	0-24 h	**1.** PNMT promoter-driven luciferase activity ↑ **2.** PNMT mRNA and cytosolic protein ↑ after 6 h, with a slight ↓ in elevation by 24 h, with a shift towards intron-retaining PNMT mRNA **3.** Egr1 mRNA ↑ rapidly and transiently, peaking at 1 h and ↓ to basal levels by 24 h **4.** Egr1 nuclear protein and Egr1-PNMT complex formation showed rapid and transient ↑, reaching peak value at 1 h **5.** Sp1 mRNA ↑ rapidly, peaking at 6 h, and remaining ↑ through 24 h **6.** Sp1 nuclear protein and Sp1-PNMT complex formation showed rapid and sustained ↑, reaching peak value at 6 h – both 105 and 95 kDa phosphorylated forms of Sp1 are expressed, with the former being more abundant **7.** No alteration in GR or Ap2 mRNA or protein, GR-PNMT complex formation, or Ap2-PNMT complex formation **8.** Egr1 and Sp1 binding site inactivation or Egr1 and Sp1 siRNA inhibit PNMT promoter stimulation by hypoxia
Crispo et al., 2011[1]	PC12 cells	CH: 5% O_2 Normoxia: 21% O_2	24 h	**1.** 1.7-fold ↑ in intracellular ROS following CH **2.** 6 μM ↓ in extracellular NO levels following CH

1.7.2 Regulation of catecholamines by intermittent hypoxia

In contrast to people who experience CH, people living at sea level can experience IH, as seen in patients with SDB and recurrent apneas. These recurrent apneas are often due to obstruction of the upper airway, as in OSA. Exposure to IH is associated with increased CA secretion from the adrenal medulla, and these patients with OSA are at an increased risk of developing HTN and stroke[168]. Patients with OSA exhibit a more pronounced rise in BP during apneic episodes, compared to normal subjects, and importantly, have a sustained elevation in BP that continues

during the daytime when apneic episodes are absent[169]. The mechanism by which augmented CA efflux occurs due to IH is in part, due to increased voltage-gated Ca^{2+} influx and intracellular Ca^{2+} stores, activation of PKC, and ultimately, an increase in the number of readily releasable pools of secretory granules[170]. A study by Kumar et al. (2006) used male Sprague-Dawley rats and exposed them to CH (4 h in 7% O_2), IH (15 s in 5% O_2; 5 min in 21% O_2; 8 h/day), or normoxia (room air)[171]. IH evoked robust effluxes of NE and Epi, whereas these responses were absent in rats exposed to CH or normoxia[171]. Furthermore, IH decreased cytosolic and mitochondrial aconitase enzyme activity, suggesting increased generation of $O_2\bullet^-$[171]. Following systemic administration of antioxidants, the effect of IH on the adrenal medulla was reversed[171]. Consistent with this study, others have also shown IH induces increased ROS levels in the adrenal medulla in adult and neonatal rats, as well as in mice[170–172]. ROS has been shown to facilitate CA efflux following IH exposure. Several studies have shown that pretreatment with the potent scavenger of ROS and SOD mimetic that scavenges $O_2\bullet^-$ without generating H_2O_2, MnTMPyP, prevented IH-induced changes in adrenal medulla functioning, including the facilitation of CA efflux, and the PKC-mediated increase in the size of the readily releasable pool of secretory vesicles[171–173]. Moreover, the increased cellular levels of ROS is governed by the balance that is tipped towards the generation of pro-oxidant enzymes, such as the nicotinamide adenine dinucleotide phosphate oxidase (NOX) family of enzymes and xanthine oxidase (XO), and decreases the action of antioxidant enzymes, including SOD1, SOD2, and catalase[173–176]. Another proposed signaling pathway involves a HIF-dependent upregulation of NOX, resulting in elevated ROS, which then upregulates Ca^{2+} channels and ryanodine receptors[173]. Lastly, IH can not only upregulate mechanisms that stimulate CA release, but it can also increase mechanisms involved in gene

transcription and translation of the enzymes involved in the CA biosynthesis pathway, and transcription factors that regulate these enzymes (Table 2).

Table 2: Studies published in the literature demonstrating the regulation of catecholamine biosynthesis enzymes by intermittent hypoxia.

Study	Animal/Tissue	Parameters	Duration	Findings
Tyrosine hydroxylase				
Hui et al., 2003[160]	Male Sprague-Dawley rats	IH: 90 s 10% O_2 and 90 s room air Normoxia: Room air	1, 3, 7, 14, or 30 days	**1.** TH protein and phosphorylation ↑ at serine-19, serine-31, and serine-40 in carotid body following IH, but was delayed, and began only after 7 days of exposure (final ↑ measured at end of 30 days' exposure to IH was 5-fold smaller than that elicited by corresponding exposures to CH) **2.** TH protein and phosphorylation ↑ at serine-19 and serine-31 in superior cervical ganglia following IH (stronger inducing effects compared to CH) **3.** TH protein and phosphorylation ↑ transiently at serine-31 and serine-40 in adrenal glands between days 3 and 7
Yuan et al., 2004[148]	PC12 cells	IH: 15 s 1.5% O_2 and 4 min 21% O_2 CH: 1.5% O_2 Normoxia: 21% O_2	IH: 60 or 120 cycles CH: 15 min-8 h	**1.** cFos mRNA and transcriptional activation ↑ in a stimulus-dependent manner, with serum responsive element (SRE) and Ca^{2+} responsive element being critical to its activation **2.** IH more potent and induced a longer activation of cFos than comparable cumulative duration of CH – comparable cumulative duration of CH had virtually no effect on cFos expression – cFos remained ↑ for at least 3 h following termination of IH, whereas it returned to control levels within 1 h of terminating CH **3.** Ap1 activity and TH mRNA ↑, since TH is an Ap1-regulated downstream gene **4.** SOD mimetic prevented IH-induced cFos, Ap1, and TH activation **5.** $O_2{\bullet}^-$ levels in mitochondria ↑, as evidenced by ↓ aconitase enzyme, and ↑ H_2O_2 levels (a stable dismutated product of $O_2{\bullet}^-$) **6.** Complex I of electron transport chain was inhibited **7.** Inhibitors of complex I mimicked effects of IH during normoxia, and occluded effects of IH on cFos activation – electron transport chain involved in generation of $O_2{\bullet}^-$ during IH **8.** TH protein was not affected by IH
Kim et al., 2004[177]	PC12 cells	IH: 30 s 1% O_2 and 3 min 21% O_2 Normoxia: 21% O_2	IH: 15 or 60 cycles	**1.** 300 μM NAC attenuated IH-induced dopamine and acetylcholine (ACh) secretion

Yuan et al., 2005[178]	PC12 cells	IH: 30 s 1.5% O_2 and 4 min 20% O_2 CH: 1.5% O_2 Normoxia: 20% O_2	IH: 120 cycles CH: 6 h	**1.** TH mRNA expression ↑, but not by CH
Kumar et al., 2006[171]	PC12 cells	IH: 15 s 1% O_2 and 4 min 21% O_2 CH: 1% O_2 Normoxia: 21% O_2	IH: 60 cycles CH: 60 or 120 min	**1.** TH activity ↑, without altering TH protein levels – comparable duration of CH ↑ TH activity, but to a lesser extent than IH **2.** IH activates TH via phosphorylation of serine residues (serine-40), in part by calcium/calmodulin-dependent protein kinase (CaMK) and PKA
Raghuraman et al., 2009[179]	Male Sprague-Dawley rats	IH_{15s}: 15 s 5% O_2 and 5 min 21% O_2 IH_{90s}: 90 s 10% O_2 and 90 2 21% O_2 Normoxia: 21% O_2	8 h/day for 10 days	**1.** TH activity, dopamine, and TH phosphorylation at serine-31 and serine-40 in the medulla oblongata ↑ following IH_{15s} **2.** PP2A activity and expression ↓ and protein kinase activity ↑ following IH_{15s} **3.** ROS generation in brainstem medullary regions ↑ following IH_{15s} **4.** Antioxidants (5 mg/kg/day MnTMPyP or 400 mg/kg/day NAC) prevented IH_{15s}-induced downregulation of PP2A or IH_{15s}-induced ↑ of protein kinase activity, resulting in reversal of serine phosphorylation of TH, TH activity, and dopamine to control levels
Khurana et al., 2018[180]	PC12 cells	IH: 30 s 1.5% O_2 and 3 min 21% O_2 Normoxia: 21% O_2	60 cycles	**1.** TH mRNA ↑
Dopamine β-hydroxylase				
Hui et al., 2003[160]	Male Sprague-Dawley rats	IH: 90 s 10% O_2 and 90 s room air Normoxia: Room air	1, 3, 7, 14, or 30 days	**1.** DBH protein ↑ for a longer duration (1, 3, 7, 14, 30 days) in superior cervical ganglia, compared to CH **2.** DBH protein ↑ in adrenal glands
Khurana et al., 2018[180]	PC12 cells	IH: 30 s 1.5% O_2 and 3 min 21% O_2 Normoxia: 21% O_2	60 cycles	**1.** DBH mRNA ↑
Phenylethanolamine N-methyltransferase				
Hui et al., 2003[160]	Male Sprague-Dawley rats	IH: 90 s 10% O_2 and 90 s room air Normoxia: Room air	1, 3, 7, 14, or 30 days	**1.** PNMT protein unchanged in adrenal glands

Yuan et al., 2005[178]	PC12 cells	IH: 30 s 1.5% O_2 and 4 min 20% O_2 CH: 1.5% O_2 Normoxia: 20% O_2	IH: 60 or 120 cycles CH: 1 h	**1.** HIF1α nuclear protein ↑ as duration of IH ↑, whereas CH requires a longer duration, and 1 h of CH is ineffective in ↑ HIF1α nuclear protein **2.** Expression of HIF1α-dependent luciferase reporter gene ↑, whereas CH did not **3.** Activation of ERK1, ERK2, c-Jun N-terminal kinase (JNK), and PKC **4.** CaMKII activity, phosphorylation of CaMKII, and intracellular Ca^{2+} ↑, whereas CH leads to only a transient (15 min) and modest ↑ in CaMKII activity **5.** Inhibitors of CaMKII prevented IH-induced HIF1α transcriptional activity, but did not prevent CH-induced HIF1α activity **6.** C-terminal transactivation domain of HIF1α ↑ (via a mechanism that is independent of Asn^{830} hydroxylation and CaMKII is required for this response) – whereas Asn^{830} hydroxylation is required for CH-evoked C-terminal transactivation domain activation **7.** Rate of O_2-dependent proline hydroxylation of HIF1α subunit ↓ by CH – whether ↓ proline hydroxylation is critical for HIF1 stabilization during IH requires further study **8.** IH-induced HIF1α transcriptional activity is independent of PI3K, whereas CH-induced HIF1α transcriptional activity requires activation of PI3K **9.** p300 and CREB are major co-activators of IH-induced HIF1 activation **10.** p300 activity ↑, and was blocked by an inhibitor of CaMKII, suggesting that CaMKII may be necessary for p300 activity
Nanduri & Nanduri, 2007[9]	PC12 cells	IH: 30 s 1.5% O_2 and 5 min 21% O_2 Normoxia: 21% O_2	5, 10, 60 cycles	**1.** PLC and inositol 1,4,5-triphosphate (IP_3) ↑, resulting in ↑ intracellular Ca^{2+} **2.** Ca^{2+} then ↑ mammalian target of rapamycin (mTOR) and CaMKII **3.** ↑ mTOR results in ↑ S6 kinase, leading to HIF1α stabilization **4.** ↑ CaMKII results in ↑ p300-CBP, leading to HIF1α transcriptional activation
Yuan et al., 2008[174]	PC12 cells	IH: 30 s 1.5% O_2 and 4 min 20% O_2 CH: 1.5% O_2 Normoxia: 20% O_2	60 cycles	**1.** mTOR-dependent HIF1α synthesis ↑, and hydroxylase-dependent HIF1α degradation ↓ **2.** HIF1α accumulation is due to ↑ generation of ROS by NOX **3.** IH-evoked HIF1α ↑ involves ROS-dependent Ca^{2+} signaling pathways involving PLC and PKC activation **4.** Phosphorylated mTOR protein synthesis and activation ↑, since rapamycin inhibits IH-induced HIF1α stabilization – whereas CH inhibits mTOR **5.** Downstream S6 kinase ↑, leading to ↑ HIF1α stabilization **6.** 50 μM MnTMPyP prevented ↑ HRE activity, and inhibited IH-evoked HIF1α protein ↑

Nanduri et al., 2015[181]	PC12 cells	IH: 30 s 1.5% O_2 and 5 min 21% O_2 Normoxia: 21% O_2	5, 10, 60 cycles	**1.** XO activity ↑, with significant activation after 5 cycles of IH **2.** NOX activation ↑, requiring a minimum of 10 cycles of IH **3.** Following treatment of cells with an inhibitor of XO (allopurinol) and exposure to IH, NOX activation was blocked – XO activation by IH precedes that of NOX **4.** NOX2 activation requires Ca^{2+}-dependent PKC activation, as well as PKC-dependent phosphorylation and subsequent translocation of the cytosolic $p47^{phox}$ and $p67^{phox}$ subunits to the membrane
Khurana et al., 2018[180]	PC12 cells	IH: 30 s 1.5% O_2 and 3 min 21% O_2 Normoxia: 21% O_2	60 cycles	**1.** Intronless and intron-retaining forms of PNMT mRNA ↑ **2.** PNMT promoter-driven luciferase activity was ↑ **3.** 200 μM $CoCl_2$ ↑ PNMT promoter-driven luciferase activity **4.** HIF1α, Egr1, Sp1, and GR mRNA ↑ **5.** PNMT and GR protein ↑ in cytoplasm of PC12 cells (immune-fluorescent microscopy) **6.** HIF1α, Egr1, and Sp1 protein ↑ in nucleus of PC12 cells (immune-fluorescent microscopy)
Blood pressure				
Hui et al., 2003[160]	Male Sprague-Dawley rats	IH: 90 s 10% O_2 and 90 s room air CH: 10% O_2 Normoxia: Room air	1, 3, 7, 14, or 30 days	**1.** At day 30, systolic and diastolic BP levels were ↑ in rats exposed to IH compared to CH
Kumar et al., 2006[171]	Male Sprague-Dawley rats	IH: 15 s 5% O_2 and 5 min 21% O_2 Normoxia: Room air	IH: 9 cycles/h and 8 h/day	**1.** 5 mg/kg/day MnTMPyP and 800 mg/kg/day NAC prevented the ↑ in BP and the ↑ in plasma CAs
Jouett et al., 2016[182]	Healthy human subject	IH: 2-3 breaths at normal tidal volume of 100% N_2 and 20-send end-expiratory apnea and recovery on room air for 40 s Normoxia: Room air	20 min	**1.** 70 mg/kg NAC ↓ muscle sympathetic nerve activity **2.** NAC ↓ systolic BP and mean arterial pressure **3.** NAC ↓ heart rate

1.8 Hypothesis and Objectives

1.8.1 Hypothesis

Current literature has shown that the CA Epi is elevated in individuals with OSA, influencing BP, and causing secondary HTN. In contrast, individuals who experience CH do not have an increased risk of cardiovascular complications. This striking contrast between the consequences of the two forms of hypoxia may be due to the increased oxidative stress in IH, as a result of the intervening periods of normoxia. We hypothesized that ROS can directly regulate the CA biosynthesis pathway in adrenal chromaffin cells, thus, providing a mechanism for hypoxia-mediated regulation of CA production, as in IH-evoked HTN. Based on the current literature, we predicted that IH will increase CA biosynthesis enzyme expression in PC12 cells. Further, we hypothesized that these changes in CA biosynthesis enzyme transcript levels would be regulated by changes in promoter activation. Studies have shown that CH leads to phenotypic remodelling and adaptive responses at the physiological and molecular level. Due to these adaptation mechanisms in response to CH, it was proposed that IH would cause more significant upregulations in CA biosynthesis enzyme expression, and their known transcription factors, compared to similar durations of CH. Lastly, we hypothesized that antioxidants and polyphenols, which have been shown to reduce BP and plasma CAs in rats and humans exposed to IH, would reduce ROS, and thus, promoter activation of PNMT.

1.8.2 Objectives

The objectives of this study were:

(1) To analyze possible regulatory effects of IH on the transcript and protein expression levels of CA biosynthesis enzymes TH, DBH, and PNMT in PC12 cells.

(2) To investigate the mechanisms involved in the transcriptional regulatory effects of IH by analyzing PNMT promoter activation, and expression of HIF1α, Egr1, Sp1, and GR.

(3) To compare the effects of IH with similar duration of CH.

(4) To examine the possible signaling mechanisms induced by both forms of hypoxia (CH, IH), as well as their combination with $CoCl_2$ or Dex.

(5) To determine the role of ROS in IH-evoked CA biosynthesis enzyme expression via antioxidant and polyphenol pretreatment.

Chapter 2: Materials and Methods

2.1 Cell culture

Rat pheochromocytoma-derived PC12 cells, originating from adrenal medullary tumour cells, were cultured in 100-mm, clear, tissue culture-treated dishes. These cells were maintained in Dulbecco's modified Eagle's medium (DMEM) and supplemented with 5% bovine calf serum (BCS), 5% equine serum (ES) and 0.05 µg/mL gentamycin sulphate (GS). Cells were maintained in a humidified Forma Series I Water Jacketed CO_2 Incubator at 37°C in an atmosphere of 95% air and 5% CO_2. Upon reaching 80% confluency, PC12 cells were either split, at a ratio of 1:2, 1:3, or 1:4, or were used in an experiment. In all experiments, cells were used when they were between passages 12 – 24. In order to disengage adherent cells from the plate and transfer them to fresh plates, cells were first washed with phosphate buffered saline (PBS), followed by incubation in trypsin. Prior to experimentation (24 h), supplemented DMEM was exchanged for charcoal-treated media (CTM; DMEM containing charcoal-treated sera) to remove endogenous hormones including GCs, growth hormones, and cytokines that may affect the expression of genes of interest. Both BCS and ES were treated with activated charcoal (1 g charcoal/50 mL of serum) by continuous stirring for 3 h at 4°C, followed by centrifugation at 2,500 x g for 30 min at 4°C, and sterile-filtration with a 0.45 µm filter. Cells were counted, and viability determined to ensure that an equal number of cells were seeded in each well. A cell viability analyzer (Vi-CELL XR), which uses a trypan blue stain to selectively colour dead cells blue, was employed to count cells. For RT-PCR and Western blot analysis, cells were plated in 6-well, clear, tissue culture-treated plates in 3 mL CTM at a density of $3x10^6$ cells/well 24 h prior to treatment. For luciferase assays, cells were plated in 24-well, clear, tissue culture-treated plates in 1 mL CTM at a density of 350,000 cells/well 48 h prior to treatment. For ROS assays, cells were plated in 96-well, clear bottom, black-sided,

tissue culture-treated plates in 200 µL CTM at a density of 150,000 cells/well 24 h prior to treatment.

2.2 Treatments

Approximately 24 h after initial seeding in CTM, PC12 cells requiring treatment were administered with appropriate agent to specified final concentration for 1 or 8 h (Table 3). If combined with hypoxia exposure, agent was added 30 min prior to placing cells in hypoxia chamber, and cells remained in drug-treated medium for remainder of hypoxia exposure.

Table 3: Properties of selected chemical agents.

Agent	Function	Solubility	Stock concentration	Final concentration
Cobalt chloride ($CoCl_2$)	Hypoxia mimetic agent	DMEM	100 mM	200 µM
Dexamethasone (Dex)	Synthetic GC	Ethanol	10 mM	1 µM
N-acetyl cysteine (NAC)	Antioxidant and free radical scavenger	DMEM	500 mM	5 mM
Epigallocatechin gallate (EGCG)	Polyphenol	DMEM	100 mM	100 µM
Methyl gallate (MG)	Polyphenol	DMEM	50 mM	50 µM
Tempol (TP)	Polyphenol	DMEM	1 mM	1 µM

2.3 Exposure of cells to hypoxia

Hypoxic conditions were achieved using a custom-built hypoxic chamber system. This was placed in a humidified incubator maintained at 37°C. The hypoxia chamber provides a means to control both the concentration of O_2, and background gas (N_2). A galvanic sensor within the chamber allows for convenient and precise indication of chamber O_2 conditions at all times throughout the program and a digital screen displays this O_2 concentration. In order to facilitate gas permeation into the media and cells, breathable sealing films (AeraSeal) were used. The protocol for normoxia, IH, and CH conditions are outlined in Table 4.

Table 4: Protocol for normoxia and hypoxia exposures.

Exposure	Protocol
Normoxia	5% CO_2 – 95% air
IH_{1h}	Hypoxia: 1% O_2 for 30 sec Normoxia: 16% O_2 for 3 min Duration: 1 h Number of cycles: 10
IH_{8h}	Hypoxia: 1% O_2 for 30 sec Normoxia: 16% O_2 for 3 min Duration: 8 h Number of cycles: 80
CH_{1h}	Hypoxia 5% O_2 Duration: 1 h
CH_{8h}	Hypoxia: 5% O_2 Duration: 8 h

2.4 RNA extraction, cDNA synthesis and RT-PCR

2.4.1 RNA extraction

Following treatment, media was aspirated, and 500 µL TRIzol reagent was added. Lysate was then transferred into a 1.5 mL microcentrifuge tube, treated with 100 µL chloroform, vortexed for 15 sec (Analog vortex mixer), and incubated for 15 min at room temperature. Following centrifugation (Centrifuge 5415 R) at 12,000 rpm for 20 min at 4°C, the aqueous phase was transferred to a new 1.5 mL microcentrifuge tube. To precipitate the RNA and remove salt, 125 µL isopropanol was added, followed by vortexing for 10 sec, and incubating the tube for 10 min at room temperature. An RNA pellet was formed upon centrifugation at 12,000 rpm for 8 min at 4°C. The supernatant was then discarded. Any residual salt was washed away from pelleted RNA by adding 250 µL of 70% anhydrous ethanol. One final centrifugation at 7,500 rpm for 5 min, at 4°C was performed, after which the ethanol was removed. The tube containing the RNA was inverted for 10 min to air-dry the pellet. Next, the RNA pellet was dissolved in 17 µL RNase-free, diethylpyrocarbonate (DEPC)-treated H_2O and placed in thermomixer at 1,000 rpm for 10 min, at 37°C. The absorbance of the RNA sample was then measured at 260 and 280 nm and the A_{260}/A_{280} ratio was used to assess RNA purity (1.8-2.1 is indicative of highly purified RNA). The RNA concentration was generated by the NanoDrop spectrophotometer (ND-1000). Samples were then stored at -80°C until further use.

Prior to DNase treatment, RNA integrity was assessed by running 500 ng of RNA sample on a denaturing 1% Tris-borate ethylenediaminetetraacetic acid (EDTA; TBE) agarose gel with 10 mg/mL ethidium bromide. Visualization of the 28S rRNA being twice as intense as the 18S rRNA band was used as an indication that RNA was completely intact. 10 µL of 1 kbp DNA ladder was loaded as a molecular weight marker.

2.4.2 DNase treatment

All samples were DNase-treated to remove any DNA contamination in the sample. 2 µg of sample RNA was treated with 2 µL of 1 U/µL Amplification Grade DNase I in 2 µL of 10X DNase reaction buffer, and DEPC-treated H_2O to a final volume of 20 µL in 0.2 mL PCR tubes. After incubation of mixture for 15 min at room temperature, 2 µL of stop solution (50 mM EDTA) was added, and tubes were heated to 70°C for 10 min in thermocycler, and then immediately chilled on ice. Final concentration of DNase-treated RNA was 2 µg RNA/22 µL volume.

2.4.3 cDNA synthesis

In the tubes with the DNase-treated RNA, 1 µg of random primers was added. Subsequently, samples were incubated for 5 min at 70°C in the thermocycler, and then immediately chilled on ice. Then, each tube was incubated for 1 h at 37°C in the thermocycler with 12.5 µL of DEPC-treated H_2O, 10 µL of 5X reaction buffer, 2.5 µL of dNTP mix (10 mM each base), and 2 µL of 200 U/µL murine leukemia virus (Mu-MLV) reverse transcriptase (RT). Final concentration of cDNA was 2 µg/50 µL volume.

2.4.4 Reverse transcriptase-polymerase chain reaction

RT-PCR was performed on 100 ng of cDNA, in a 25 µL reaction volume in 0.2 mL PCR tube strips containing 14.375 µL MilliQ H_2O, 5 µL 5X Green GoTaq Flexi reaction buffer, 1.5 µL of 25 mM $MgCl_2$, 0.5 µL dNTPs (10 mM each base), 0.5 µL of 100 ng/µL forward primer, 0.5 µL of 100 ng/µL reverse primer, and 0.125 µL of 5 U/µL of GoTaq Flexi DNA polymerase. Primer sets and thermocycler protocols for each gene from *Rattus norvegicus* are described in Table 5. The 28S RNA gene was used as a housekeeping gene. Following RT-PCR, amplicons were

resolved on a 2% Tris-acetate EDTA (TAE) agarose gel with 10 mg/mL ethidium bromide. 10 μL of 1 kbp DNA ladder was loaded as a molecular weight marker. Gel was visualized under UV light using Chemidoc XRS and quantified by Quantity One analysis software. All samples were run in triplicate, and the experiment was performed at least 3 times.

Table 5: Primer sets and cycling conditions.

Gene	Primer sequence (5'-3')	Primer name	Target Amplicon	Amplification conditions
PNMT X75333	**F**: CAGACTTCTTGGAGGTCAACCG	rPNMT ss1	715/605 bp	1. Initial denaturing 94°C, 3 min 2. Denaturing: 94°C, 1 min 3. Annealing: 58°C, 1 min 4. Synthesis: 72°C, 1 min 5. Go to step 2, 34 times 6. Final extension: 70°C, 10 min
	R: AGCAGCGTCGTGATATGATAC	rPNMTE3 as		
HIF1α NM024359	**F**: GGTGCTAACAGATGATGGTGAC	rHIF1α ss	161 bp	1. Initial denaturing 94°C, 3 min 2. Denaturing: 94°C, 1 min 3. Annealing: 58°C, 1 min 4. Synthesis: 72°C, 1 min 5. Go to step 2, 26 times 6. Final extension: 70°C, 10 min
	R: CTCGGTGAGATAGTTCTGC	rHIF1α as		
Egr1 AY551092	**F**: TTTCCACAACAACAGGGAGAC	rEgr1 ss (Q)	261 bp	1. Initial denaturing 94°C, 3 min 2. Denaturing: 94°C, 1 min 3. Annealing: 58°C, 1 min 4. Synthesis: 72°C, 1 min 5. Go to step 2, 34 times 6. Final extension: 70°C, 10 min
	R: CTCAACAGGGCAAGCATACG	rEgr1 as		
Sp1 NM012655	**F**: CAGACTAGCAGCAGCAATACCA	rSP1 ss (Q)	224 bp	1. Initial denaturing 94°C, 3 min 2. Denaturing: 94°C, 1 min 3. Annealing: 58°C, 1 min 4. Synthesis: 72°C, 1 min 5. Go to step 2, 26 times 6. Final extension: 70°C, 10 min
	R: TGAAGGCCAAGTTGAGCTCCAT	rSP1 as		
GR AY066016	**F**: CTCTGGAGGACAGATGTACCA	rGR ss (Q)	232 bp	1. Initial denaturing 94°C, 3 min 2. Denaturing: 94°C, 1 min 3. Annealing: 58°C, 1 min 4. Synthesis: 72°C, 1 min 5. Go to step 2, 26 times 6. Final extension: 70°C, 10 min
	R: GCTTACATCTGGTCTCATTCC	rGR as		
TH L22651	**F**: GCGACAGAGTCTCATCGAGGAT	rTHss	303 bp	1. Initial denaturing 94°C, 3 min 2. Denaturing: 94°C, 1 min 3. Annealing: 52°C, 1 min 4. Synthesis: 72°C, 1 min 5. Go to step 2, 20 times 6. Final extension: 70°C, 10 min
	R: GGCACCTCGAAGCGCACAAAA	THas2		
DBH NM_013158	**F**: TTCCCCATGTTCAACGGACC	rDBHss	449 bp	1. Initial denaturing 94°C, 3 min 2. Denaturing: 94°C, 1 min 3. Annealing: 58°C, 1 min 4. Synthesis: 72°C, 1 min 5. Go to step 2, 27 times 6. Final extension: 70°C, 10 min
	R: GCGAGCACAGTAATCACCTTCC	rDBHas		
28S RNA V01270	**F**: GACCTCAGATCAGACGTGGC	R28S rRNAss	429 bp	1. Initial denaturing 94°C, 3 min 2. Denaturing: 94°C, 30 sec 3. Annealing: 58°C, 30 sec 4. Synthesis: 72°C, 30 sec 5. Go to step 2, 19 times 6. Final extension: 70°C, 10 min
	R: ACCTCTTAACGGTTTCACGCC	R28S rRNAas429		

2.5 Western blot

2.5.1 Cytosolic and nuclear protein extraction

Following treatment, PC12 cells were washed once with 1 mL of cold 1X PBS. Cells were then scraped off the plate using 1.5 mL of cold 1X PBS and cell scrapers, and collected into 1.5 mL microcentrifuge tubes. The cells were pelleted by centrifugation at 13,000 rpm for 10 sec at 4°C, and supernatant was removed. Cells were resuspended in 200 µL of lysis buffer A for cell swelling (10 mM HEPES-KOH [pH 7.9], 1.5 mM $MgCl_2$, 10 mM KCl, 10 mM dithiothreitol [DTT], 0.2 mM phenylmethylsulfonyl fluoride [PMSF] and protease inhibitor in H_2O) for 10 min on ice. The sample was drawn into a 1 mL syringe with a 22-gauge needle, and force ejected into the tube 10 times. Next, samples were vortexed for 10 sec, centrifuged at 13,000 rpm for 10 sec at 4°C, and the supernatant containing cytosolic protein extract was collected into a 1.5 mL microcentrifuge tube. Nuclear protein extract was then prepared by hypotonic lysis in which nuclei were resuspended in 50 µL of lysis buffer C (20 mM HEPES-KOH [pH 7.9], 1.5 mM $MgCl_2$, 420 mM NaCl, 25% glycerol, 0.2 mM EDTA, 0.5 mM DTT, 0.2 mM PMSF and protease inhibitor cocktail in H_2O) and incubated on ice for 20 min for high salt extraction. Following incubation, nuclei were centrifuged at 13,000 rpm for 2 min at 4°C, and supernatant containing nuclear protein extract was collected into a 1.5 mL microcentrifuge tube.

Protein concentration for cytosolic and nuclear extracts was determined using the Bradford method. This assay employed a protein standard made with immunoglobulin G (IgG) antibody ranging from 1-20 µg. These standards, as well as sample dilutions, were plated in a total well volume of 20 µL in a 96-well, clear plate, and incubated for 5 min at room temperature with 250 µL of 1X protein assay dye reagent concentrate. The absorbance was measured at a wavelength of

595 nm using the PowerWave XS microplate spectrophotometer, and analyzed using KC4 software. Samples were then stored at -20°C.

2.5.2 Sample preparation

Cytosolic and nuclear protein samples were prepared by adding 15-40 µg of protein to a mixture of 6X loading dye (300 mM Tris-HCL, 12% sodium dodecyl sulfate [SDS], 12 mM EDTA, 6% β-mercaptoethanol, 60% glycerol, 6% bromophenol blue, pH 6.8), and respective lysis buffer, to a volume of 60 µL. For cytosolic extracts, 0.1 M DTT was also added. Cytosolic and nuclear samples were then denatured by heating to 95°C for 15 and 5 min on a block heater, respectively.

2.5.3 Gel electrophoresis

Samples were loaded onto an SDS polyacrylamide 4% stacking gel (3.2 mL H_2O, 0.5 mL 40% acrylamide/bis-acrylamide [37.5:1] solution, 1.25 mL stacking buffer [0.5 M Tris-HCl, 8 mM EDTA, 0.4% SDS, pH 6.8], 50 µL 10% SDS, 50 µL ammonium persulfate [APS] and 10 µL tetramethylethylenediamine [TEMED]), and a 10% resolving gel (4.9 mL H_2O, 2.5 mL 40% acrylamide/bis-acrylamide [37.5:1] solution, 2.5 mL resolving buffer [1.5 M Tris-HCl, 8 mM EDTA, 0.4% SDS, pH 8.8], 100 µL APS and 10 µL TEMED). This gel was placed in 1X running buffer (25 mM Tris, 192 mM glycine, 0.1% SDS) between 1.5 mm spaced plates with a 10-well comb. The samples loaded in the gel were electrophoresed at 100 V for 1.5 h to separate proteins based on their differences in molecular weight. 10 µl of PageRuler prestained protein ladder was loaded as a molecular weight marker.

2.5.4 Protein transfer

Proteins were transferred from the polyacrylamide gel electrophoresis (PAGE) gel to a polyvinylidene difluoride (PVDF) membrane. This was performed using a transfer cassette, and the immersed tank system containing 1X transfer buffer (48 mM Tris, 39 mM glycine, 0.037% SDS, 20% methanol), at 100 V for 1 h. Protein transfer was verified by Ponceau S stain, which reversibly binds to protein bands.

2.5.5 Antibody incubation

Membranes were blocked with 5% milk in Tris-buffered saline with Tween 20 (TBS-T; 10 mM Tris-HCl pH 8.0, 150 mM NaCl, 0.05% Tween-20) for 30 min at room temperature, with gentle agitation on the Belly Dancer. After washing with TBS-T (5 mL for 5 min at room temperature, 3x), the membrane was incubated with the appropriate primary antibody (5 mL, refer to Table 6) overnight at 4°C, with gentle agitation. Following incubation, membrane was washed with TBS-T (5 mL for 10 min at room temperature, 4x), and then incubated with appropriate horseradish peroxidase (HRP) conjugated secondary antibody (5 mL, refer to Table 7) for 1 h at room temperature, with gentle agitation. The secondary antibody is directed at a species-specific portion of the primary antibody.

Table 6: Primary antibodies.

Antibody	Vendor	Source	Dilution	Incubation period	Molecular weight
PNMT	Abcam ab69579 (Cambridge, United Kingdom) Lot# GR129455-1	Rabbit	1:1500 diluted in 5% milk in TBS-T	Overnight 4°C	31 kDa
TH	Novus Biologicals NB300-173 (Littleton, Colorado, USA) Lot# AJ0514y	Rabbit	1:4000 diluted in 5% milk in TBS-T	Overnight 4°C	62 kDa
DBH	Santa Cruz sc-7487 (Dallas, Texas, USA) Lot# I2006	Goat	1:250 diluted in 1% bovine serum albumin (BSA) in TBS-T	Overnight 4°C	69 kDa
GR	Santa Cruz sc-1004 Lot# H2712	Rabbit	1:250 diluted in 5% milk in TBS-T	Overnight 4°C	97 kDa
HIF1α	Novus Biologicals NB100-134 Lot# M-3	Rabbit	1:1000 diluted in 5% milk in TBS-T	Overnight 4°C	120 kDa
Egr1	Santa Cruz sc-189 Lot# G2114	Rabbit	1:250 diluted in 5% milk in TBS-T	Overnight 4°C	58 kDa
Sp1	Santa Cruz sc-59 Lot# E1414	Rabbit	1:250 diluted in 5% milk in TBS-T	Overnight 4°C	95 kDa
GAPDH	Abcam ab9245 Lot# GR232949-3	Mouse	1:10,000 diluted in 5% milk in TBS-T	Overnight 4°C	36 kDa
PCNA	Santa Cruz sc-56 Lot# A1113	Mouse	1:500 diluted in 5% milk in TBS-T	Overnight 4°C	36 kDa

Table 7: Secondary antibodies.

Antibody	Vendor	Source	Dilution	Incubation period
Anti-rabbit	Pierce Biotechnology (Waltham, Massachusetts, USA) Lot# IA110693	Goat	1:2000 diluted in 5% milk in TBS-T	1 h Room temperature
Anti-mouse	Santa Cruz sc-2005 Lot# B2014	Goat	1:2000 diluted in 5% milk in TBS-T	1 h Room temperature
Anti-goat	Santa Cruz sc-2768 Lot# J0713	Rabbit	1:2000 diluted in 1% BSA in TBS-T	1 h Room temperature

2.5.6 Enhanced chemiluminescence and autoradiography

Following a final wash with TBS-T (5 mL for 10 min at room temperature, 4x), proteins were detected by enhanced chemiluminescence (ECL) using ECL A (Tris-HCl pH 8.5, luminol, p-coumaric acid), and ECL B (Tris-HCl pH 8.5, 30% H_2O_2) in a 1:1 ratio. In a darkroom, these membranes were then exposed to CL-XPosure film, which were placed in an x-ray cassette. Exposure times were chosen to allow bands to be just under saturation. Films were developed using a SRX 101A Konica Film Processor and reagents as per the manufacturer's instructions. Densitometry of bands were then quantified by Quantity One software and the Bio-Rad UV ChemiDoc analyzer. Cytosolic and nuclear protein bands were normalized to glyceraldehyde 3-phosphate dehydrogenase (GAPDH), and proliferating cell nuclear antigen (PCNA), respectively.

2.5.7 Membrane stripping

A harsh membrane stripping protocol (Abcam) was followed in order to remove antibodies bound to proteins on the membrane, and re-probe with different antibodies. To do so, a harsh stripping buffer (10% SDS, 0.5 M Tris-HCl pH 6.8, β-mercaptoethanol and MilliQ H_2O) was added to a container enclosing the membrane and placed in a shaking H_2O bath for 30 min at 50°C. Buffer was then disposed, and the membrane rinsed with deionized (DI) H_2O. Membrane was washed with TBS-T (5 mL for 10 min at room temperature, 5x), and moved to a new container to avoid traces of β-mercaptoethanol. The membrane was then blocked in 5% milk with TBS-T for 30 min at room temperature with gentle agitation. After a final washing with TBS-T (5 mL for 10 min at room temperature, 4x), the primary antibody was incubated on membrane overnight at 4°C.

2.6 Analysis of phenylethanolamine N-methyltransferase promoter activation

2.6.1 Plasmid

A rat PNMT promoter luciferase reporter gene construct, pGL3RP893 (5731 bp), was previously generated by subcloning the *XhoI-HindIII* restriction fragment from pRP863LUC[127], a plasmid containing the rat PNMT proximal promoter sequence from -893 to +20 bp (913 bp), into the corresponding multiple cloning region of the pGL3 basic vector (4818 bp).

2.6.2 Bacterial transformation

The heat-shock method was performed by thawing artificially competent Douglas Hanahan 5α (DH5α) *Escherichia coli* (*E. coli*) cells on ice for 10 min. In a round bottom tube, 50 ng (0.2 µL pGL3RP893) was combined with 75 µL of competent DH5α cells, and the tube was flicked gently to mix. Following incubation on ice for 20 min, the tube was placed in 42°C H_2O bath (Isotemp 202) for 45 sec (heat shock), and then immediately placed back on ice for 2 min. Next, 1 mL of super optimal broth with catabolite repression (SOC) was added to the tube near a flame to ensure sterility. To help cells recover from stress, and to allow for plasmid expression, the tube was incubated in 37°C shaker incubator (Innova 42) at 250 rpm for 1 h. Using a glass plate spreader, 100 µL of the transformed bacteria was smeared evenly onto a Luria Bertani broth (LB) agar petri dish containing 100 µg/mL ampicillin, and placed in 37°C incubator for 18 h. Ampicillin is used in order to select for the cells that have acquired the plasmid. Therefore, only transformed cells that have acquired pGL3RP893 are able to grow on the plates. Using a pipette tip, colonies were scraped off the LB agar, and inoculated in 5 mL of LB containing 100 µg/mL ampicillin in round bottom tubes. These tubes were then placed in a 37°C shaker incubator at 250 rpm for 18 h.

The contents of the most turbid tubes (turbidity indicating sufficient bacterial growth) were transferred into a flask containing 100 mL of LB with 100 µg/mL ampicillin, which was subsequently placed into a 37°C shaker incubator at 250 rpm for 10 h. Finally, 100 mL of growing bacteria was transferred into 1 L of LB with 100 µg/mL ampicillin, and then into a 37°C shaker incubator at 250 rpm for 16 h.

2.6.3 Plasmid extraction

Plasmid DNA was extracted from DH5α cells using the PureLink HiPure Plasmid DNA Purification Maxipreps Kit as per the manufacturer's instructions. The purification is based on an anion-exchange chromatography using a column, containing a resin composed of small particles with uniform pore size. Following the extraction, the NanoDrop spectrophotometer was used to measure the concentration of DNA in the sample. A yield of approximately 450 µg in 100 µL volume was obtained. Plasmid concentration was then diluted further in TE buffer (10 mM Tris-HCl, pH 8.0 and 0.1 mM EDTA) to produce a final concentration of 1 µg/µL. Plasmid was then stored at 4°C until further use.

2.6.4 Restriction enzyme digest

To validate that the plasmid was correctly isolated, a restriction enzyme double digest was performed with restriction endonucleases to cleave DNA within a specific nucleotide sequence at a restriction site (Figure 5). To do so, pGL3RP893, restriction enzymes, 10X buffer, and MilliQ H_2O was added to a 0.2 mL PCR tube, and samples were incubated for 1 h at 37°C in thermocycler (Table 8). Following incubation, 6X loading buffer (30% glycerol and 0.25% bromophenol blue) was added, and samples were resolved on 1% TAE agarose gel with 10 µL ethidium bromide (10

mg/mL) per 200 mL of solution for a final concentration of 0.5 µg/mL. 10 µL of 1 kbp DNA ladder was loaded as a molecular weight marker.

Table 8: Restriction digest of pGL3RP893 and expected products.

Sample	Plasmid	Restriction enzyme	Buffer	MilliQ H_2O	Expected products
Uncut	1 µL	-	-	19 µL	Supercoiled: > 5731 bp Nicked: < 5731 bp
BamHI and HindIII	1 µL	1 µL of each	2 µL of NEBuffer 3.1	15 µL	3780 bp 1951 bp
HpaI and HindIII	1 µL	1 µL of each	2 µL of NEBuffer 4	15 µL	3882 bp 1849 bp

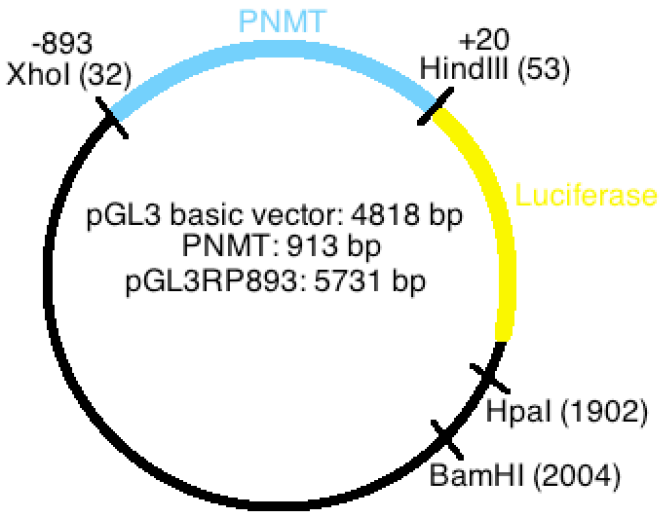

Figure 5: pGL3RP893 and restriction sites.

2.6.5 Transfection

A polyethylenimine (PEI)-mediated transient transfection[183] was performed using linear PEI, which is a cationic polymer containing repeating units composed of all secondary amine groups, and a two carbon aliphatic CH_2CH_2 spacer. PEI condenses DNA into positively charged particles, which bind to anionic cell surface residues, transporting DNA into the cell via

endocytosis. Once inside the cell, protonation of the amines of PEI results in an influx of counter-ions, and a lowering of the osmotic potential, which ultimately results in osmotic swelling and a bursting of the vesicle, releasing the polymer-DNA complex into the cytoplasm. Once this complex unpacks, the plasmid is able to freely diffuse into the nucleus. In order to determine the transfection time, the ratio of DNA to PEI, and the PEI type, the protocol was first worked out using 1 μg/μL pTracer cytomegalovirus (CMV) 2 green fluorescent protein (GFP) mammalian expression vector in 150 mM NaCl. This transfection was then visualized using microscopy to ensure its success. Following 24 h of transfection, 3.7% paraformaldehyde (2 mL), 0.2% Triton X-100 (1 mL), and 1:5000 4'6-diamidino-2-phenylindole (DAPI; 200 μL) was added to each well (6-well plate). Coverslips were mounted using a drop of PermaFluor mounting medium, and viewed on Zeiss Axioplan 2 Imaging Microscope. All images were focused for GFP, using the 40X objective, and images taken with the 63X oil objective. Finally, the percentage of transfected cells was calculated by determining the number of GFP-expressing cells divided by the number of DAPI expressing cells, and multiplying by 100.

The transfection was performed by diluting 1 μg of pGL3RP893 in 16 μL of 150 mM NaCl in a 15 mL conical tube, and diluting 4 μL of 10 mM linear PEI in 13 μL NaCl in a 1.5 microcentrifuge tube. Both tubes were incubated for 10 min at room temperature. Next, the contents of the microcentrifuge tube (PEI mixture) was added to the contents of the conical tube (DNA mixture), vortexed immediately, and this 1 DNA:4 PEI mixture was incubated for 10 min at room temperature. Lastly, 466 μL of CTM was added to create a mixture of PEI-DNA-NaCl-CTM with a total volume of 0.5 mL. In the meantime, medium was removed from the cells, and they were washed once with PBS. The transfection mixture was added directly to each well containing PC12 cells, and incubated for 3 h, after which it was carefully removed and replaced

with 1 mL of CTM for 21 h (24 h total transfection time), and incubated at 37°C and 5% CO_2-95% air. Once transfection was complete, treatments with either chemical agent or hypoxia were conducted as outlined in Table 3 and 4.

2.6.6 Luciferase assay

The reporter vector pGL3 basic contains the *luc*+ modified luciferase gene from the firefly *Photinus pyralis*, which encodes a 61 kDa enzyme that oxidizes D-luciferin in the presence of adenosine triphosphate (ATP), O_2, and Mg^{2+}, yielding oxyluciferin in an electronically excited state. This reaction releases a photon of light, as oxyluciferin returns to the ground state. This method allows the assessment of PNMT promoter activity by an indirect measure of released light[49].

Following treatment, medium was removed from transfected cells, and washed with 1 mL cold 1X PBS. Next, 100 µL of 1X cell lysis reagent (25 mM Tris-phosphate pH 7.8, 2 mM DTT, 2 mM 1,2-cyclohexylenedinitrilotetraacetic acid (CDTA), 10% glycerol, and 1% Triton X-100) was added to each well, and stored at -80°C for at least 1 h. Plates were then thawed at room temperature on the Belly Dancer, and then transferred to a 96-well, clear, v-shaped bottom plate, and centrifuged at 3,000 rpm for 10 min at 4°C to separate out the cellular debris. Next, 20 µL of cleared cell lysate was transferred to a 96-well, white, round-shaped bottom plate, and 50 µL of luciferase assay buffer (2X luciferase cocktail [40 mM tricine, 2.14 mM $MgCO_3 \cdot 5H_2O$, 5.34 mM $MgSO_4$, and 0.2 mM EDTA], 5X luciferin-DTT [2.35 mM D-luciferin potassium salt and 166.5 mM DTT], 100X coenzyme A [27 mM coenzyme A sodium salt] and 200X ATP [0.1 M ATP sodium salt]) was injected into each well. Luciferase activity was determined using the FLUOstar Optima microplate luminometer. Total protein in the lysate was determined by Bradford method,

and luciferase activity was then adjusted for protein concentration to correct for variations in cell density in each well of the 24-well cell culture plate. Luciferase activity was expressed as relative light units (RLU) per μg protein.

2.7 Reactive oxygen species assay

The DCFDA Cellular ROS Detection Assay Kit was used to measure intracellular ROS activity. This kit uses the cell permeant reagent 2'7'-dichlorofluorescin diacetate (DCFH-DA), a fluorogenic dye. Once the dye diffuses into the PC12 cells, cellular esterases deacetylate DCFH-DA to a non-fluorescent compound (DCFH). This compound is then oxidized by ROS into 2'7'-dichlorofluorescein (DCF), a highly fluorescent compound with maximum excitation (Ex) spectra of 495 nm and maximum emission (Em) spectra of 529 nm. Following the protocol of this kit, 100 μL of 1X buffer (Hank's buffered salt solution [HBSS]) was added to each well. 1X buffer was removed, cells were stained by adding 100 μL per well of 25 μM DCFDA solution, and cells were incubated for 45 min at 37°C in the dark. Following incubation, DCFDA solution was removed, and cells were washed with 100 μL/well of 1X buffer, followed by 100 μL of CTM for the duration of treatment. Plate was then measured at Ex/Em of 485/535 nm on a fluorescence plate reader.

2.8 Statistical analyses

All data are presented as the mean ± standard error mean (SEM; n=3-9). Fold change differences were calculated between normoxia control and treated cells. Statistical significance between experimental and control groups was determined by one-way analysis of variance (ANOVA), followed by post-hoc comparisons using Tukey's multiple comparison test, which compares all possible pairs of means based on a studentized range distribution (q), and then

identifies any difference between two means that is greater than the expected standard error. When only two treatment groups were being analyzed, statistical significance was determined by unpaired two-tailed t-test with Tukey's correction, which is a single-step multiple comparison test. Calculated p-values of $p \leq 0.05$ (95% confidence interval) were considered statistically significant. Statistical and graphical analysis was performed using GraphPad Prism.

Chapter 3: Results

3.1 Objective 1: Regulation of catecholamine biosynthesis enzymes by intermittent hypoxia

PC12 cells were treated for 1 h or 8 h with IH, and transcript levels of TH, DBH, and both intron-retaining and intronless PNMT were measured using RT-PCR in order to determine the effects of IH on expression of the CA biosynthesis enzymes in adrenal chromaffin cells. Transcript levels were compared to PC12 cells in normoxia (control). Additionally, PC12 cells were exposed to 8 h of IH, and cytosolic protein levels of these three enzymes were measured using Western blot analysis to determine the effects of IH on protein translation and/or protein stability of the CA biosynthesis enzymes.

3.1.1 Tyrosine hydroxylase

Results from the RT-PCR analysis of PC12 cells exposed for 1 or 8 h with IH show specific changes in TH mRNA (Figure 6-A). IH_{1h} increased TH mRNA levels by 1.45-fold ($p \leq 0.05$), and these levels remained elevated for 8 h of IH (1.56-fold; $p \leq 0.05$), in comparison to cells exposed to normoxia (Figure 6-E). At the protein level, IH_{8h} elevated TH cytosolic protein by 4.74-fold ($p \leq 0.0001$).

3.1.2 Dopamine β-hydroxylase

Results from the RT-PCR analysis of PC12 cells exposed for 1 or 8 h with IH show specific changes in DBH mRNA (Figure 6-B). IH_{1h} increased DBH mRNA levels by 1.54-fold ($p \leq 0.05$), and these transcript levels were further increased by 2.41-fold when exposed to the longer duration

of IH_{8h} ($p \leq 0.0001$), compared to normoxia control. These mRNA levels are also reflected by the elevation in DBH cytosolic protein expression levels following IH_{8h} (1.61-fold; $p \leq 0.0001$; Figure 6-F).

3.1.3 Phenylethanolamine N-methyltransferase

Results from the RT-PCR analysis of PC12 cells exposed for 1 or 8 h with IH show specific changes in PNMT mRNA. IH_{1h} increased intron-retaining PNMT mRNA by 2.77-fold ($p \leq 0.0001$), and IH_{8h} further elevated these levels (5.06-fold; $p \leq 0.0001$), compared to normoxia (Figure 6-C). In contrast, only IH_{1h} increased intronless PNMT mRNA, and this fold change (1.29-fold; $p \leq 0.05$) was much more inappreciable compared to the effect of IH on the intron-retaining form of PNMT (Figure 6-D). At the protein level, PNMT cytosolic protein was significantly elevated following IH_{8h} (2.29-fold; $p \leq 0.0001$), compared to normoxia-exposed cells (Figure 6-G).

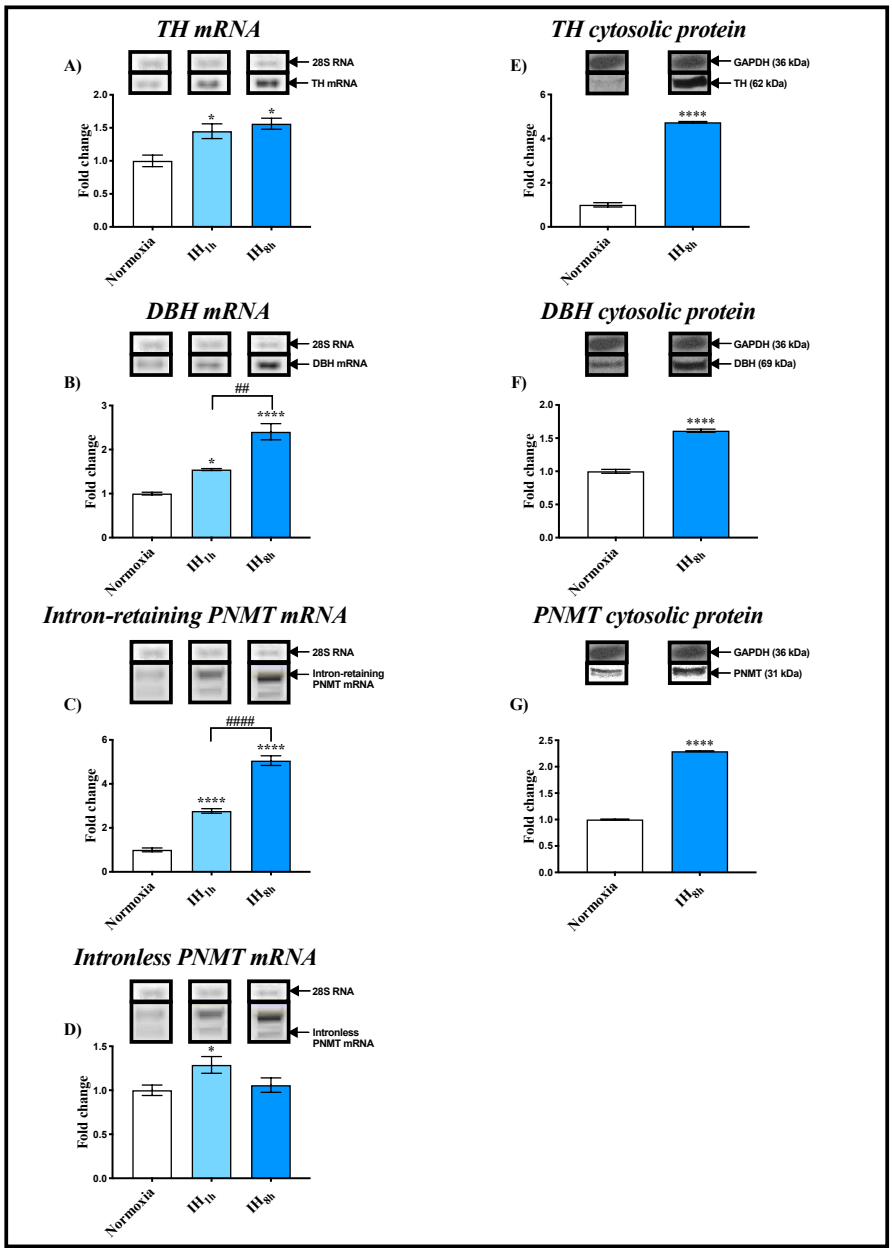

Figure 6: Gene and protein expression of catecholamine biosynthesis enzymes after time-variable treatment of PC12 cells with intermittent hypoxia. Image shows mRNA levels of TH (A), DBH (B), intron-retaining PNMT (C), and intronless PNMT (D), as well as cytosolic protein levels of TH (E), DBH (F), and PNMT (G), detected by RT-PCR and Western blotting, respectively. For transcript levels, PC12 cells were exposed to either IH_{1h} or IH_{8h}. For protein expression levels, PC12 cells were exposed to IH_{8h} only. Image shown above its respective graph is the representative gel bands of each treatment. Fold changes were normalized to untreated controls. mRNA and protein data were normalized to 28s RNA and GAPDH, respectively. One-way ANOVA with a post-hoc Tukey test was used for analyzing transcript levels, and unpaired two-tailed t-test with Tukey's correction was used for analyzing protein levels. Data are presented as mean ± SEM (n = 3). *, **, ***, and **** indicate significance from untreated controls where $p \leq 0.05$, $p \leq 0.01$, $p \leq 0.001$, and $p \leq 0.0001$ respectively. All other significant differences between groups are bracketed using the following symbol #.

3.2 Objective 2: Mechanisms involved in the transcriptional regulatory effects and phenylethanolamine N-methyltransferase promoter activation by intermittent hypoxia

To analyze the mechanism by which IH can elevate PNMT transcription, the effects of IH on the transcriptional machinery involved in PNMT promoter activation was investigated. PC12 cells were treated for 1 h or 8 h with IH, and transcript levels of HIF1α, Egr1, Sp1, and GR were measured using RT-PCR in order to determine the effects of IH on the expression of the known transcription factors of the PNMT promoter in adrenal chromaffin cells. Transcript levels were compared to PC12 cells in normoxia (control). Additionally, PC12 cells were exposed to 8 h of IH, and nuclear protein levels of these four transcription factors, as well as the cytosolic levels of GR were measured using Western blot analysis to determine the effects of IH on protein translation and/or protein stability of the transcription factors known to act on the promoter of the CA biosynthesis enzymes. Finally, to determine if IH-induced regulation of PNMT transcript levels are caused by changes in promoter activation, a PNMT promoter-driven luciferase vector was used. PC12 cells were transfected with the PNMT promoter-driven luciferase vector, pGL3RP893, prior to treatment with IH for 8 h. Results from this study show that IH has strong transcriptional effects on PNMT promoter activation.

3.2.1 Hypoxia-inducible factor 1α

Results from the RT-PCR analysis of PC12 cells exposed for 1 or 8 h with IH show specific changes in HIF1α mRNA (Figure 7-A). IH_{1h} elevated HIF1α mRNA by 1.94-fold ($p \leq 0.01$), and these levels remained elevated following the duration of IH_{8h} (1.76-fold; $p \leq 0.01$), compared to normoxic cells. Furthermore, results from the Western blot analysis show similar results to RT-

PCR. IH_{8h} increased HIF1α nuclear protein by 3.35-fold ($p \leq 0.0001$), compared to control (Figure 7-E).

3.2.2 Early growth response protein 1

There were significant increases in Egr1 transcript levels when PC12 cells were exposed to either IH_{1h} (1.43-fold; $p \leq 0.05$) or IH_{8h} (1.36-fold; $p \leq 0.05$), compared to normoxia (Figure 7-B). The fold changes produced in the Egr1 nuclear protein levels were much larger, with IH_{8h} causing a 3.12-fold increase ($p \leq 0.0001$), compared to cells exposed to normoxia (Figure 7-F).

3.2.3 Specificity protein 1

Treatment of PC12 cells with 1 and 8 h of IH caused significant increases in Sp1 transcript levels (Figure 7-C). IH_{1h} augmented Sp1 mRNA levels by 2.38-fold ($p \leq 0.0001$), and these levels remained significantly elevated following 8 h of IH (1.66-fold; $p \leq 0.01$), in comparison to normoxia-exposed cells. However, following IH_{8h}, the fold changes in Sp1 transcript levels was significantly decreased ($p \leq 0.01$) compared to the large induction by IH_{1h}. Although the Sp1 transcript levels after IH_{8h} were not as elevated as they were following IH_{1h}, the nuclear protein levels of Sp1 were still strongly increased by IH_{8h}, with a 4.00-fold change ($p \leq 0.0001$), compared to control (Figure 7-G).

3.2.4 Glucocorticoid receptor

Although IH_{1h} did not cause any induction in GR mRNA, the longer duration of IH_{8h} did produce a significant upregulation in GR transcript levels (1.82-fold; $p \leq 0.01$), compared to normoxia (Figure 7-D). Interestingly, IH_{8h} did not cause any change in GR nuclear protein (Figure

7-H), however it did produce a significant induction in the GR protein that is localized to the cytoplasm (1.86-fold; $p \leq 0.0001$; Figure 7-I).

3.2.5 Phenylethanolamine N-methyltransferase promoter activity

Before the transfection of the PNMT pGL3RP893 luciferase vector, the protocol to ensure success of transfection was refined and achieved using the pTracer CMV2 GFP vector. Immunofluorescent microscopy demonstrates the overlapping fluorescence of DAPI and GFP, and the localization of GFP to the cytoplasm in the transfected PC12 cells compared to control (Figure 8-A). Following the transfection of pGL3RP893 and exposure of cells to IH_{8h}, PNMT luciferase activity was significantly increased by 3.06-fold ($p \leq 0.0001$; Figure 8-B).

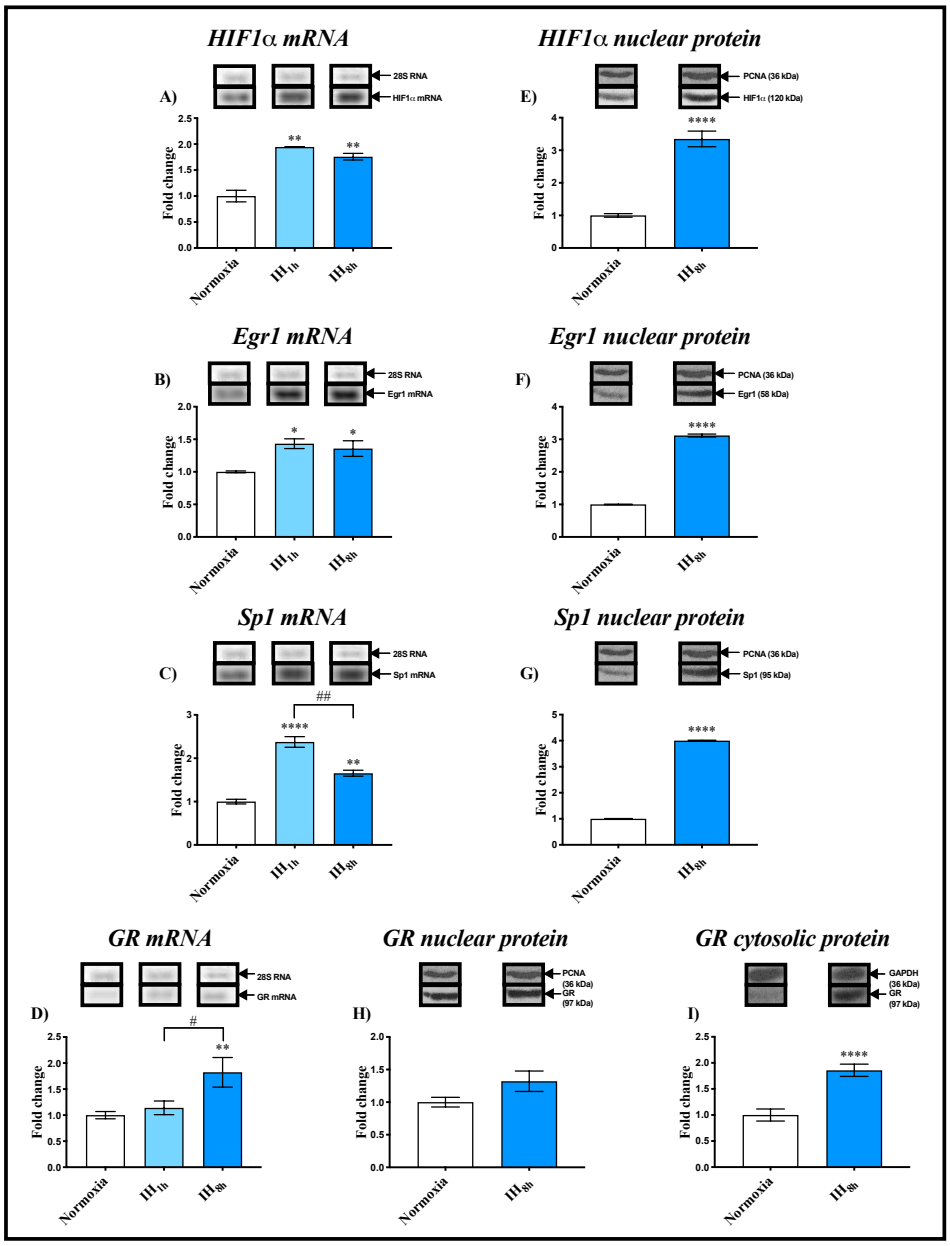

Figure 7: Gene and protein expression of transcriptional regulators after time-variable treatment of PC12 cells with intermittent hypoxia. Image shows mRNA levels of HIF1α (A), Egr1 (B), Sp1 (C), and GR (D), as well as nuclear protein levels of HIF1α (E), Egr1 (F), Sp1 (G), and GR (H), and cytosolic protein levels of GR (I) detected by RT-PCR and Western blotting, respectively. For transcript levels, PC12 cells were exposed to either IH_{1h} or IH_{8h}. For protein expression levels, PC12 cells were exposed to IH_{8h} only. Image shown above its respective graph is the representative gel bands of each treatment. Fold changes were normalized to untreated controls. mRNA and protein data were normalized to 28s RNA and GAPDH, respectively. One-way ANOVA with a post-hoc Tukey test was used for analyzing transcript levels, and unpaired two-tailed t-test with Tukey's correction for analyzing protein levels. Data are presented as mean ± SEM (n = 3). *, **, ***, and **** indicate significance from untreated controls where $p \leq 0.05$, $p \leq 0.01$, $p \leq 0.001$, and $p \leq 0.0001$ respectively. All other significant differences between groups are bracketed using the following symbol #.

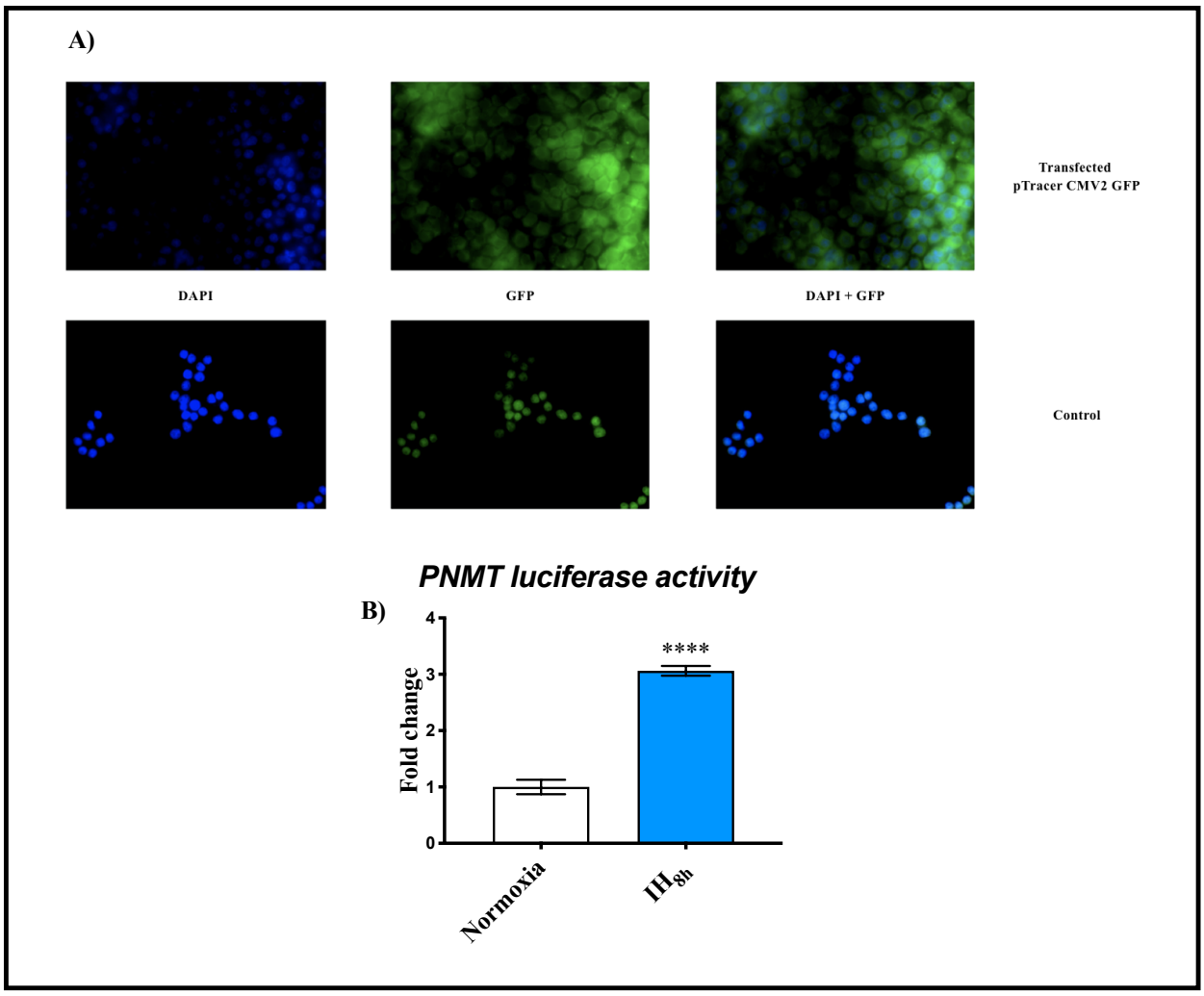

Figure 8: Intermittent hypoxia regulation of phenylethanolamine N-methyltransferase promoter activation. PC12 cells were transfected with PNMT pGL3RP893 luciferase vector prior to treatment with IH_{8h}. To optimize transfection, immunofluorescent microscopy was used to visualize the success of transfection using pTracer CMV2 GFP. DAPI exhibits blue fluorescent emission, and is localized to the nucleus (A; left column). GFP exhibits green fluorescent emission, and is localized to the cytosol (A; middle column). Overlapping fluorescence of DAPI and GFP demonstrate the achievement of transfection of the plasmid (A; top panel), and only the nuclei stained in the control cells (A; bottom panel). A separate experiment was then carried out to assess luciferase activity, which was calculated relative to protein expression, and normalized to the normoxic sample. The fold change in the IH_{8h}-treated group relative to the normoxic group is represented graphically (B). Statistical significance between normoxia and IH_{8h} treatment was determined by unpaired two-tailed t-test with Tukey's correction. Data are presented as mean ± SEM (n = 3). **** indicates significance from untreated controls where $p \leq 0.0001$.

3.3 Objective 3: Compare the effects of intermittent hypoxia with similar duration of continuous hypoxia

As demonstrated above, PC12 cells exposed to IH_{8h} caused significant changes to CA biosynthesis enzymes and their transcription factors at the gene and protein level, as well as inducing PNMT promoter activation. Next, these effects were compared to cells exposed to similar duration of CH, to determine whether these two forms of hypoxia produced similar or different alterations in CA biosynthesis enzyme expression. PC12 cells were treated for 1 h or 8 h with IH or CH, and transcript levels of TH, DBH, both intron-retaining and intronless PNMT, HIF1α, Egr1, Sp1, and GR were measured using RT-PCR in order to compare the effects of CH with IH on the expression of the CA biosynthesis enzymes and their transcription factors in adrenal chromaffin cells. Additionally, PC12 cells were exposed to 8 h of IH or CH, and cytosolic protein levels of these three enzymes and GR, as well as nuclear protein levels of the four transcription factors were measured using Western blot analysis to compare the effects of CH with IH on protein translation and/or protein stability of the CA biosynthesis enzymes and their transcriptional machinery. Moreover, to compare the effects of CH with IH in terms of changes to transcription rate and promoter activation, the PNMT promoter-driven luciferase vector, pGL3RP893, was transfected into PC12 cells, followed by treatment with CH_{8h} or IH_{8h}.

3.3.1 Tyrosine hydroxylase

When the effects of both time points of IH exposure were compared to normoxia alone, they demonstrated modest, yet significant increases in TH mRNA. Similarly, both CH_{1h} and CH_{8h} caused a significant increase in TH mRNA levels by 2.16-fold ($p \leq 0.001$) and 1.86-fold ($p \leq 0.01$), respectively, compared to normoxic control (Figure 9-A). However, CH_{1h} produced a significantly

greater elevation in TH mRNA compared to IH_{1h} ($p \leq 0.05$). In contrast, Western blot analysis demonstrated the opposite, with IH_{8h} producing a significantly larger increase in TH cytosolic protein compared to CH_{8h} ($p \leq 0.0001$; Figure 9-E). Still, CH_{8h} did produce a significant elevation in TH protein with a 2.26-fold change, compared to normoxia alone ($p \leq 0.0001$).

3.3.2 Dopamine β-hydroxylase

RT-PCR analysis demonstrated that both CH_{1h} and CH_{8h} produced significant changes in DBH mRNA (Figure 9-B). CH_{1h} resulted in a 1.98-fold change ($p \leq 0.001$), whereas CH_{8h} caused a 1.60-fold increase in transcript levels ($p \leq 0.01$), compared to normoxia. When comparing these changes to similar durations of IH, the shorter duration of CH produced a more significant increase in DBH mRNA compared to IH_{1h} ($p \leq 0.05$). However, the opposite occurred with the longer duration of hypoxia, in which IH_{8h} produced a larger elevation in transcript levels compared to CH_{8h} ($p \leq 0.001$). Although there were significant differences in DBH mRNA levels between CH- and IH-exposed cells, these differences did not appear following Western blot analysis. CH_{8h} induced a 1.52-fold elevation in DBH cytosolic protein ($p \leq 0.0001$), compared to cells in normoxic conditions (Figure 9-F).

3.3.3 Phenylethanolamine N-methyltransferase

CH_{1h} produced a 1.78-fold increase ($p \leq 0.01$), and CH_{8h} caused a 1.40-fold increase ($p \leq 0.05$) in intron-retaining PNMT transcript levels, compared to normoxia-exposed cells (Figure 9-C). Although both time points of CH exposure produced significant increases in intron-retaining PNMT mRNA, both CH_{1h} and CH_{8h} were significantly lower than similar durations of IH ($p \leq 0.001$ and $p \leq 0.0001$, respectively). In contrast, intronless PNMT mRNA was not significantly

changed by either duration of CH, and CH effects were not significantly different from IH exposure effects (Figure 9-D). Following Western blot analysis, PNMT cytosolic protein was significantly elevated by CH_{8h} by 2.01-fold ($p \leq 0.0001$), compared to control (Figure 9-G). However, these protein levels caused by CH_{8h} exposure were significantly less compared to the elevation caused by IH_{8h} ($p \leq 0.0001$).

3.3.4 Hypoxia-inducible factor 1α

At the transcript level, CH_{1h} and CH_{8h} caused a significant increase in HIF1α mRNA by 1.54-fold ($p \leq 0.05$) and 1.48-fold ($p \leq 0.05$), respectively, compared to control (Figure 10-A). At the transcript level, there were no significant changes between CH- and IH-exposed cells. However, at the protein level, IH and CH caused significantly different fold changes. CH_{8h} resulted in a 2.12-fold change ($p \leq 0.05$) in HIF1α nuclear protein (Figure 10-E). However, IH_{8h} caused a significantly greater induction of HIF1α protein ($p \leq 0.01$).

3.3.5 Early growth response protein 1

Only the shorter duration of CH caused a significant increase in Egr1 mRNA, with a 1.44-fold change ($p \leq 0.05$), compared to normoxia-exposed cells (Figure 10-B). When comparing CH with IH, there were no significant differences at the transcript level between both forms of hypoxia. However, both time points of IH exposure caused significant increases in Egr1 mRNA, unlike CH. At the protein level, CH_{8h} resulted in a 2.00-fold increase in Egr1 nuclear protein ($p \leq 0.0001$), compared to control (Figure 10-F). However, the transcription factor elevation caused by IH was significantly higher than the increase caused by similar duration of CH ($p \leq 0.0001$).

3.3.6 Specificity protein 1

Both CH_{1h} and CH_{8h} caused significant increases at the transcript level of the transcription factor, Sp1 (Figure 10-C). The shorter duration of CH caused a 1.64-fold increase ($p \leq 0.01$), and the longer duration of CH caused a 1.63-fold change ($p \leq 0.01$), compared to normoxia. When comparing the effects of CH with IH, IH_{1h} produced a significantly greater elevation in Sp1 mRNA compared to similar duration of CH ($p \leq 0.01$). Following Western blot analysis, CH_{8h} resulted in a 2.19-fold increase in Sp1 nuclear protein ($p \leq 0.0001$), compared to normoxia (Figure 10-G). However, IH_{8h} caused a greater increase in protein levels compared to CH_{8h} ($p \leq 0.0001$).

3.3.7 Glucocorticoid receptor

Unlike the significant increase in GR mRNA caused by IH_{8h}, CH at both time points did not cause any significant changes in GR at the transcript level (Figure 10-D). Furthermore, even though neither IH nor CH produced any significant differences in GR nuclear protein, the change caused by CH_{8h} was significantly lower than the change in nuclear protein caused by IH_{8h} ($p \leq 0.05$; Figure 10-H). Interestingly, IH_{8h} did produce a strong elevation in GR cytosolic protein, whereas no change was produced following CH_{8h} (Figure 10-I). The elevation in GR cytosolic protein caused by IH_{8h} was therefore significantly greater than that caused by CH_{8h} ($p \leq 0.05$).

3.3.8 Phenylethanolamine N-methyltransferase promoter activity

Like IH_{8h}, similar duration of CH produced a significant elevation in PNMT luciferase activity. CH_{8h} caused a 2.45-fold change in this activity ($p \leq 0.0001$; Figure 11). However, the increase caused by IH_{8h} was significantly greater than that following CH_{8h} exposure ($p \leq 0.05$).

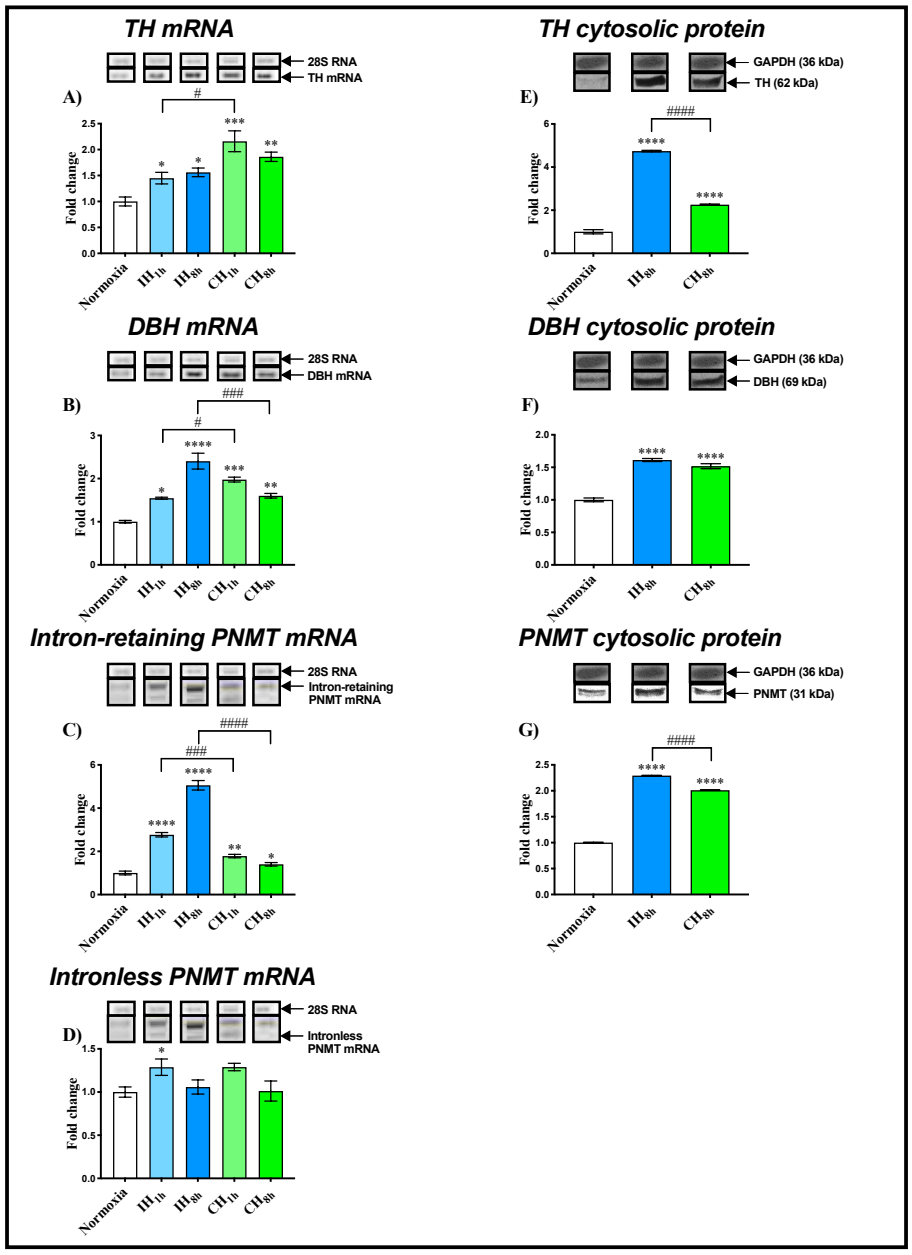

Figure 9: Comparing gene and protein expression levels of catecholamine biosynthesis enzymes after time-variable treatment of PC12 cells with intermittent hypoxia or continuous hypoxia. Image shows mRNA levels of TH (A), DBH (B), intron-retaining PNMT (C), and intronless PNMT (D), as well as cytosolic protein levels of TH (E), DBH (F), and PNMT (G), detected by RT-PCR and Western blotting, respectively. For transcript levels, PC12 cells were exposed to either IH_{1h}, IH_{8h}, CH_{1h}, or CH_{8h}. For protein expression levels, PC12 cells were exposed to IH_{8h} or CH_{8h}. Image shown above its respective graph is the representative gel bands of each treatment. Fold changes were normalized to untreated controls. mRNA and protein data were normalized to 28s RNA and GAPDH, respectively. One-way ANOVA with a post-hoc Tukey test was used for analyzing transcript and protein levels. Data are presented as mean ± SEM (n = 3). *, **, ***, and **** indicate significance from untreated controls where $p \leq 0.05$, $p \leq 0.01$, $p \leq 0.001$, and $p \leq 0.0001$ respectively. All other significant differences between groups are bracketed using the following symbol #.

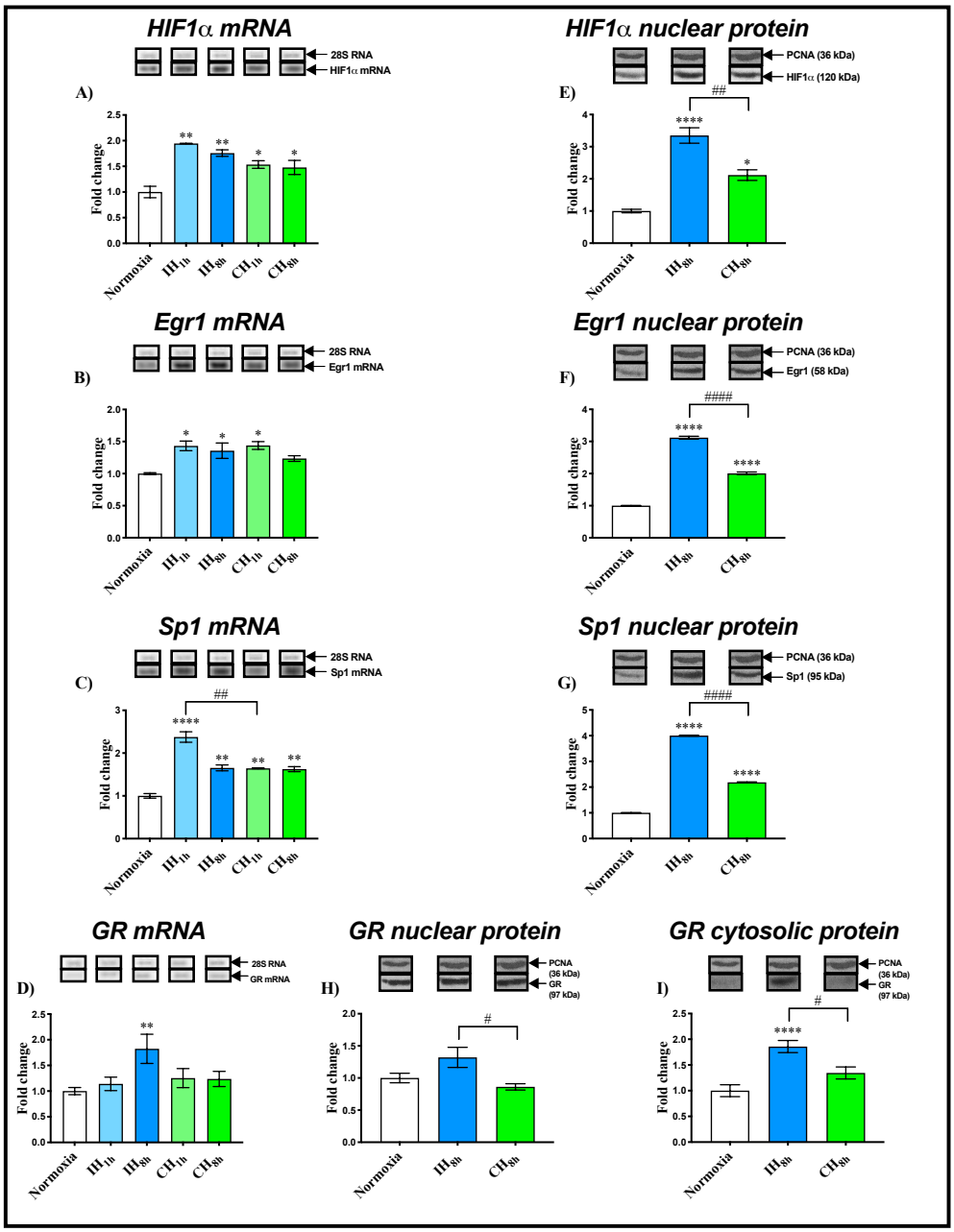

Figure 10: Comparing gene and protein expression of transcriptional regulators after time-variable treatment of PC12 cells with intermittent hypoxia or continuous hypoxia. Image shows mRNA levels of HIF1α (A), Egr1 (B), Sp1 (C), and GR (D), as well as nuclear protein levels of HIF1α (E), Egr1 (F), Sp1 (G), and GR (H), and cytosolic protein levels of GR (I) detected by RT-PCR and Western blotting, respectively. For transcript levels, PC12 cells were exposed to either IH_{1h}, IH_{8h}, CH_{1h}, or CH_{8h}. For protein expression levels, PC12 cells were exposed to IH_{8h} or CH_{8h}. Image shown above its respective graph is the representative gel bands of each treatment. Fold changes were normalized to untreated controls. mRNA and protein data were normalized to 28s RNA and GAPDH, respectively. One-way ANOVA with a post-hoc Tukey test was used for analyzing transcript and protein levels. Data are presented as mean ± SEM (n = 3). *, **, and **** indicate significance from untreated controls where $p \leq 0.05$, $p \leq 0.01$, and $p \leq 0.0001$ respectively. All other significant differences between groups are bracketed using the following symbol #.

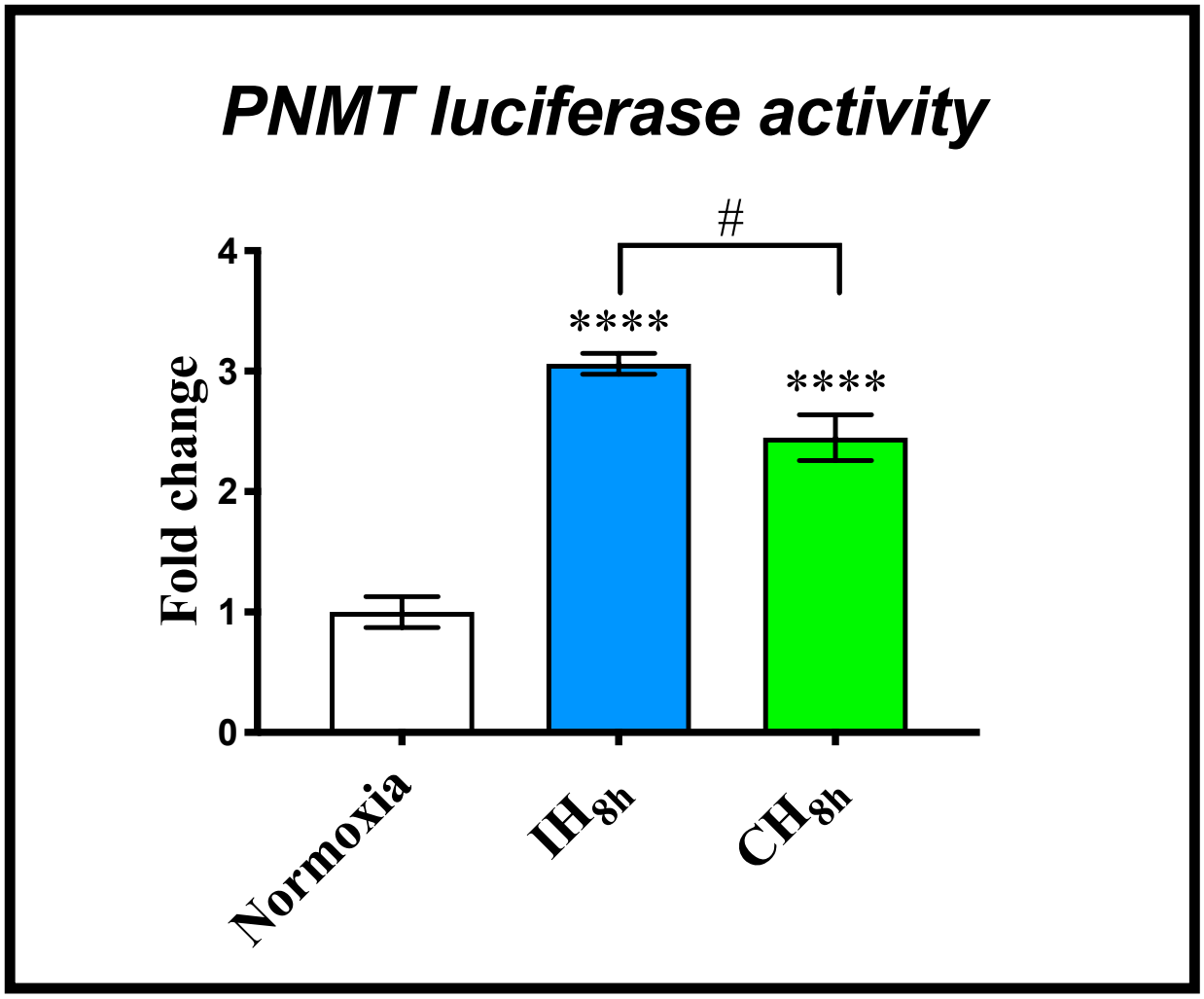

Figure 11: Comparing phenylethanolamine N-methyltransferase promoter activation by intermittent hypoxia or continuous hypoxia. PC12 cells were transfected with PNMT pGL3RP893 luciferase vector prior to treatment with IH_{8h} or CH_{8h}. Luciferase activity was calculated relative to protein expression, and normalized to the normoxic sample. The fold change in the IH_{8h}- and CH_{8h}-treated group relative to the normoxic group is represented graphically. Statistical significance between normoxia and hypoxia treatments was determined by one-way ANOVA with a post-hoc Tukey test. Data are presented as mean ± SEM (n = 3). * and **** indicate significance from untreated controls where $p \leq 0.05$ and $p \leq 0.0001$ respectively. All other significant differences between groups are bracketed using the following symbol #.

3.4 Objective 4: Signaling mechanisms and combination treatments involving cobalt chloride and dexamethasone

In the previous objectives above, it was shown that both forms of hypoxia upregulate the CA biosynthesis enzymes, as well as their known transcription factors. However, the extent to

which this elevation occurs is dependent on the type of hypoxia, and the duration of exposure. In order to further investigate the potential signaling mechanisms involved, as well as the potential for additive or synergistic interaction, we treated cells with a hypoxia mimetic agent, or a synthetic GC prior to exposing them to hypoxia as in Objective 2. PC12 cells were treated with 200 μM $CoCl_2$ or 1 μM Dex for 8 h. In addition, PC12 cells were also treated with the combination of drug treatment with IH or CH for 1 or 8 h. Transcript levels of TH, DBH, both intron-retaining and intronless PNMT, HIF1α, Egr1, Sp1, and GR were measured using RT-PCR to determine the effects of CH or IH, and their combination with signaling inducers, on the expression of the CA biosynthesis enzymes and their transcription factors in adrenal chromaffin cells. Interestingly, the condition with the combination of IH_{8h} and $CoCl_2$ resulted in extensive apoptosis of PC12 cells and were therefore omitted from all analyses (Figure 14).

3.4.1 Tyrosine hydroxylase

Following 8 h of $CoCl_2$ treatment, TH mRNA increased by 1.53-fold ($p \leq 0.05$), compared to cells exposed to normoxia (Figure 12-A). When $CoCl_2$ and IH_{1h} were in combination, a similar increase was observed (1.60-fold; $p \leq 0.05$). Either treatment of CH_{1h} or CH_{8h} with $CoCl_2$ also caused a comparable increase in TH transcript levels (1.62-fold and 1.53-fold, respectively; $p \leq 0.05$). Following 8 h of Dex treatment, TH mRNA significantly increased by 1.58-fold ($p \leq 0.05$), compared to normoxia. When in combination with IH_{1h}, IH_{8h}, or CH_{1h}, TH mRNA increased to a similar extent as Dex treatment alone (1.60-fold, 1.59-fold, and 1.60-fold, respectively; $p \leq 0.05$). Interestingly, the longer duration of CH with Dex caused a greater significant increase, compared to Dex treatment alone (1.98-fold; $p \leq 0.0001$).

3.4.2 Dopamine β-hydroxylase

Following 8 h of $CoCl_2$ treatment, DBH mRNA rose significantly by 1.73-fold ($p \leq 0.0001$) compared to control (Figure 12-B). Similarly, both IH_{1h} or CH_{1h} with $CoCl_2$ caused a corresponding increase in DBH transcript levels (1.62-fold and 1.59-fold, respectively; $p \leq 0.0001$). Although the combination of CH_{8h} with $CoCl_2$ caused a significant increase in mRNA (1.35-fold; $p \leq 0.001$), this increase was significantly lower than $CoCl_2$ alone ($p \leq 0.001$). Dex treatment alone, IH_{1h} and Dex, or IH_{8h} and Dex, all caused a significant elevation in DBH mRNA (1.48-fold, 1.43-fold, and 1.57-fold, respectively; $p \leq 0.0001$), compared to control. Similarly, CH_{1h} and Dex caused a 1.39-fold induction in DBH mRNA ($p \leq 0.001$), compared to normoxia. Interestingly, the combination of the longer duration of CH with Dex caused a significantly larger induction than Dex alone ($p \leq 0.0001$), producing a 2.14-fold change ($p \leq 0.0001$).

3.4.3 Phenylethanolamine N-methyltransferase

Like the expression levels of DBH mRNA, $CoCl_2$, IH_{1h} with $CoCl_2$, or CH_{1h} with $CoCl_2$ all caused a similar induction in intron-retaining PNMT mRNA (2.78-fold, 3.24-fold, and 3.25-fold, respectively; $p \leq 0.0001$), compared to control (Figure 12-C). However, the combination of CH_{8h} with $CoCl_2$ caused a more distinct increase in PNMT transcript levels compared to $CoCl_2$ alone ($p \leq 0.01$), producing a 3.64-fold change ($p \leq 0.0001$). Following 8 h of Dex treatment, there was no change in intron-retaining PNMT mRNA, compared to normoxia-exposed cells. Interestingly, the combination of Dex with IH_{1h}, IH_{8h}, or CH_{1h} all caused a more significant increase in intron-retaining PNMT mRNA compared to Dex treatment alone (2.73-fold, $p \leq 0.0001$; 3.24-fold, $p \leq 0.0001$; and 2.07-fold, $p \leq 0.01$, respectively). In striking contrast, the combination of Dex with CH_{8h} produced a significant decrease in intron-retaining PNMT mRNA,

which was significantly lower than Dex treatment alone ($p \leq 0.001$). When analyzing the intronless PNMT mRNA levels, the fold changes were overall, much smaller among the different treatment groups, with the exception of CH_{8h} and Dex (Figure 12-D). First, $CoCl_2$ treatment caused a 1.51-fold increase in the intronless form of PNMT compared to normoxia ($p \leq 0.01$). The combination of $CoCl_2$ treatment with IH_{1h} did not cause any change in this form of PNMT. Moreover, CH_{1h} with $CoCl_2$ resulted in significantly decreased intronless PNMT transcript compared to $CoCl_2$ alone (0.53-fold; $p \leq 0.0001$). CH_{8h} with $CoCl_2$ caused no change in intronless PNMT transcript, compared to normoxia. Unlike the intron-retaining form of PNMT, 8 h of Dex treatment caused a significant increase in intronless PNMT mRNA (2.62-fold; $p \leq 0.0001$), compared to normoxia. However, when IH_{1h} and Dex were in combination, there was no change in the intronless PNMT form. On the other hand, the longer duration of IH with Dex caused a similar induction in intronless PNMT mRNA (2.23-fold; $p \leq 0.0001$), as compared to Dex treatment alone. The shorter duration of CH with Dex also caused a relatively similar upregulation in transcript levels of the intronless PNMT form (1.99-fold; $p \leq 0.001$), compared to Dex treatment alone, whereas the longer duration of CH with Dex actually caused the most significant increase in intronless PNMT mRNA (5.03-fold; $p \leq 0.0001$). This combination treatment caused a more robust increase in transcript levels of the intronless PNMT form compared to Dex treatment alone ($p \leq 0.0001$), and this change demonstrated synergistic effects.

3.4.4 Hypoxia-inducible factor 1α

Following 8 h of $CoCl_2$ treatment, HIF1α mRNA increased by 1.89-fold ($p \leq 0.01$), compared to normoxia-exposed cells (Figure 13-A). When $CoCl_2$ was used in combination with IH_{1h}, it resulted in a 1.70-fold increase in HIF1α mRNA ($p \leq 0.05$). However, when CH was used

in combination with $CoCl_2$, it resulted in no change in HIF1α transcript levels. Unlike $CoCl_2$, Dex treatment resulted in no change to HIF1α mRNA levels. In addition, the only form of hypoxia in combination with Dex that resulted in a significant increase was CH_{1h}, which caused a 1.61-fold change ($p \leq 0.05$), and this caused a significantly greater elevation in mRNA levels compared to Dex alone ($p \leq 0.01$).

3.4.5 Early growth response protein 1

Egr1 mRNA levels increased significantly by 1.50-fold ($p \leq 0.001$) following 8 h of $CoCl_2$ treatment, compared to normoxia (Figure 13-B). When in combination with IH_{1h}, Egr1 transcript levels increased to a similar extent compared to $CoCl_2$ alone (1.54-fold; $p \leq 0.0001$). In contrast, CH_{1h} or CH_{8h} in combination with $CoCl_2$, caused a significantly greater elevation in Egr1 mRNA levels (1.95-fold and 2.10-fold, respectively; $p \leq 0.0001$) compared to $CoCl_2$ treatment alone ($p \leq 0.001$ and $p \leq 0.0001$, respectively). When analyzing effects of Dex treatment, 8 h of Dex resulted in a significant increase in Egr1 mRNA 1.53-fold ($p \leq 0.001$), compared to control. Similarly, IH_{1h}, IH_{8h}, CH_{1h}, or CH_{8h} in combination with Dex caused a significant increase in Egr1 transcript levels that was similar to that caused by Dex alone (1.39-fold, $p \leq 0.01$; 1.38-fold, $p \leq 0.01$; 1.39-fold, $p \leq 0.01$; and 1.51-fold, $p \leq 0.001$, respectively).

3.4.6 Specificity protein 1

Sp1 mRNA levels rose significantly by 1.78-fold ($p \leq 0.001$), 1.92-fold ($p \leq 0.001$), and 1.90-fold ($p \leq 0.0001$) when exposed to $CoCl_2$, IH_{1h} in combination with $CoCl_2$, or CH_{1h} and $CoCl_2$, respectively, compared to control (Figure 13-C). Interestingly, when $CoCl_2$ was used in combination with CH_{8h}, it resulted in no change to Sp1 transcript levels, and it produced

significantly lower levels compared to $CoCl_2$ treatment alone ($p \leq 0.01$). Treatment with 8 h of Dex resulted in a significant elevation in Sp1 mRNA by 2.04-fold ($p \leq 0.0001$), compared to normoxia. When in combination with IH_{1h} or IH_{8h}, the shorter duration of IH caused a 1.73-fold ($p \leq 0.001$), and the longer duration resulted in a 1.38-fold change ($p \leq 0.05$). Similarly, CH_{1h} and CH_{8h} caused a significant increase in Sp1 mRNA by 1.81-fold ($p \leq 0.0001$) and 1.43-fold ($p \leq 0.05$). Both the longer durations of hypoxia (IH_{8h} and CH_{8h}) resulted in a significantly lower elevation in mRNA compared to Dex treatment alone ($p \leq 0.001$).

3.4.7 Glucocorticoid receptor

Neither $CoCl_2$ alone, or in combination with either form of hypoxia caused any change in GR mRNA (Figure 13-D). In contrast, 8 h of Dex treatment caused a significant increase in GR mRNA by 2.09-fold ($p \leq 0.05$), compared to normoxia. Interestingly, when Dex was used in combination with either form of hypoxia, the GR transcript levels were comparable to the normoxic condition. In fact, CH_{8h} in combination with Dex resulted in significantly lower GR mRNA compared to Dex treatment alone ($p \leq 0.05$).

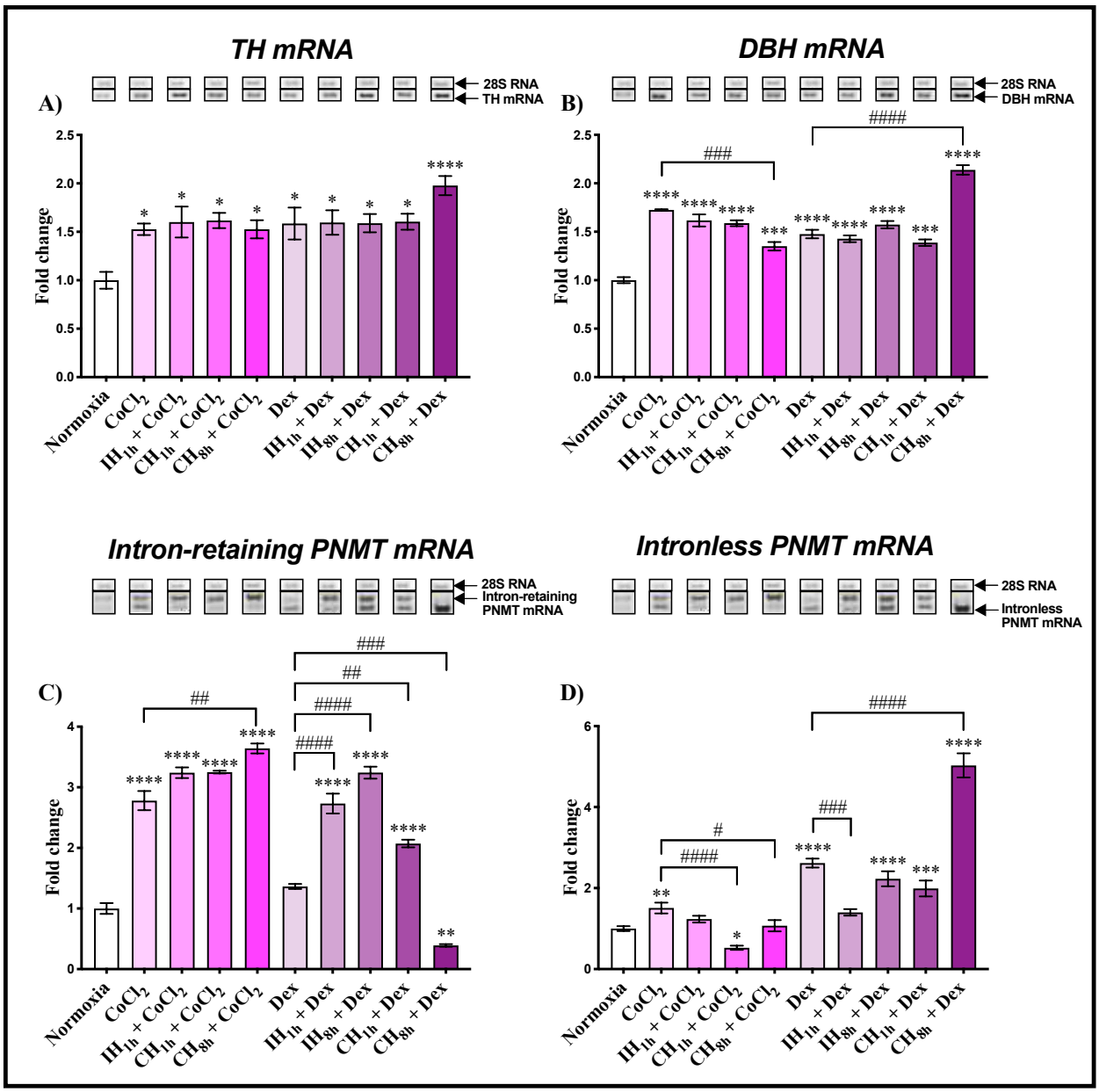

Figure 12: Gene expression of catecholamine biosynthesis enzymes after time-variable treatment of PC12 cells with the hypoxia mimetic agent (cobalt chloride) or the synthetic glucocorticoid (dexamethasone), and their combination with either intermittent hypoxia or continuous hypoxia. Image shows mRNA levels of TH (A), DBH (B), intron-retaining PNMT (C), and intronless PNMT (D) detected by RT-PCR. PC12 cells were exposed to either 200 µM $CoCl_2$ (8 h), 1 µM Dex (8 h), or the combination of drug treatment and hypoxia (IH_{1h}, IH_{8h}, CH_{1h}, CH_{8h}). Note that there is no representation of IH_{8h} with $CoCl_2$ treatment. Image shown above its respective graph is the representative gel bands of each treatment. Fold changes were normalized to untreated controls. mRNA data was normalized to 28s RNA. One-way ANOVA with a post-hoc Tukey test was used for analyzing transcript levels. Data are presented as mean ± SEM (n = 3). *, **, ***, and **** indicate significance from untreated controls where $p \leq 0.05$, $p \leq 0.01$, $p \leq 0.001$, and $p \leq 0.0001$ respectively. All other significant differences between groups are bracketed using the following symbol #.

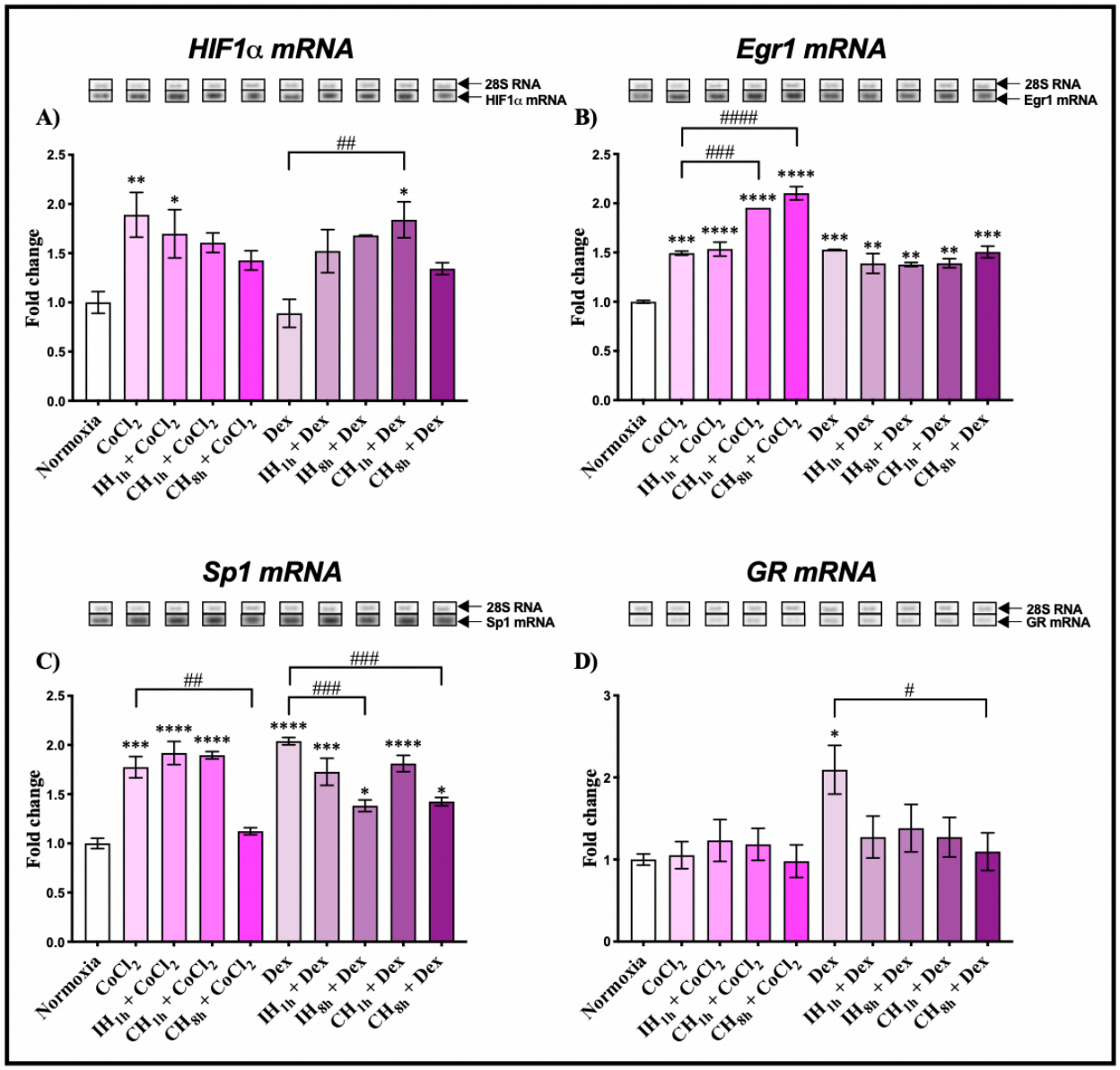

Figure 13: Gene expression of transcriptional regulators after time-variable treatment of PC12 cells with the hypoxia mimetic agent (cobalt chloride) or the synthetic glucocorticoid (dexamethasone), and their combination with either intermittent hypoxia or continuous hypoxia. Image shows mRNA levels of HIF1α (A), Egr1 (B), Sp1 (C), and GR (D) detected by RT-PCR. PC12 cells were exposed to either 200 µM $CoCl_2$ (8 h), 1 µM Dex (8 h), or the combination of drug treatment and hypoxia (IH_{1h}, IH_{8h}, CH_{1h}, CH_{8h}). Note that there is no representation of IH_{8h} with $CoCl_2$ treatment. Image shown above its respective graph is the representative gel bands of each treatment. Fold changes were normalized to untreated controls. mRNA data was normalized to 28s RNA. One-way ANOVA with a post-hoc Tukey test was used for analyzing transcript levels. Data are presented as mean ± SEM (n = 3). *, **, ***, and **** indicate significance from untreated controls where $p \leq 0.05$, $p \leq 0.01$, $p \leq 0.001$, and $p \leq 0.0001$ respectively. All other significant differences between groups are bracketed using the following symbol #.

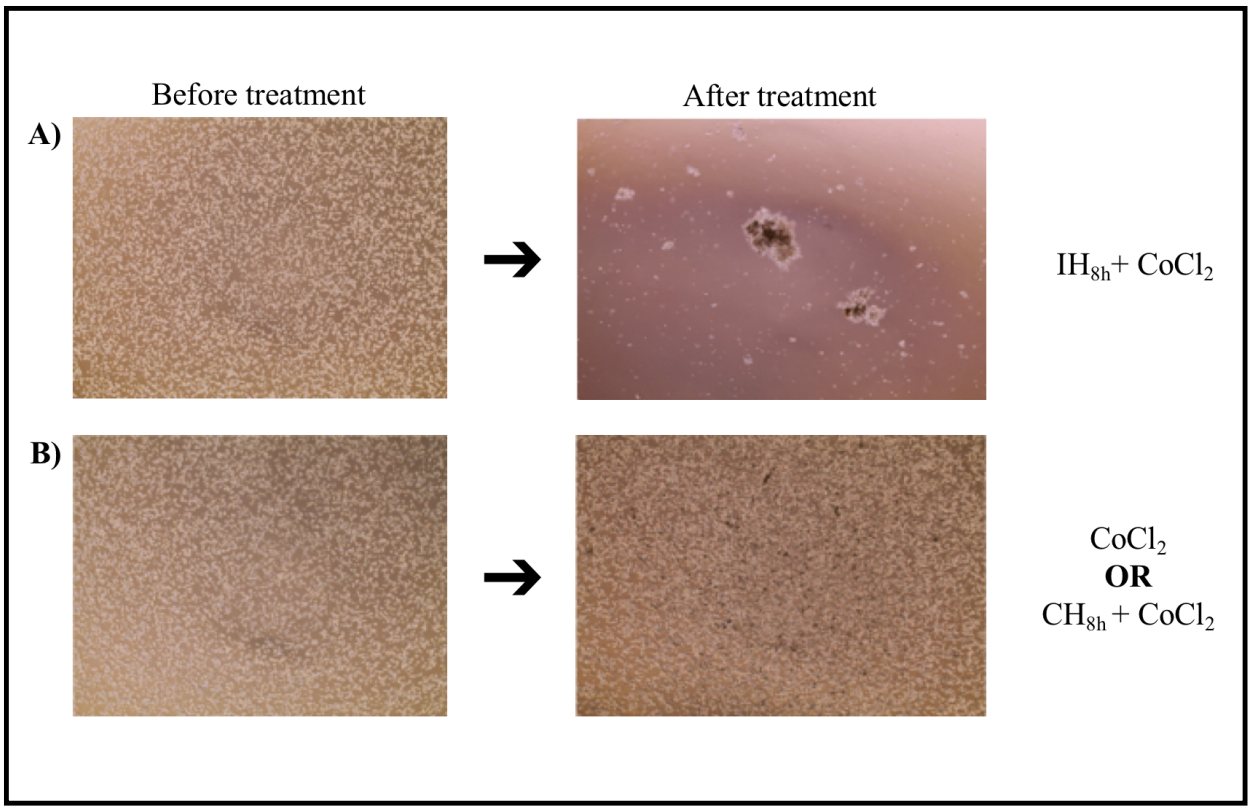

Figure 14: Apoptosis resulting from the combination of intermittent hypoxia and the hypoxia mimetic agent (cobalt chloride). The left column demonstrates PC12 cells before treatment while in normoxic conditions, and the right column shows the effects to confluency and integrity of PC12 cells following either the combination of 8 h of IH and $CoCl_2$ (panel A), or the treatment with either 8 h of $CoCl_2$ alone, or the combination of 8 h of CH and $CoCl_2$ (panel B).

3.5 Objective 5: Role of reactive oxygen species in intermittent hypoxia-evoked catecholamine biosynthesis enzyme expression via antioxidant and polyphenol pretreatment

A major feature that distinguishes IH from CH is the intervening periods of normoxia, where ROS are produced, resulting in increased oxidative stress[13]. In order to determine the role of ROS in the elevation of CA biosynthesis enzymes, their transcription factors, and PNMT promoter activation, expression levels with IH or CH were compared to those with antioxidant pretreatment. PC12 cells were first pretreated with 30 min of the chemical antioxidant, 5 mM NAC, and then treated with IH or CH for 1 h or 8 h, with continued antioxidant treatment for the remainder of the hypoxia exposure. Transcript levels of TH, DBH, and both intron-retaining and intronless PNMT, as well as HIF1α, Egr1, Sp1, and GR were measured using RT-PCR. Transcript levels were compared to PC12 cells in normoxia (control). Additionally, cytosolic protein levels of these three enzymes and GR, as well as nuclear protein levels of the four transcription factors were measured using Western blot analysis to determine the effects of NAC on protein expression.

3.5.1 Tyrosine hydroxylase

At the transcript level, NAC did not affect the fold change in TH mRNA in comparison to IH_{1h} or IH_{8h} alone (Figure 15-A). In contrast, the antioxidant was able to significantly lower mRNA to control levels in cells exposed to CH_{1h} ($p \leq 0.001$). NAC was ineffective at decreasing TH mRNA in cells exposed to the longer duration of CH. At the protein level, NAC was only able to significantly lower TH cytosolic protein expression levels in cells exposed to IH_{8h} ($p \leq 0.0001$), but was unable to reduce these levels in cells exposed to CH_{8h} (Figure 16-A).

3.5.2 Dopamine β-hydroxylase

At the transcript level, the antioxidant was effective in significantly decreasing DBH mRNA to normoxic control levels in IH_{1h}- and IH_{8h}-exposed PC12 cells ($p \leq 0.001$; Figure 15-B). However, NAC was only able to significantly decrease DBH transcript levels to basal expression levels in cells exposed to the shorter duration of CH ($p \leq 0.05$). At the protein level, NAC was only capable of reducing cytosolic protein levels in cells that were exposed to IH_{8h}, whereas it had no effect in cells exposed to CH_{8h} (Figure 16-B).

3.5.3 Phenylethanolamine N-methyltransferase

At the transcript level, NAC was only successful in decreasing the intron-retaining form of PNMT mRNA in PC12 cells that were exposed to the longer duration of IH ($p \leq 0.0001$), whereas it had no significant effect in cells exposed to either IH_{1h}, CH_{1h}, or CH_{8h} (Figure 15-C). As for the intronless form of PNMT, NAC was effective in decreasing mRNA levels in cells exposed to the shorter durations of either IH or CH ($p \leq 0.01$ and $p \leq 0.0001$, respectively), but was not able to do the same for cells exposed to the longer duration of either IH or CH (Figure 15-D). At the protein level, unlike the other CA biosynthesis enzymes, NAC was successful in lowering PNMT cytosolic protein in cells exposed to both forms of hypoxia ($p \leq 0.0001$; Figure 16-C).

3.5.4 Hypoxia-inducible factor 1α

At the transcript level, the synthetic antioxidant, NAC was only able to effectively decrease HIF1α mRNA to normoxia control levels in cells that were exposed to IH_{1h} ($p \leq 0.05$), whereas these levels were unchanged by NAC in cells that were exposed to IH_{8h}, CH_{1h}, or CH_{8h} (Figure 17-

A). At the protein level, NAC was capable of significantly lowering nuclear protein levels in cells that were exposed to IH_{8h} only ($p \leq 0.001$; Figure 18-A).

3.5.5 Early growth response protein 1

At the transcript level, NAC significantly decreased Egr1 mRNA expression levels to basal expression levels, as compared to cells exposed to IH_{1h} or IH_{8h} alone ($p \leq 0.01$ and $p \leq 0.05$, respectively; Figure 17-B). In distinct contrast, this antioxidant was unable to decrease Egr1 mRNA in cells that were exposed to either duration of CH. At the protein level, Egr1 nuclear protein levels significantly decreased with NAC pretreatment in cells that were exposed to IH_{8h} ($p \leq 0.0001$); however, in cells exposed to CH_{8h}, NAC was not only able to decrease Egr1 protein levels, it actually increased them ($p \leq 0.05$; Figure 18-B).

3.5.6 Specificity protein 1

Similar to Egr1, at the transcript level, Sp1 mRNA was significantly decreased by NAC in cells exposed to IH_{1h} and IH_{8h} ($p \leq 0.0001$ and $p \leq 0.001$, respectively; Figure 17-C). In addition, NAC was unable to effectively decrease Sp1 mRNA in cells exposed to either form of CH. The similarity between Sp1 and Egr1 also persisted when examining protein levels. NAC significantly decreased Sp1 nuclear protein in cells exposed to IH_{8h} ($p \leq 0.0001$), and again, actually increased nuclear protein levels in cells exposed to CH_{8h} ($p \leq 0.0001$; Figure 18-C).

3.5.7 Glucocorticoid receptor

As demonstrated in the results above, GR mRNA was only elevated significantly by IH_{8h}. When NAC was pretreated in cells exposed to IH_{8h}, it did not significantly decrease GR mRNA

levels, although the mRNA levels with NAC were reduced to basal expression levels (Figure 17-D). NAC did not cause any changes to the expression levels in cells treated with IH_{1h}, CH_{1h}, or CH_{8h}. Furthermore, as demonstrated above, GR nuclear protein levels were unchanged by either form of hypoxia, and NAC pretreatment did not affect these levels either (Figure 18-D). However, GR cytosolic protein levels were significantly elevated by IH_{8h} ($p \leq 0.0001$; Figure 18-E). NAC pretreatment did not significantly lower GR cytosolic protein levels in cells exposed to IH_{8h}, although it did reduce the fold change and its significance ($p \leq 0.01$). CH_{8h} did not elevate GR cytosolic protein levels, nor did NAC affect these fold changes.

3.5.8 Phenylethanolamine N-methyltransferase promoter activity

To determine the effects of ROS on PNMT promoter activation, chemical antioxidant pretreatment was applied to PC12 cells that were transfected with the PNMT promoter-driven luciferase vector, pGL3RP893, and then exposed to IH_{8h} or CH_{8h}. The results demonstrate that both forms of hypoxia can significantly increase PNMT promoter activity. However, when pretreated with the antioxidant, NAC, only the cells that were exposed to IH_{8h} were able to significantly decrease their PNMT activity to control levels as seen by the luciferase assay data ($p \leq 0.0001$; Figure 19). In contrast, cells that were pretreated with NAC and then exposed to CH_{8h} maintained their elevated PNMT promoter activity.

3.5.9 Reactive oxygen species and antioxidant/polyphenol pretreatment

Lastly, the levels of ROS were measured in PC12 cells following exposure to both forms of hypoxia. PC12 cells were stained with 25 μM DCFDA solution for 45 min, followed by treatment with either 200 μM $CoCl_2$ for 8 h, IH_{8h}, or CH_{8h}. Then, they were compared to IH_{8h}- or

CH_{8h}-treated cells that were pretreated with chemical antioxidant, NAC (5 mM), or three different polyphenols, namely 100 μM EGCG, 50 μM MG, or 1 μM TP. If ROS were produced in the culture media, they oxidized the deacetylated DCFDA compound, namely DCF, which is a highly fluorescent compound that was then measured by a fluorescence plate reader. Following 8 h of 200 μM $CoCl_2$ treatment, levels of ROS produced by PC12 cells increased significantly by 1.97-fold ($p \leq 0.0001$; Figure 20). Similarly, IH_{8h} significantly elevated ROS by 2.1-fold ($p \leq 0.0001$). Interestingly, pretreatment with the chemical antioxidant, NAC ($p \leq 0.001$), as well as pretreatment with the polyphenols, EGCG ($p \leq 0.001$), MG ($p \leq 0.0001$), or TP ($p \leq 0.01$) significantly decreased ROS to normoxia control levels. In contrast, CH_{8h} did not elevate ROS by PC12 cells as compared to cells in normoxia. Neither NAC, nor the three polyphenols significantly decreased ROS levels in CH_{8h}-treated cells.

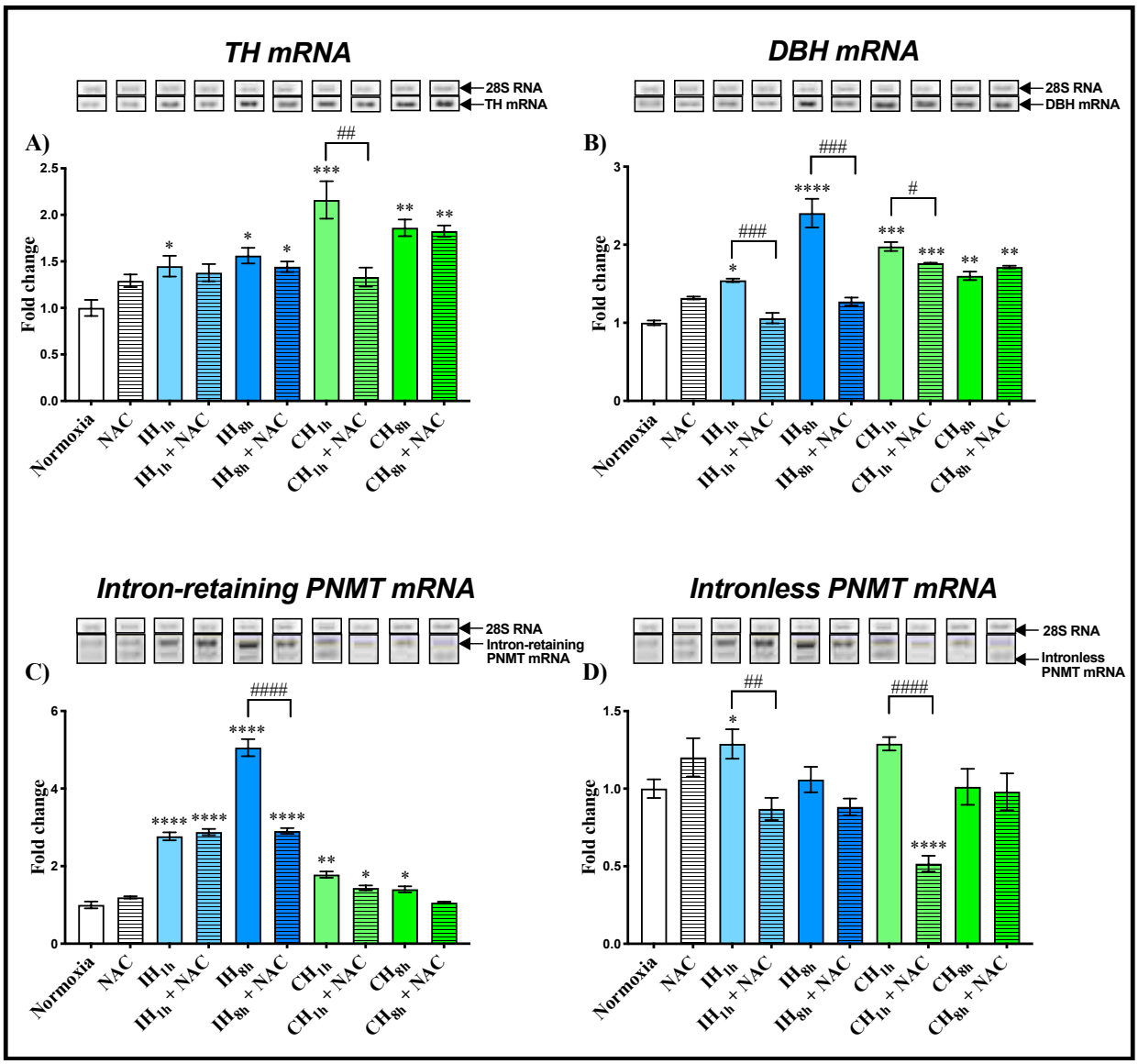

Figure 15: Gene expression of catecholamine biosynthesis enzymes after time-variable treatment of PC12 cells with intermittent hypoxia or continuous hypoxia, and the effects of antioxidant pretreatment. Image shows mRNA levels of TH (A), DBH (B), intron-retaining PNMT (C), and intronless PNMT (D) detected by RT-PCR. PC12 cells were exposed to either IH_{1h}, IH_{8h}, CH_{1h}, or CH_{8h}. These transcript levels were also compared to levels following antioxidant pretreatment with 5 mM NAC (30 min), and continued antioxidant treatment for the duration of hypoxia. Image shown above its respective graph is the representative gel bands of each treatment. Fold changes were normalized to untreated controls. mRNA data was normalized to 28s RNA. One-way ANOVA with a post-hoc Tukey test was used for analyzing transcript levels. Data are presented as mean ± SEM (n = 3). *, **, ***, and **** indicate significance from untreated controls where $p \leq 0.05$, $p \leq 0.01$, $p \leq 0.001$, and $p \leq 0.0001$ respectively. All other significant differences between groups are bracketed using the following symbol #.

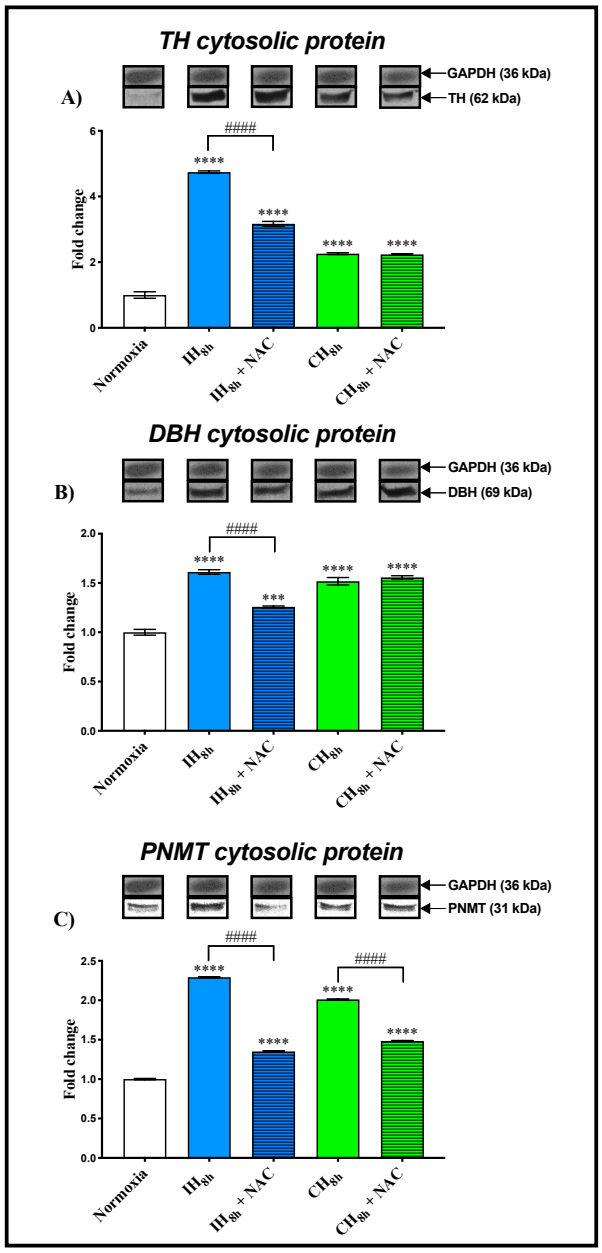

Figure 16: Protein expression of catecholamine biosynthesis enzymes after time-variable treatment of PC12 cells with intermittent hypoxia or continuous hypoxia, and the effects of antioxidant pretreatment. Image shows cytosolic protein levels of TH (A), DBH (B), and PNMT (C) detected by Western blotting. PC12 cells were exposed to either IH_{1h}, IH_{8h}, CH_{1h}, or CH_{8h}. These protein levels were also compared to levels following antioxidant pretreatment with 5 mM NAC (30 min), and continued antioxidant treatment for the duration of hypoxia. Image shown above its respective graph is the representative gel bands of each treatment. Fold changes were normalized to untreated controls. Protein data was normalized to GAPDH. One-way ANOVA with a post-hoc Tukey test was used for analyzing protein levels. Data are presented as mean ± SEM (n = 3). *, **, ***, and **** indicate significance from untreated controls where $p \leq 0.05$, $p \leq 0.01$, $p \leq 0.001$, and $p \leq 0.0001$ respectively. All other significant differences between groups are bracketed using the following symbol #.

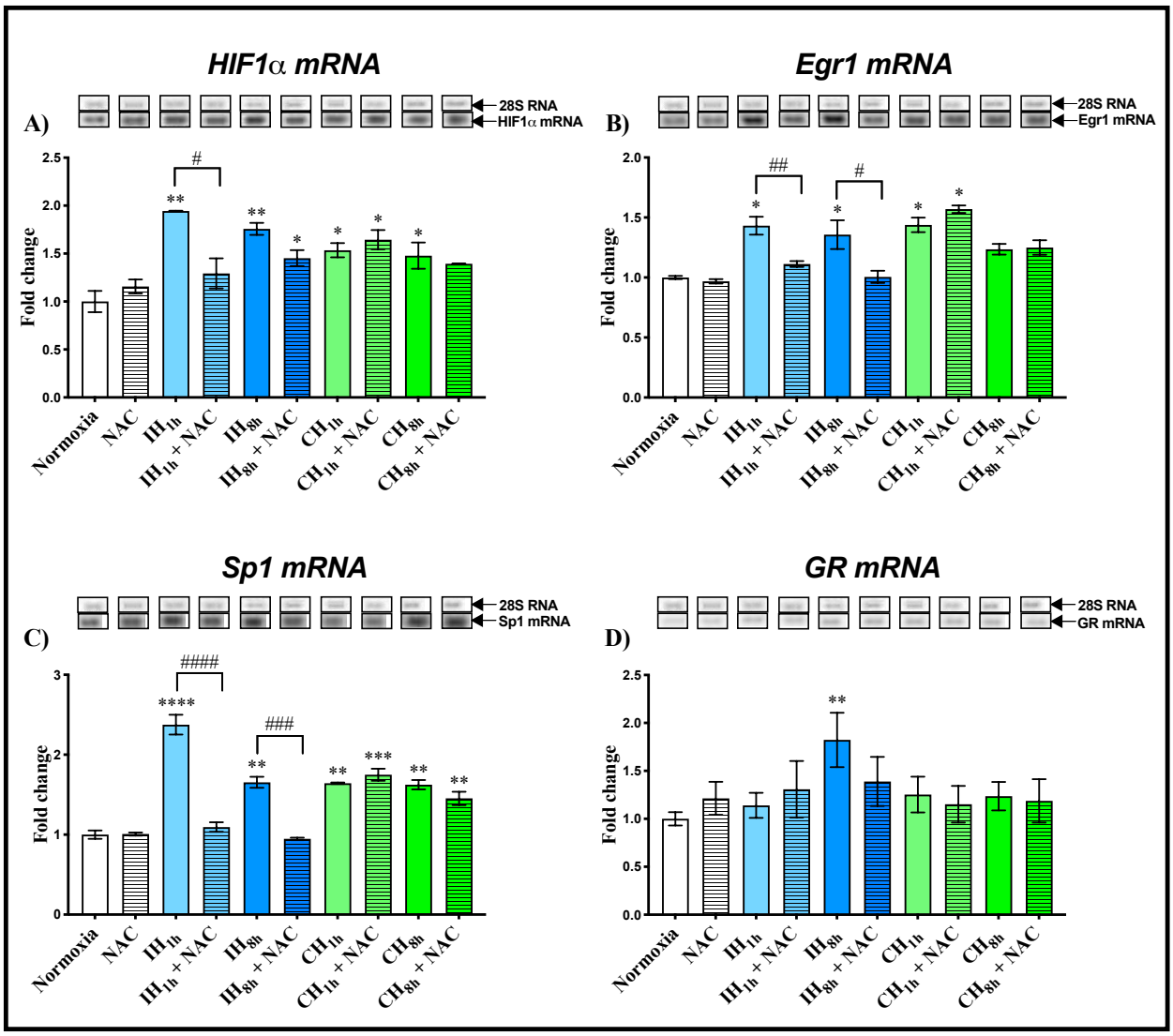

Figure 17: Gene expression of transcriptional regulators after time-variable treatment of PC12 cells with intermittent hypoxia or continuous hypoxia, and the effects of antioxidant pretreatment. Image shows mRNA levels of HIF1α (A), Egr1 (B), Sp1 (C), and GR (D) detected by RT-PCR. PC12 cells were exposed to either IH_{1h}, IH_{8h}, CH_{1h}, or CH_{8h}. These transcript levels were also compared to levels following antioxidant pretreatment with 5 mM NAC (30 min), and continued antioxidant treatment for the duration of hypoxia. Image shown above its respective graph is the representative gel bands of each treatment. Fold changes were normalized to untreated controls. mRNA data was normalized to 28s RNA. One-way ANOVA with a post-hoc Tukey test was used for analyzing transcript levels. Data are presented as mean ± SEM (n = 3). *, **, ***, and **** indicate significance from untreated controls where $p \leq 0.05$, $p \leq 0.01$, $p \leq 0.001$, and $p \leq 0.0001$ respectively. All other significant differences between groups are bracketed using the following symbol #.

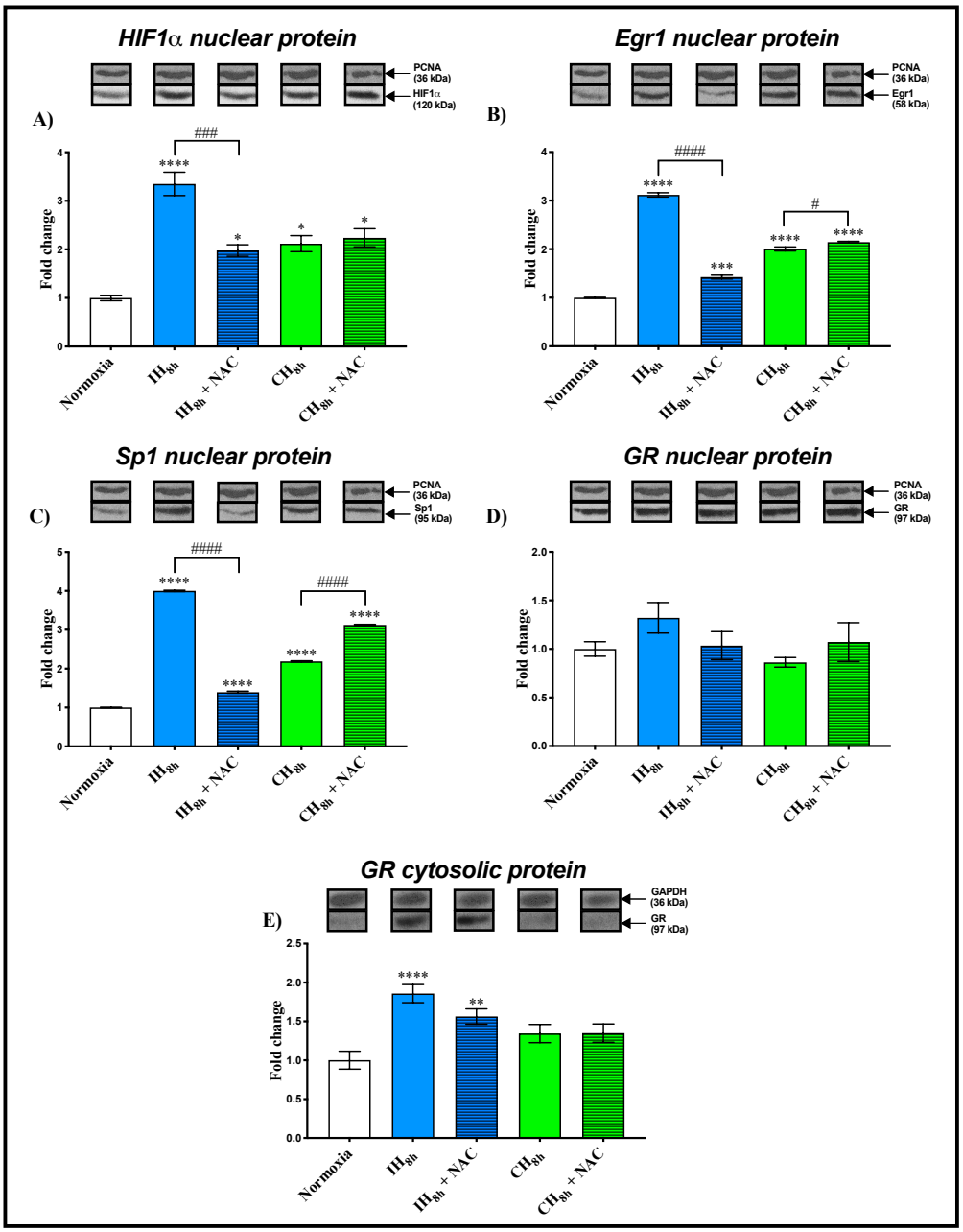

Figure 18: Protein expression of transcriptional regulators after time-variable treatment of PC12 cells with intermittent hypoxia or continuous hypoxia, and the effects of antioxidant pretreatment. Image shows nuclear protein levels of HIF1α (A), Egr1 (B), Sp1 (C), and GR (D), as well as cytosolic protein levels of GR (E) detected by Western blotting. PC12 cells were exposed to either IH_{1h}, IH_{8h}, CH_{1h}, or CH_{8h}. These protein levels were also compared to levels following antioxidant pretreatment with 5 mM NAC (30 min), and continued antioxidant treatment for the duration of hypoxia. Image shown above its respective graph is the representative gel bands of each treatment. Fold changes were normalized to untreated controls. Protein data was normalized to GAPDH. One-way ANOVA with a post-hoc Tukey test was used for analyzing protein levels. Data are presented as mean ± SEM (n = 3). *, **, ***, and **** indicate significance from untreated controls where $p \leq 0.05$, $p \leq 0.01$, $p \leq 0.001$, and $p \leq 0.0001$ respectively. All other significant differences between groups are bracketed using the following symbol #.

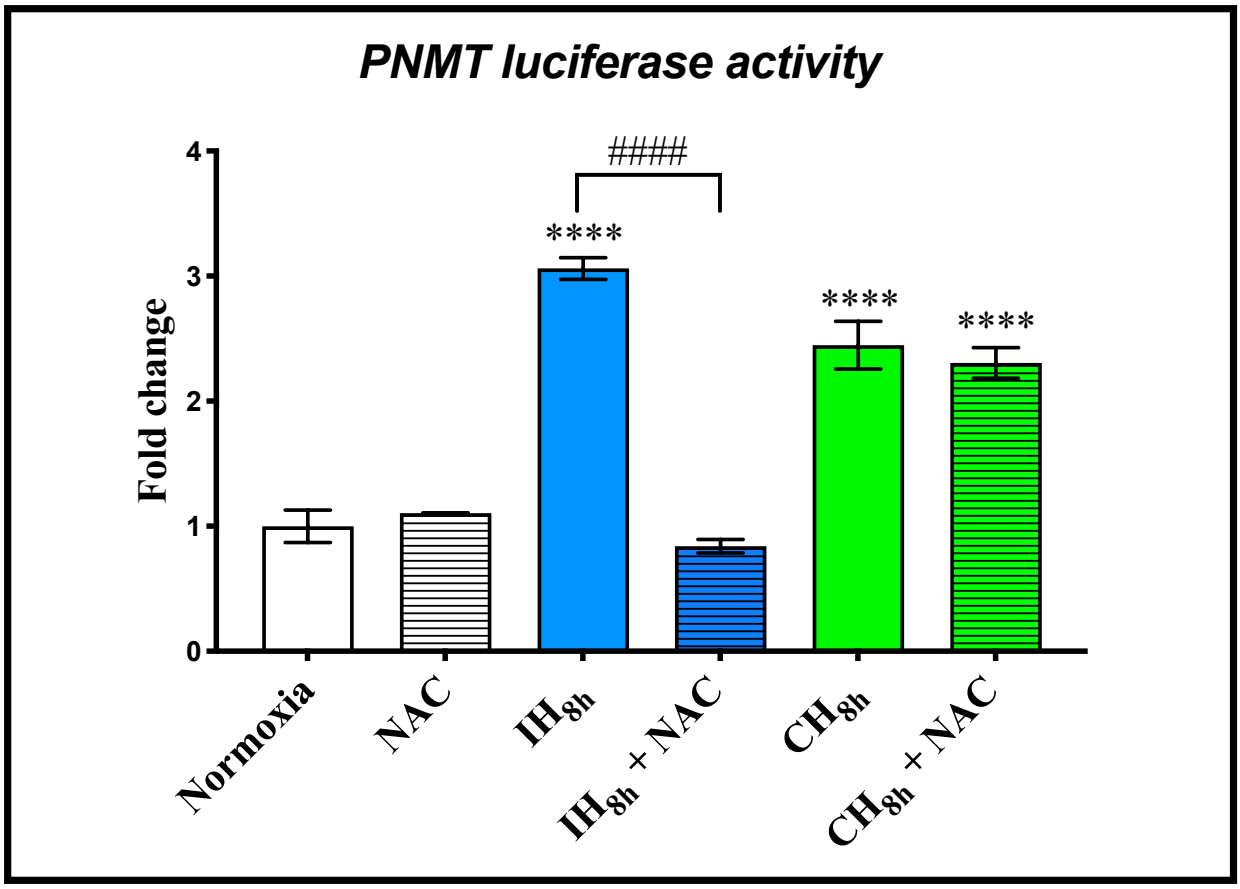

Figure 19: Phenylethanolamine N-methyltransferase promoter activation by intermittent hypoxia or continuous hypoxia, and the effects of antioxidant pretreatment. PC12 cells were transfected with PNMT pGL3RP893 luciferase vector prior to treatment with IH_{8h} or CH_{8h}. Luciferase activity was also compared to activity following antioxidant pretreatment with 5 mM NAC (30 min), with continued antioxidant treatment for the duration of hypoxia. Luciferase activity was calculated relative to protein expression, and normalized to the normoxic sample. The fold changes relative to the normoxic group is represented graphically. Statistical significance between normoxia and hypoxia treatments was determined by one-way ANOVA with a post-hoc Tukey test. Data are presented as mean ± SEM (n = 3). **** indicate significance from untreated controls where $p \leq 0.0001$. All other significant differences between groups are bracketed using the following symbol #.

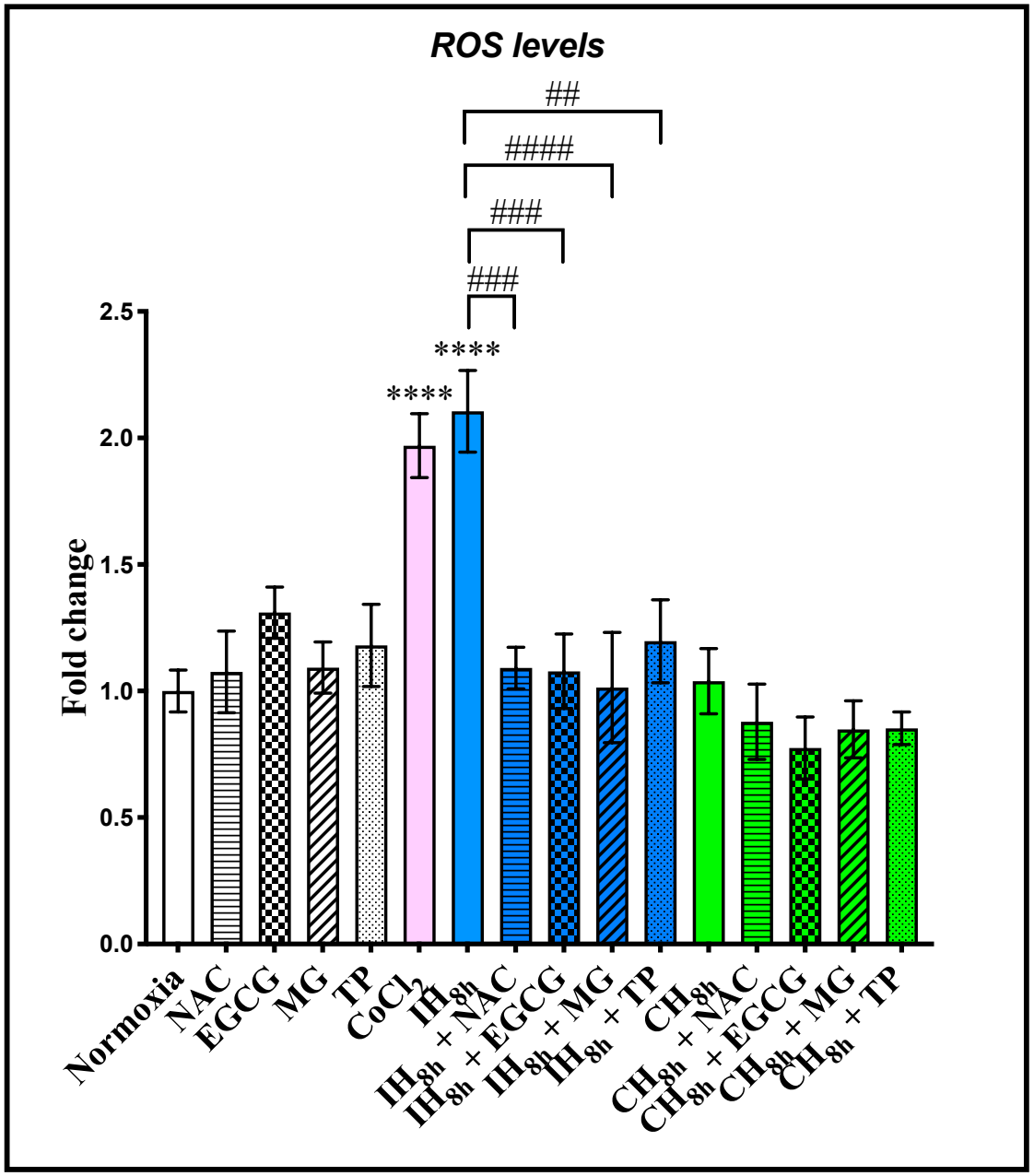

Figure 20: Fold change in levels of reactive oxygen species following intermittent hypoxia or continuous hypoxia, and the effects of synthetic antioxidant or polyphenol pretreatment. PC12 cells were stained with 25 μM DCFDA solution (45 min), and then began treatment. Cells were treated with either 200 μM $CoCl_2$, IH for 8 h (IH_{8h}), CH for 8 h (CH_{8h}), or the combination of hypoxia with 5 mM NAC, 100 μM EGCG, 50 μM MG, or 1 μM TP. DCFDA is deacetylated by cellular esterases to a non-fluorescent compound, which is later oxidized by ROS into DCF. DCF is a highly fluorescent compound that is measured by a fluorescence plate reader at Ex/Em = 485/535. The fold changes relative to the normoxic group is represented graphically. Statistical significance between normoxia and treatments was determined by one-way ANOVA with a post-hoc Tukey test. Data are presented as mean ± SEM (n = 3). **, ***, and **** indicate significance from untreated controls where $p \leq 0.01$, $p \leq 0.001$, and $p \leq 0.0001$ respectively. All other significant differences between groups are bracketed using the following symbol #.

Chapter 4: Discussion

Humans can experience various forms of hypoxia, including continuous exposure, as tolerated in high-altitude inhabitants, or intermittent exposure, as endured by those afflicted with OSA. The crucial difference between these two manifestations of hypoxia is the intervening period of reoxygenation occurring in IH, which contributes to the formation of ROS, and culminates in a tremendous amount of oxidative stress[13]. Whereas physiological systems adapt to the continuous form, which may paradoxically provide protection from cardiovascular complications, this protection is not afforded when hypoxia occurs intermittently, and rather than adapting, the system undergoes pathological change[6,148]. Exposure to IH is associated with increased secretion of CAs, specifically Epi, from the adrenal medulla[168,184]. Epi is an important neurohormone that plays a key role in the stress response and BP regulation. PNMT is the final enzyme in the CA biosynthesis pathway, converting NE to Epi, and this gene has been linked with HTN[185]. This study presents the first investigation into the role of PNMT in PC12 cells under both IH and CH conditions, in order to elucidate the mechanism by which HTN occurs in individuals experiencing IH, and how this may compare to the physiological process that occurs when individuals are exposed to CH.

The present study provides compelling evidence that adrenal medullary chromaffin cells respond to various forms of hypoxia, and these distinct forms affect the enzymes involved in the CA biosynthesis pathway to contrasting magnitudes. For the first time in PC12 cells, the role of both IH and CH exposure in TH, DBH, and PNMT gene regulation is investigated, with specific differences at both the gene and protein level of these enzymes (Figure 9). These contrasting results between IH and CH exposure were also sustained when observing their effects on transcription factors that regulate CA biosynthesis enzymes, especially in *de novo* protein synthesis, as well as

their effects on PNMT promoter activation (Figures 10-11). This study also demonstrated that chromaffin cells have the capacity to integrate ROS and GC signaling, resulting in context-specific gene regulation of CA biosynthesis enzymes and their transcription factors (Figures 12-13). Further, novel findings were ascertained when comparing the effects of pretreatment with the chemical antioxidant, NAC, prior to either IH or CH exposure, on the transcript levels and protein expression of TH, DBH, and PNMT, and their transcription factors, as well as on PNMT promoter activation (Figures 15-19). The last major finding of this study was the identification of altered levels of ROS from IH versus CH exposure, and the variations in response to polyphenol pretreatment (Figure 20).

Due to the scarcity of opportunities for patient investigation, there have remained several gaps in the understanding of the pathophysiology of OSA. To overcome this limitation, several animal and tissue models of OSA have been developed to mimic this form of SDB in humans. IH exposure is now established as the predominant model for studies on the molecular effects of OSA, where the animal or tissue is housed in ventilated chambers, and cyclically exposed to either normoxia (O_2-enriched air) or hypoxia (N_2-enriched air)[186]. Each group of researchers have applied their own IH parameters, which differ in the animal/tissue treated, the severity of hypoxia, the number of hypoxic episodes per h, and the duration of exposure; these discrepancies may compromise the direct comparison of results. The experiments presented here use a PC12 cell culture model, which has allowed for comprehensive inquiry into the effects of IH at the cellular level, especially the mechanisms involved in signal transduction and CA regulation. The severity of hypoxia in the IH condition reaches 1% O_2, since hypoxia of 5% or less usually mimics severe forms of OSA[186]. The duration of exposure was 1 h, to mimic acute IH conditions, and 8 h, which is approximately the average duration of sleep, with 10 episodes of hypoxia per h. It is important

to note that the duration of exposure seems to affect the study outcomes more than the rate of hypoxic cycling[186]. For CH exposure, 5% O_2 was used for 1 and 8 h, as previously demonstrated by our lab[5,44,49,100].

The first enzyme in the CA biosynthesis pathway that was examined in this study was TH, which demonstrates that both durations of IH elevate TH mRNA (Figure 6). A recent study by Khurana et al. (2018), displayed an equivalent increase in TH mRNA in PC12 cells by 60 cycles of IH[180]. This increase is potentially caused by the upregulation of cFos caused by IH, which then forms a heterodimer with cJun, resulting in the formation of Ap1, a transcription factor that binds to Ap1-regulated genes, including TH, in the promoter region[148]. In terms of protein expression, the results show a novel finding that TH cytosolic protein is augmented following IH_{8h} exposure in PC12 cells (Figure 6). Previous studies have shown that IH does not affect TH enzyme expression in PC12 cells; rather, it increases TH enzyme activity via the phosphorylation of serine residues, mainly serine-40, in part by CaMK and PKA[171]. Further, comparable duration of CH (1% O_2) increased TH activity, but to a lesser extent than IH[171]. Hui et al. (2003) did in fact confirm that both TH protein and phosphorylation were increased transiently in the adrenal glands of rats exposed to IH[160]. When comparing both forms of hypoxia, CH_{1h} was more potent than IH_{1h} in elevating TH mRNA; however, IH_{8h} was more potent than CH_{8h} in elevating TH cytosolic protein (Figure 9). As shown in a study by Czyzyk-Krzeska et al. (1994), CH (5% O_2) caused an increase in TH mRNA following 1 h of exposure, with peak expression at 6 h, and these levels remained elevated for 24 h in PC12 cells[158]. In addition to these findings, they concluded that cAMP is not the primary regulator of TH transcription during CH[158]. Further, a study by Millhorn et al. (1997) found that PC12 cells exposed to CH (5% O_2) increases cFos and JunB binding to the Ap1 promoter site upstream of the TH gene[159]. However, unlike IH, PKA activity was decreased during

CH, and they concluded that the cAMP/PKA pathway was not required for CH-mediated TH gene regulation in PC12 cells[159]. HIFs, on the other hand, are important regulators of the TH gene during CH, which stimulates HIF/TH HRE (-272) binding complex formation[161]. Yuan et al. (2004) found that IH (60 or 120 cycles) was more potent and induced a longer activation of cFos than comparable duration of CH in PC12 cells[148]. Although CH_{1h} caused a more significant rise in TH mRNA, this difference was abolished with the longer exposure of hypoxia (Figure 9). A study by Hui et al. (2003) found that TH cytosolic protein was only modestly increased at later time points by CH (10% O_2) in rat adrenal glands[160]. Taken together, these findings provide evidence that at more acute durations, CH_{1h} elevates TH mRNA to a greater extent than similar duration of IH_{1h}, with the importance of HIFs in gene transcription. However, these differences between IH and CH are not as pronounced following longer exposures, with the cAMP/PKA pathway and cFos being fundamental to IH-mediated (and not CH-mediated) TH mRNA and protein elevation, as well as serine-41 phosphorylation being critical to TH enzyme activity by IH. As shown by Kroll et al. (1998), HIF1α activation and ROS signaling in PC12 cells are important in inducing TH mRNA levels[154]. The present study demonstrated this induction following $CoCl_2$ treatment (Figure 12). However, $CoCl_2$ did not elevate mRNA levels any further when used in combination with either form of hypoxia (Figure 12). GC signaling in PC12 cells can also be induced with the synthetic GC, Dex. This pathway is crucial in chromaffin cells due to the close proximity of these cells to the adrenal cortex. In this study, Dex elevated TH mRNA, which has been previously shown by Lewis et al. (1987); however, in combination with either form of hypoxia, Dex did not further elevate TH mRNA (Figure 12)[187]. Next, the effect of a chemical antioxidant was used to examine its effect on TH mRNA and protein expression prior to exposure of PC12 cells with either IH or CH. One previous study by Kroll and Czyzyk-Krzeska (1998) demonstrated that CH (5% O_2)

reduced H_2O_2 concentration, and this resulted in an induction of TH mRNA[154]. Here, NAC pretreatment abrogated the CH_{1h}-mediated elevation in TH mRNA, whereas it failed to do so at the longer time point following CH_{8h} (Figure 15). This demonstrates that ROS signaling may be of importance at the shorter duration of CH, whereas the TH mRNA induction may be mediated by other mechanisms following longer exposures to CH. Unlike in CH-exposed cells, NAC pretreatment did not attenuate TH mRNA induction following either duration of IH exposure (Figure 15). Interestingly, NAC did diminish the IH-evoked induction of TH cytosolic protein, whereas it failed to do so for cells exposed to CH (Figure 16). In a study by Yuan et al. (2004), MnTMPyP, a SOD mimetic, which is a potent scavenger of $O_2\bullet^-$, prevented IH-induced cFos, Ap1, and TH mRNA activation in PC12 cells[148]. They demonstrated that ROS contribute to TH gene activation by 120 cycles of IH[148]. Since the present study only exposed PC12 cells with IH up to 80 cycles, perhaps longer duration of IH exposure is needed to demonstrate the role of ROS in TH gene regulation. In rats, NAC pretreatment also resulted in reversal of IH-induced serine phosphorylation of TH and TH enzyme activity[179]. It follows from these observations that the longer duration of IH produces a more robust increase in $O_2\bullet^-$, which may play a key role in cFos and Ap1 activation, as well as TH enzyme expression. In contrast, ROS may be elevated by only short durations of CH, and thus, other mechanisms in TH gene activation and protein expression may be activated by longer durations of CH.

Once L-DOPA is produced by TH, it is rapidly decarboxylated to dopamine. Cytoplasmic dopamine in chromaffin cells is then taken up into storage vesicles, and hydroxylated by DBH to produce NE. DBH, like TH, also requires O_2 as a cofactor. This experiment demonstrates that both forms of IH elevate DBH mRNA (Figure 6). Khurana et al. (2018) also showed a similar induction in DBH transcript by 60 cycles of IH in PC12 cells[180]. No known HREs are present in the promoter

of DBH, suggesting that HIF1α is not directly responsible for DBH transcription, but possibly indirectly due to the increase in Ap1 by IH[48,148]. For the first time, IH_{8h} was proven to also upregulate DBH cytosolic protein in PC12 cells (Figure 6). A study by Hui et al. (2003) presented a corresponding increase in DBH protein in adrenal glands by IH, however, this was in an animal model[160]. Yet, the increase in DBH enzyme expression did not correlate with the increased NE levels in the adrenal gland[160]. Instead, the authors postulated that longer exposures to IH may elevate NE in this tissue through augmented DBH activity[160]. When comparing both forms of hypoxia, CH_{1h} was more potent than IH_{1h} in elevating DBH mRNA; however, this was reversed after the longer hypoxia exposures (Figure 9). A study by Kato et al. (2012) showed that immunoreactivity for DBH is transiently increased in glomus cells of rat carotid bodies by short-term CH (10% O_2). They suggested that a CRE in the promoter region of the DBH gene is essential for its transcription, which is regulated by the phosphorylated CREB. Thus, it is possible that the difference in the time course of DBH mRNA between IH and CH is due to differences in the transcriptional factors that regulate DBH[166]. The present study also shows that both IH_{8h} and CH_{8h} produce an equivalent upregulation in DBH cytosolic protein (Figure 9). Although Hui et al. (2003) showed that DBH protein was induced for a longer duration by IH compared to CH exposure, this occurred in the superior cervical ganglia, and instead, DBH may show a tissue-specific response since both forms of hypoxia increased DBH protein to a similar extent in the adrenal medullary cells, in order to produce NE[160]. The present study shows for the first time the induction of DBH following $CoCl_2$ treatment (Figure 12). However, the simultaneous treatment of cells with either form of hypoxia and $CoCl_2$ did not cause any synergistic effects (Figure 12). Administration of the synthetic GC, Dex, significantly increased DBH at the transcript level (Figure 12), as previously demonstrated by Kim et al. (1993)[188]. Although not additive nor

synergistic, the simultaneous treatment of PC12 cells with CH_{8h} and Dex caused a significantly greater increase in DBH mRNA compared to CH_{8h} or Dex alone, suggesting that these two signaling pathways interact to stimulate further transcription of DBH (Figure 12). The present study is the first to demonstrate the role of ROS in DBH gene and protein activation. Following both durations of IH, the use of antioxidant pretreatment completely abolished the IH-mediated induction to control levels (Figure 15). This is in stark contrast to the use of antioxidant prior to CH treatment, in which NAC only moderately decreased DBH mRNA levels following only the acute duration of CH, and this decrease was not to control levels (Figure 15). Similarly, NAC pretreatment significantly decreased the IH-mediated upregulation of DBH cytosolic protein levels, whereas it failed to do so in cells exposed to CH (Figure 16). It follows from these observations that the shorter duration of CH causes a more potent increase in DBH mRNA at first, however, as both hypoxia treatments become more chronic, IH_{8h} causes the most robust changes in DBH mRNA. Further, the IH-induced ROS plays a key role in IH-mediated upregulation of both DBH mRNA and protein, whereas the CH-mediated induction of DBH is presumably caused by other signaling mechanisms, such as transcriptional regulation via CREB.

In the final step of the CA biosynthesis pathway, NE is methylated to produce Epi by the cytoplasmic enzyme PNMT using AdoMET as methyl donor and cofactor. The adrenergic chromaffin cells of the adrenal medulla are where PNMT is mainly localized, making the adrenal gland the primary organ for Epi biosynthesis[4]. PNMT can be regulated by post-transcriptional processing that involves an alternative splicing mechanism and intron retention or removal. This alternative splicing produces two different forms of PNMT mRNA; (1) the intron-retaining PNMT, which produces a truncated PNMT protein that appears to be inactive, and (2) the intronless PNMT, which produces a full length, functionally active PNMT enzyme following protein

translation[94]. This experiment shows that IH elevated the intron-retaining PNMT mRNA, with the most robust induction following the IH_{8h} (Figure 6). Furthermore, IH_{1h} increased the intronless PNMT mRNA (Figure 6); whereas it was unchanged by CH (Figure 9). Khurana et al. (2018) also showed that both the intron-retaining and intronless PNMT transcript are increased by IH in PC12 cells[180]. When comparing both forms of hypoxia, both durations of IH exposure were more potent in inducing intron-retaining PNMT mRNA, compared to their respective durations of CH exposure (Figure 9). Following Western blot analysis, IH_{8h} significantly elevated PNMT cytosolic protein (Figure 6). This result was similar to that reported by Khurana et al. (2018), in which PNMT protein was upregulated in the cytoplasm of PC12 cells, as measured by immune-fluorescent microscopy[180]. Furthermore, IH was more effective in raising PNMT cytosolic protein levels compared to the same duration of CH (Figure 9). Following the transfection of PC12 cells with the PNMT promoter-luciferase reporter gene construct pGL3RP893 and exposure to IH_{8h}, PNMT luciferase activity markedly increased (Figure 8), as previously shown by Khurana et al. (2018) with 60 cycles of IH[180]. IH was more potent in stimulating PNMT promoter activity, compared to the same duration of CH exposure (Figure 11). A study by Tai et al. (2010) showed that CH (5% O_2) caused an elevation in PNMT promoter-driven luciferase activity, as well as PNMT mRNA and cytosolic protein, peaking at 6 h, with a slight decline in elevation by 24 h, and a shift towards the intron-retaining PNMT mRNA form[5]. However, the findings described in this present study are novel, since they are comparing the effects of IH with CH exposure, and demonstrate that IH is more potent in elevating PNMT mRNA, protein, and luciferase activity compared to CH. $CoCl_2$ administration was used to induce intracellular ROS levels in PC12 cells, and as expected, both forms of PNMT mRNA were elevated, with the intron-retaining form being most significantly increased (Figure 12); this was previously demonstrated in a study by Crispo et al. (2011)[1]. When

$CoCl_2$ was applied to cells simultaneously with CH exposure, there was an increase in intron-retaining PNMT mRNA, with a concomitant decrease in the intronless form (Figure 12). Either form of PNMT mRNA was unaffected by the addition of $CoCl_2$ to IH, compared to $CoCl_2$ or IH alone (Figure 12). Since IH already produces a significant amount of ROS, then it may be reasoned that the supplemental ROS provided by $CoCl_2$ will be less effective at altering PNMT mRNA levels, compared to when given concurrently with CH exposure, where less ROS is produced. The effect of Dex, and its combination with hypoxia was then determined. GC sensitivity has been reported for PNMT promoter activity, and three putative GREs have been identified in the PNMT gene[106]. In the present study, Dex alone caused a significant upregulation of PNMT mRNA, with a shift to the intronless variant (Figure 12), as shown previously by Crispo et al. (2011)[1]. However, when used in combination with either form of hypoxia, it appeared as though the simultaneous treatment of Dex and IH caused a greater induction in intron-retaining PNMT, whereas Dex and CH acted synergistically to shift PNMT mRNA to a much greater increase in the intronless PNMT form (Figure 12). Crispo et al. (2011) demonstrated this synergism in PC12 cells following the combination treatment of Dex and $CoCl_2$, suggesting further post-transcriptional regulation by these drugs[1]. Crispo et al. (2011) also investigated the role of ROS in the regulation of the PNMT gene[1]. Following antioxidant pretreatment with NAC prior to $CoCl_2$ administration, both the intron-retaining and intronless PNMT mRNA were significantly decreased compared to $CoCl_2$ alone[1]. Their findings confirmed the upregulation of both PNMT transcript forms via $CoCl_2$-induced ROS and HIF1α stabilization, and the abolishment of this response when treated jointly with $CoCl_2$ and NAC[1]. The present study is the first to examine the role of IH-induced ROS, and its effect on PNMT at the transcript and protein level, as well as in PNMT promoter activation. NAC was only effective in reducing intron-retaining PNMT mRNA when used in combination

with IH_{8h} compared to IH_{8h} alone, whereas it was unsuccessful in reducing CH-induced intron-retaining transcript levels (Figure 15). Furthermore, NAC was effective in reducing the intronless variant of PNMT when used in combination with either form of the shorter duration of hypoxia, compared to IH_{1h} or CH_{1h} alone (Figure 15). At the protein level, NAC was able to significantly decrease PNMT cytosolic protein when used together with IH_{8h} or CH_{8h}, compared to either form of hypoxia alone (Figure 16). Following transfection of PC12 cells with pGL3RP893, NAC when used in combination with IH_{8h} was successful in attenuating PNMT luciferase activity to control levels, compared to IH_{8h} alone, whereas NAC failed to do so in CH_{8h}-exposed cells (Figure 19). NAC is a known antioxidant, serving as a prodrug to L-cysteine, which is the precursor to the biologic antioxidant glutathione (GSH) whose thiol group confers the ability to reduce free radicals. It is surprising then that although CH_{8h} does not change the level of ROS in PC12 cells (Figure 20), NAC was still able to reduce PNMT cytosolic protein following CH_{8h}. This may be due to NAC's anti-inflammatory effects via inhibiting nuclear factor κ-light-chain-enhancer of activated B cells (NFκB) and modulating cytokine synthesis, rather than via NAC's antioxidant effects[189]. Therefore, a potential mechanism for CH-mediated upregulation in PNMT at the protein level, and subsequent reduction of this response by NAC, may be due to increased proinflammatory cytokines by CH, which can then modulate CA levels, as described by Byrne et al. (2018)[190]. It follows from these observations that IH is more potent than CH in elevating the intron-retaining variant of PNMT, PNMT cytosolic protein, and PNMT promoter activity. The IH-induced ROS seems to be the dominant signaling mechanism in increasing PNMT at the transcript and protein level, as well as in promoter activation, whereas CH-induced cytokines may play a stronger role in increasing PNMT mRNA and protein, yet not as crucial in altering PNMT promoter activation.

The sustained activation of PNMT by some stressors and not others suggests that multiple mechanisms of activation are involved in regulating PNMT. Transcriptional regulation of PNMT may play a key role in generating these differences. The 5' upstream region of the PNMT promoter has been studied, with several key transcription factor-binding sites identified, including HIF1α, Egr1, Sp1, and GR. In the present study, HIF1α, Egr1, and Sp1 mRNA were elevated by both durations of IH (Figure 7). Only IH_{8h} was able to significantly elevate GR mRNA (Figure 7). A study by Khurana et al. (2018) also examined the effects of IH (60 cycles) on transcript levels of PNMT transcription factors in PC12 cells, and demonstrated comparable fold changes[180]. Following Western blot analysis, HIF1α, Egr1, and Sp1 nuclear protein were significantly increased by IH_{8h} (Figure 7). Only GR cytosolic, and not nuclear, protein was induced by IH_{8h} (Figure 7). Khurana et al. (2018), via immune-fluorescent microscopy, also demonstrated an induction of HIF1α, Egr1, and Sp1 protein in the nucleus of PC12 cells, and GR protein in the cytoplasm[180]. When comparing both forms of hypoxia, Sp1, at the mRNA level, was the only transcription factor to be upregulated by IH, to a greater extent than its respective duration of CH (Figure 10). In addition, both durations of CH were able to increase HIF1α and Sp1 mRNA, only CH_{1h} was capable of increasing Egr1 mRNA, and both durations of CH were unable to induce GR mRNA in PC12 cells (Figure 10). A study by Tai et al. (2009) demonstrated a similar induction in HIF1α mRNA by CH (5% O_2), with peak stimulation at 6 h, and declining to basal levels by 24 h[100]. In 2010, Tai et al. also showed a comparable elevation in the remaining transcription factors by CH (5% O_2)[5]. Specifically, they showed that Egr1 mRNA was rapidly and transiently increased, with peak induction at 1 h; Sp1 mRNA showed rapid and sustained increase, peaking at 6 h; and GR mRNA was unaltered[5]. IH_{8h} was more potent than CH_{8h} in elevating all four transcription factor protein levels (Figure 10). Further, CH_{8h} was able to increase nuclear protein of HIF1α,

Egr1, and Sp1, but was ineffective in altering both nuclear and cytosolic GR protein (Figure 10). The effects of CH (5% O_2) on protein levels of these transcription factors have been previously published, and showed comparable results[5,100]. Yuan et al. (2005) also showed an increase in HIF1α nuclear protein, as duration of IH increased, whereas CH requires a longer duration of exposure to significantly increase the levels of HIF1α mRNA[178]. $CoCl_2$ administration was used to induce intracellular ROS levels and stabilize HIF1α in PC12 cells, and as expected, HIF1α, Egr1, and Sp1 mRNA were induced compared to control, whereas GR mRNA was unaffected (Figure 13). This can be attributed to the increased expression of HIF1α by oxidative stress, which in turn, induces Egr1 and Sp1 expression[100]. Although GR mRNA was unchanged by $CoCl_2$, a study by Kitagawa et al. (2007) demonstrated that $CoCl_2$ increases stabilized GR protein within the cell[191]. To continue, PC12 cells were also treated with Dex to mimic the effects of endogenous GCs produced in the adrenal cortex. Dex caused a significant increase in Egr1, Sp1, and GR mRNA, whereas HIF1α mRNA was unaffected (Figure 13). A study by Nguyen et al. (2015) demonstrated similar results in which rats exposed to Dex in utero had increased Egr1, Sp1, and GR mRNA[192]. When $CoCl_2$ or Dex were administered in combination with either form of hypoxia, there were no additive nor synergistic effects produced (Figure 13). The present study also examined the role of IH-induced ROS, and its effect on PNMT transcription factors at the mRNA and protein level, and these effects were compared to those caused by NAC when used in conjunction with CH exposure. NAC pretreatment was successful in abolishing IH_{1h}-induced HIF1α, Egr1, and Sp1 mRNA to control levels, as well as IH_{8h}-induced Egr1 and Sp1 mRNA (Figure 17). Furthermore, this antioxidant was effective in reducing HIF1α, Egr1, and Sp1 nuclear protein (Figure 18). Although not significant, NAC reduced IH-induced GR mRNA and cytosolic protein (Figure 18). In distinct contrast, NAC failed to reduce CH-induced upregulation of all

transcription factors at the mRNA and protein level (Figure 17-18). It follows from these observations that IH is more potent than CH in elevating Sp1 mRNA, nuclear protein levels of HIF1α, Egr1, Sp1, and GR, as well as GR cytosolic protein. Furthermore, IH-induced ROS seems to be a primary signaling mechanism in the upregulation of transcription factors by IH, whereas other signaling mechanisms appear to play a role in CH-induced upregulation of HIF1α, Egr1, and Sp1. A study by Yuan et al. (2008) confirmed that IH-induced HIF1α accumulation is due to increased generation of ROS by NOX2[174]. XO activation by IH precedes that of NOX[181]. NOX2 activation requires Ca^{2+}-dependent PKC activation, as well as PKC-dependent phosphorylation and subsequent translocation of the cytosolic p47phox and p67phox subunits to the membrane[181]. Other potential differences in IH versus CH-mediated signaling mechanisms in PC12 cells are presented here. IH results in increased PLC and IP_3, as well as $ERK_{1/2}$, JNK, and PKC, resulting in increased intracellular Ca^{2+}, which then upregulates mTOR and CaMKII[9,174,178]. In contrast, CH lead to only a transient and modest increase in CaMKII activity[178]. CaMKII is also necessary for IH-induced, but not CH-induced, HIF1α transcriptional activity[178]. Some mechanisms that are upregulated following CH include cAMP, PKA, PLC, PKC, PI3K, $ERK_{1/2}$, and MAPK[44]. In addition, PI3K is required for CH-induced HIF1α transcriptional activity, whereas IH-induced HIF1α activity is independent of PI3K[178]. The HIF1α C-terminal transactivation domain activation by IH is independent of Asn^{830} hydroxylation, whereas this hydroxylation is required for CH-evoked HIF1α activation[178]. The increased mTOR by IH also results in upregulation of S6 kinase, leading to HIF1α stabilization and synthesis[9]. mTOR targets rapamycin, which normally inhibits IH-induced HIF1α stabilization[174]. Interestingly, CH inhibits mTOR[174]. IH also causes a decrease in hydroxylase-dependent HIF1α degradation[174]. Furthermore, the increase in CaMKII causes an increase in p300 and CBP, which lead to HIF1α transcriptional activation[9]. The present

study also demonstrated an increase in cytosolic GR following IH, but not CH, exposure. The cooperation of GR and HIF1α has been regarded as a point of interaction and regulation between the HPA and oxidative stress pathways[193,194].

Recently, polyphenolic compounds have received much attention due to their antioxidant properties[195]. For the first time, their protective effects are investigated in PC12 cells following exposure to IH and CH exposure. IH_{8h} caused a robust increase in intracellular ROS levels that was similar to that produced by $CoCl_2$, a known inducer of ROS, and the synthetic antioxidant, NAC, was successful in attenuating this induction (Figure 20). EGCG, an abundant catechin in tea, effectively reduced ROS to basal levels when administered prior to IH_{8h} exposure (Figure 20). A study by Crispo et al. (2010) demonstrated similar findings in which EGCG increased viability of PC12 cells under non-stressed conditions, and lowered intracellular ROS caused by $CoCl_2$ treatment[196]. MG is another polyphenol found in various plants, fruit extracts, and wine, and in the present study, MG successfully decreased ROS when administered prior to IH_{8h} exposure (Figure 20). MG has been shown to increase cell viability in H_2O_2-stressed cells, lower intracellular ROS caused by $CoCl_2$ and H_2O_2, and increase NO and total GSH in H_2O_2-stressed cells[196]. TP is a synthetic polyphenol, and when used in combination with IH_{8h}, decreased intracellular ROS (Figure 20). In contrast, CH_{8h} did not significantly elevate ROS levels, and its combination with the synthetic antioxidant or the polyphenols did not alter ROS levels (Figure 20). There appears to be some controversy over the production of ROS by CH. For example, there is a study that demonstrates that following 1 h of CH, ROS production increased in PC12 cells compared to normoxia, however, this increase in ROS production only paralleled the CH-induced gene transcription, rather than caused it[155]. In contrast, a different study using the same cell line demonstrated that ROS production decreased with increasing time, and this actually induced an

increase in that same gene expression[154]. When using a different cell line, namely fibroblasts, a sharp decrease in ROS was observed with exposure to CH (0.5% O_2) after 20 min, followed by a consistent and progressive decline of cellular ROS while maintaining cells up to 24 h under CH[197]. Another study demonstrated that exposure to 24 h of CH increased intracellular ROS, but decreased extracellular NO[1]. With these conflicting findings in previous studies, perhaps the greater elevation in ROS by IH compared to CH in our study can be attributed to the type of tissue studied, the duration of hypoxia, the form of hypoxia including its parameters and O_2 concentrations, as well as the method of measuring ROS and the type of species detected.

This study demonstrates the reduction of ROS due to hypoxia-induced injury by antioxidants and polyphenols in IH-exposed cells only. Furthermore, the present study demonstrated that when PC12 cells were treated with both IH_{8h} and $CoCl_2$ simultaneously, it caused widespread apoptosis of adrenal chromaffin cells, which was not generated by the same duration of CH with $CoCl_2$, or 8 h $CoCl_2$ alone (Figure 14). This may be due to the increase in ROS due to the combination of a ROS-producing agent, $CoCl_2$, and IH. ROS are highly reactive molecules that can damage cell structures, carbohydrates, nucleic acids, lipids, and proteins, as well as induce proinflammatory responses and alter cell function[198]. A study by Gozal et al. (2005) presented findings that suggested different signaling pathways are involved in CH and IH-induced cell injury[199]. Specifically, IH induces an earlier and more extensive apoptotic response than CH, and that this response is at least partially dependent on caspase-mediated pathways[199]. These findings suggest that CH does not elevate ROS as extensively as IH, and suggests that cells may adapt more quickly to low O_2 tensions, compared to IH exposure.

Chapter 5: Conclusion

Findings from the present study suggest that: (1) IH is more potent than CH in upregulating CA biosynthesis enzymes at the transcript and protein level, especially following a more sustained duration of exposure; (2) mechanisms involved in this IH-mediated induction include a more robust increase in HIF1α, Egr1, Sp1, and GR, leading to a more enhanced activation of the PNMT promoter, compared to that resulting from CH exposure; (3) chromaffin cells have the capacity to integrate ROS and GC signaling, resulting in context-specific gene regulation of CA biosynthesis enzymes and their transcription factors; (4) CH may be more potent than IH in generating TH and DBH mRNA following the shorter exposure, however, PC12 cells soon become desensitized by hypoxic conditions, and CH-induced ROS may decline to baseline levels; (5) IH-induced oxidative stress and ROS play a pivotal role in the induction of CA biosynthesis enzymes and their transcription factors, as well as PNMT promoter activity, and both NAC and select polyphenols were able to abolish these IH-mediated inductions. These findings support the possibility of a novel mechanism, whereby IH-induced ROS in OSA patients regulate CA biosynthesis in the adrenal gland, and may help explain how this syndrome, characterized by intermittent O_2 deficiency, may contribute to the progression of HTN.

Chapter 6: Limitations and Future Directions

Limitations in the current study includes an inability to verify that O_2 level fluctuations in the medium were in fact achieved during the course of a given experiment. A study by Yuan et al. (2004) described the changes in PO_2 by IH versus CH in PC12 cells, in which IH resulted in only a modest decrease in PO_2 (~20 mmHg) near the cells, while a comparable cumulative duration of CH caused a more pronounced drop in PO_2 (~70 mmHg) near the cells[148]. IH and CH profiles, as well as the type of hypoxic chamber system used, differs between studies; although breathable sealing films were employed, and O_2 concentrations were monitored within the chamber in the present study, the O_2 concentration at the level of the cells should also be measured in our lab's custom-built hypoxic chamber. The current study only examined IH and CH following 1 h and 8 h of exposure. Many of the results in the present study were compared to data by Tai et al. (2010), in which the effects of CH (5% O_2) on PNMT and its transcription factors were determined over a 24 h period. Future research should examine the influence of IH on CA biosynthesis enzymes, and their transcription factors over a longer time-course, allowing the establishment of peak induction and fluctuations in these levels. Also, the sample size in the present study ranged from n = 3-9, and therefore, sample size could be expanded to increase the robustness of the data, as well as the use of RT-qPCR to measure quantified mRNA expression more precisely, compared to RT-PCR. Furthermore, the levels of ROS produced by IH versus CH were measured after 8 h of hypoxia exposure only. In order to achieve a better understanding in the role of ROS following these two forms of hypoxia, more acute and chronic durations of exposure should be performed, especially in determining whether CH results in a significant production of ROS initially, followed by physiological adaptation to CH in which ROS levels return to basal levels, or whether ROS levels

continuously oscillate with time as CH exposure becomes more chronic. Furthermore, the relative contribution of various forms of ROS including $O_2\bullet^-$, H_2O_2, and OH• to IH-induced changes in adrenal medullary chromaffin cells remains to be investigated. In the present study, mRNA and protein levels were measured following IH and CH, and the effects of a known antioxidant was administered to determine the effects of ROS on these levels. Future studies should examine protein-DNA complex formation, binding site mutation, and protein activity of CA biosynthesis enzymes following CH and IH in order to gain a clearer understanding of how these two different forms of hypoxia differ in their role of CA production and regulation in the adrenal gland. Finally, an interesting future direction for research on the molecular mechanisms involved in HTN secondary to OSA, may be the effect of OSA on the core clock genes, and how these may interact with the CA biosynthesis pathway in producing the metabolic and cardiovascular derangements associated with OSA. The rational for this study is supported by the evidence that OSA causes sleep disturbances, which can lead to clock gene dysfunction, and affect a person's circadian rhythm, as well as the evidence which demonstrates that deregulation of the clock can lead to HTN[200,201].

References

1. Crispo, J. A. G., Ansell, D. R., Ubriaco, G. & Tai, T. C. Role of reactive oxygen species in the neural and hormonal regulation of the PNMT gene in PC12 cells. *Oxid. Med. Cell. Longev.* **2011**, 1–10 (2011).
2. W.B.Cannon & Paz, D. D. La. Emotional stimulation of adrenal secretion. *Am. J. Physiol.* **28**, 64–70 (1911).
3. Wong, D. L. Epinephrine biosynthesis: Hormonal and neural control during stress. *Cell. Mol. Neurobiol.* **26**, 891–900 (2006).
4. Kvetnansky, R., Sabban, E. L. & Palkovits, M. Catecholaminergic systems in stress: Structural and molecular genetic approaches. *Physiol. Rev.* **89**, 535–606 (2009).
5. Tai, T. C., Wong-Faull, D. C., Claycomb, R. & Wong, D. L. Hypoxia and adrenergic function: Molecular mechanisms related to Egr-1 and Sp1 activation. *Brain Res.* **1353**, 14–27 (2010).
6. Semenza, G. L. Oxygen sensing, homeostasis, and disease. *N. Engl. J. Med.* **365**, 537–547 (2011).
7. Beall, C. M. Tibetan and Andean patterns of adaptation to high-altitude hypoxia. *Hum. Biol.* **72**, 201–228 (2000).
8. Simonson, T. S. *et al.* Genetic evidence for high-altitude adaptation in Tibet. *Science* **329**, 72–75 (2010).
9. Nanduri, J. & Nanduri, R. P. Cellular mechanisms associated with intermittent hypoxia. *Essays Biochem.* **43**, 91–104 (2007).
10. Mohsenin, V. Obstructive sleep apnea and hypertension: A critical review. *Current hypertension reports* **16**, (2014).
11. Prabhakar, N. R., Kumar, G. K., Nanduri, J. & Semenza, G. L. ROS signaling in systemic and cellular responses to chronic intermittent hypoxia. *Antioxid Redox Signal* **9**, 1397–1403 (2007).
12. Eisele, H.-J., Markart, P. & Schulz, R. Obstructive sleep apnea, oxidative stress, and cardiovascular disease: Evidence from human studies. *Oxid. Med. Cell. Longev.* **2015**, 608438 (2015).
13. Prabhakar, N. R. *et al.* Oxygen sensing during intermittent hypoxia: Cellular and molecular mechanisms. *J. Appl. Physiol.* **90**, 1986–1994 (2001).
14. Dopp, J. M., Reichmuth, K. J. & Morgan, B. J. Obstructive sleep apnea and hypertension: Mechanisms, evaluation, and management. *Curr. Hypertens. Rep.* **9**, 529–534 (2007).
15. Phillips, C. L. & O'Driscoll, D. M. Hypertension and obstructive sleep apnea. *Nat. Sci. Sleep* **5**, 43–52 (2013).
16. Naish, J. & Syndercombe Court, D. Medical sciences. *Saunders elsevier* **2**, 562 (2015).
17. Mayet, J. & Hughes, A. Cardiac and vascular pathophysiology in hypertension. *Heart* **89**, 1104–1109 (2003).
18. Rossier, B. C., Bochud, M. & Devuyst, O. The hypertension pandemic: An evolutionary perspective. *Physiology* **32**, 112–125 (2017).
19. Jun, J. C., Chopra, S. & Schwartz, A. R. Sleep apnea. *Eur. Respir. Rev.* **25**, (2016).
20. Motamedi, K. K., McClary, A. C. & Amedee, R. G. Obstructive sleep apnea: A growing problem. *Ochsner J.* **9**, 149–153 (2009).
21. Victor, L. Obstructive sleep apnea. *Am. Fam. Physician* **60**, 2279–2286 (1999).
22. Ganten, D. (Detlev) & Ruckpaul, K. *Encyclopedic reference of genomics and proteomics*

in molecular medicine. (Springer, 2006).
23. Physicians, A. A. of F. *The international classification of sleep disorders, revised*. *American academy of sleep medicine* (2001).
24. Sterling, P. & Eyer, J. Allostasis: A new paradigm to explain arousal pathology. *Handb. life Stress. Cogn. Heal.* 629–649 (1988).
25. Cannon, W. B. Bodily changes in pain, hunger, fear and rage. *D. Applet. Co.* 40–65 (1915).
26. Semenza, G. L. HIF-1: Mediator of physiological and pathophysiological responses to hypoxia. *J. Appl. Physiol.* **88**, 1474–1480 (2000).
27. Melmed, S., Polonsky, K. S., Larsen, P. R. & Kronenberg, H. *Williams textbook of endocrinology*. (Elsevier, 2016).
28. Carmichael, C. Y. & Wainford, R. D. Hypothalamic signaling mechanisms in hypertension. *Curr. Hypertens. Rep.* **17**, 39 (2015).
29. McCorry, L. K. Physiology of the autonomic nervous system. *Am. J. Pharm. Educ.* **71**, 78 (2007).
30. Guillemin, R. Hypothalamic hormones a.k.a. hypothalamic releasing factors. *J. Endocrinol.* **184**, 11–28 (2005).
31. Ulrich-Lai, Y. M. & Herman, J. P. Neural regulation of endocrine and autonomic stress responses. *Neuroscience* **10**, 397–409 (2009).
32. Kvetnanský, R. *et al.* Sympathoadrenal system in stress: Interaction with the hypothalamic-pituitary-adrenocortical system. *Ann. N. Y. Acad. Sci.* **771**, 131–58 (1995).
33. Smith, S. M. & Vale, W. W. The role of the hypothalamic-pituitary-adrenal axis in neuroendocrine responses to stress. *Dialogues Clin. Neurosci.* **8**, 383–395 (2006).
34. Cawley, N. X., Li, Z. & Loh, Y. P. 60 years of POMC: Biosynthesis, trafficking, and secretion of pro-opiomelanocortin-derived peptides. *J. Mol. Endocrinol.* **56**, T77-97 (2016).
35. Herman, J. P. *et al.* Regulation of the hypothalamic-pituitary-adrenocortical stress response. *Compr. Physiol.* **6**, 603–621 (2016).
36. Wurtman, R. J. Stress and the adrenocortical control of epinephrine synthesis. *Metabolism.* **51**, 11–4 (2002).
37. Nicolaides, N. C., Galata, Z., Kino, T., Chrousos, G. P. & Charmandari, E. The human glucocorticoid receptor: Molecular basis of biologic function. *Steroids* **75**, 1–12 (2010).
38. Asok, M. *et al.* A study on comparison of salivary cortisol circadian rhythm in periodontal diseases with external stressors and clinical parameters. *Biomed. Pharmacol. J.* **9**, 679–688 (2016).
39. Liberzon, I., Krstov, M. & Young, E. A. Stress-restress: Effects on ACTH and fast feedback. *Psychoneuroendocrinology* **22**, 443–453 (1997).
40. Colomer, C., Martin, A., Desarménien, M. & Guérineau, N. Gap junction-mediated intercellular communication in the adrenal medulla: An additional ingredient of stimulus–secretion coupling regulation. *Biochim. Biophys. Acta* **1818**, 1937–1951 (2011).
41. Desarménien, M. G. *et al.* Gap junction signalling is a stress-regulated component of adrenal neuroendocrine stimulus-secretion coupling in vivo. *Nat. Commun.* **4**, 2938 (2013).
42. Fitzgerald, P., Gardner, D. & Shoback, D. Adrenal medulla and paraganglia. in *Greenspan's basic & clinical endocrinology* (McGraw-hill global education holdings, LLC., 2011).
43. Fitzpatrick, P. F. Tetrahydropterin-dependent amino acid hydroxylases. *Annu. Rev. Biochem.* **68**, 355–381 (1999).
44. Wong, D. L. *et al.* Stress and adrenergic function: HIF1α, a potential regulatory switch. *Cell. Mol. Neurobiol.* **30**, 1451–1457 (2010).

45. Lieberman, M. & Marks, A. *Marks' basic medical biochemistry*. (Lippincott Williams & Wilkins, 2013).
46. Fuller, R. W. Pharmacology of brain epinephrine neurons. *Annu. Rev. Pharmacol. Toxicol.* **22**, 31–55 (1982).
47. Molinoff, P. B. Alpha- and beta-adrenergic receptor subtypes properties, distribution and regulation. *Drugs* **28 Suppl 2**, 1–15 (1984).
48. Sabban, E. L. & Kvetnanský, R. Stress-triggered activation of gene expression in catecholaminergic systems: Dynamics of transcriptional events. *Trends Neurosci.* **24**, 91–98 (2001).
49. Wong, D. L., Tai, T. C., Wong-Faull, D. C., Claycomb, R. & Kvetnansky, R. Genetic mechanisms for adrenergic control during stress. in *Annals of the New York academy of sciences* **1018**, 387–397 (2004).
50. Majewski, H. & Rand, M. J. A possible role of epinephrine in the development of hypertension. *Med. Res. Rev.* **6**, 467–486 (1986).
51. Nguyen, P. *et al.* Regulation of the phenylethanolamine N-methyltransferase gene in the adrenal gland of the spontaneous hypertensive rat. *Neurosci. Lett.* **461**, 280–284 (2009).
52. Grandbois, J. *et al.* Phenylethanolamine N-methyltransferase gene expression in adrenergic neurons of spontaneously hypertensive rats. *Neurosci. Lett.* **635**, 103–110 (2016).
53. Peltsch, H. *et al.* Cardiac phenylethanolamine N-methyltransferase: Localization and regulation of gene expression in the spontaneously hypertensive rat. *Can. J. Physiol. Pharmacol.* **94**, 363–372 (2016).
54. Kepp, K. *et al.* Resequencing PNMT in european hypertensive and normotensive individuals: No common susceptibilily variants for hypertension and purifying selection on intron 1. *BMC Med. Genet.* **8**, (2007).
55. Powell, J. F., Boni, C., Lamouroux, A., Craig, I. W. & Mallet, J. Assignment of the human tyrosine hydroxylase gene to chromosome 11. *FEBS Lett.* **175**, 37–40 (1984).
56. Bonnefoy, E., Ferrara, P., Rohrer, H., Gros, F. & Thibault, J. Role of the N-terminus of rat pheochromocytoma tyrosine hydroxylase in the regulation of the enzyme's activity. *Eur. J. Biochem.* **174**, 685–90 (1988).
57. Dunkley, P. R., Bobrovskaya, L., Graham, M. E., Von Nagy-Felsobuki, E. I. & Dickson, P. W. Tyrosine hydroxylase phosphorylation: Regulation and consequences. *J. Neurochem.* **91**, 1025–1043 (2004).
58. Nagatsu, T. & Ichinose, H. Regulation of pteridine-requiring enzymes by the cofactor tetrahydrobiopterin. *Mol. Neurobiol.* **19**, 79–96 (1999).
59. Kumer, S. C. & Vrana, K. E. Intricate regulation of tyrosine hydroxylase activity and gene expression. *J. Neurochem.* **67**, 443–62 (1996).
60. Raghuraman, G., Prabhakar, N. R. & Kumar, G. K. Differential regulation of tyrosine hydroxylase by continuous and intermittent hypoxia. *Adv. Exp. Med. Biol.* **758**, 381–385 (2012).
61. Haycock, J. W., George, R. J. & Waymire, J. C. In situ phosphorylation of tyrosine hydroxylase in chromaffin cells: Localization to soluble compartments. *Neurochem. Int.* **7**, 301–308 (1985).
62. Grima, B., Lamouroux, A., Blanot, F., Biguet, N. F. & Mallet, J. Complete coding sequence of rat tyrosine hydroxylase mRNA. *Proc. Natl. Acad. Sci. U. S. A.* **82**, 617–621 (1985).
63. Haycock, J. W. Phosphorylation of tyrosine hydroxylase in situ at serine 8, 19, 31, and 40. *J. Biol. Chem.* **265**, 11662–11691 (1990).

64. Ramsey, A. J. & Fitzpatrick, P. F. Effects of phosphorylation on binding of catecholamines to tyrosine hydroxylase: Specificity and thermodynamics. *Biochemistry* **39**, 773–778 (2000).
65. Ramsey, A. J. & Fitzpatrick, P. F. Effects of phosphorylation of serine 40 of tyrosine hydroxylase on binding of catecholamines: Evidence for a novel regulatory mechanism. *Biochemistry* **37**, 8980–8986 (1998).
66. Lewis-Tuffin, L. J., Quinn, P. G. & Chikaraishi, D. M. Tyrosine hydroxylase transcription depends primarily on cAMP response element activity, regardless of the type of inducing stimulus. *Mol. Cell. Neurosci.* **25**, 536–547 (2004).
67. Suzuki, T., Yamakuni, T., Hagiwara, M. & Ichinose, H. Identification of ATF-2 as a transcriptional regulator for the tyrosine hydroxylase gene. *J. Biol. Chem.* **277**, 40768–40774 (2002).
68. Maharjan, S., Serova, L. & Sabban, E. L. Transcriptional regulation of tyrosine hydroxylase by estrogen: opposite effects with estrogen receptors α and β and interactions with cyclic AMP. *J. Neurochem.* **93**, 1502–1514 (2005).
69. Papanikolaou, N. A. & Sabban, E. L. Ability of Egr1 to activate tyrosine hydroxylase transcription in PC12 cells. *J. Biol. Chem.* **275**, 26683–26689 (2000).
70. Nakashima, A., Ota, A. & Sabban, E. L. Interactions between Egr1 and AP1 factors in regulation of tyrosine hydroxylase transcription. *Mol. brain Res.* **112**, 61–69 (2003).
71. Hagerty, T., Morgan, W. W., Elango, N. & Strong, R. Identication of a glucocorticoid-responsive element in the promoter region of the mouse tyrosine hydroxylase gene. *J. Neurochem.* **76**, 825–834 (2001).
72. Sheela Rani, C. S., Elango, N., Wang, S., Kobayashi, K. & Strong, R. Identification of an activator protein-1-like sequence as the glucocorticoid response element in the rat tyrosine hydroxylase gene. *Mol. Pharmacol.* **75**, 589–598 (2009).
73. Craig, S. P., Buckle, V. J., Lamouroux, A., Mallet, J. & Craig, I. W. Localization of the human dopamine beta hydroxylase (DBH) gene to chromosome 9q34. *Cytogenet. Cell Genet.* **48**, 48–50 (1988).
74. Cubells, J. F. & Zabetian, C. P. Human genetics of plasma dopamine beta-hydroxylase activity: Applications to research in psychiatry and neurology. *Psychopharmacology (Berl).* **174**, 463–476 (2004).
75. Kobayashi, K., Kurosawa, Y., Fujita, K. & Nagatsu, T. Human dopamine beta-hydroxylase gene: Two mRNA types having different 3'-terminal regions are produced through alternative polyadenylation. *Nucleic Acids Res.* **17**, 1089–1102 (1989).
76. McMahon, A., Geertman, R. & Sabban, E. L. Rat dopamine beta-hydroxylase: Molecular cloning and characterization of the cDNA and regulation of the mRNA by reserpine. *J. Neurosci. Res.* **25**, 395–404 (1990).
77. Feng, Z., Angeletti, R. H., Levin, B. E. & Sabban, E. L. Glycosylation and membrane insertion of newly synthesized rat dopamine beta-hydroxylase in a cell-free system without signal cleavage. *J. Biol. Chem.* **267**, 21808–21815 (1992).
78. Lewis, E. J. & Asnani, L. P. Soluble and membrane-bound forms of dopamine beta-hydroxylase are encoded by the same mRNA. *J. Biol. Chem.* **267**, 494–500 (1992).
79. Shaskus, J., Greco, D., Asnani, L. P. & Lewis, E. J. A bifunctional genetic regulatory element of the rat dopamine beta-hydroxylase gene influences cell type specificity and second messenger-mediated transcription. *J. Biol. Chem.* **267**, 18821–18830 (1992).
80. Weinshilboum, R. & Axel, J. Serum dopamine-beta-hydroxylase activity. *Circ. Res.* **28**,

307–315 (1971).
81. Weinshilboum, R. M., Kvetnansky, R., Axelrod, J. & Kopin, I. J. Elevation of serum dopamine-beta-hydroxylase activity with forced immobilization. *Nat. New Biol.* **230**, 287–288 (1971).
82. Cheng, S.-Y., Serova, L. I., Glazkova, D. & Sabban, E. L. Regulation of rat dopamine beta-hydroxylase gene transcription by early growth response gene 1 (Egr1). *Brain Res.* **1193**, 1–11 (2008).
83. Shaskus, J., Zellmer, E. & Lewis, E. J. A negative regulatory element in the rat dopamine beta-hydroxylase gene contributes to the cell type specificity of expression. *J. Neurochem.* **64**, 52–60 (1995).
84. Kim, H.-S., Seo, H., Yang, C., Brunet, J.-F. & Kim, K.-S. Noradrenergic-specific transcription of the dopamine b-hydroxylase gene requires synergy of multiple cis-acting elements including at least two phox2a-binding sites. *J. Neurosci.* **18**, 8247–8260 (1998).
85. Greco, D., Zellmer, E., Zhang, Z. & Lewis, E. Transcription factor AP-2 regulates expression of the dopamine beta-hydroxylase gene. *J. Neurochem.* **65**, 510–6 (1995).
86. Kim, H.-S., Hong, S. J., LeDoux, M. S. & Kim, K.-S. Regulation of the tyrosine hydroxylase and dopamine β-hydroxylase genes by the transcription factor AP-2. *J. Neurochem.* **76**, 280–294 (2009).
87. Swanson, D., Zellmer, E. & Lewis, E. Ap1 proteins mediate the cAMP response of the dopamine beta-hydroxylase gene. *J. Biol. Chem.* **273**, 24065–24074 (1998).
88. Xu, H., Firulli, A. B., Zhang, X. & Howard, M. J. HAND2 synergistically enhances transcription of dopamine-β-hydroxylase in the presence of Phox2a. *Dev. Biol.* **262**, 183–193 (2003).
89. Zellmer, E. *et al.* A homeodomain protein selectively expressed in noradrenergic tissue regulates transcription of neurotransmitter biosynthetic genes. *J. Neurosci.* **15**, 8109–8120 (1995).
90. Swanson, D. J., Zellmer, E. & Lewis, E. J. The homeodomain protein Arix interacts synergistically with cyclic AMP to regulate expression of neurotransmitter biosynthetic genes. *J. Biol. Chem.* **272**, 27382–27392 (1997).
91. Seo, H., Yang, C., Kim, H. S. & Kim, K. S. Multiple protein factors interact with the cis-regulatory elements of the proximal promoter in a cell-specific manner and regulate transcription of the dopamine beta-hydroxylase gene. *J. Neurosci.* **16**, 4102–4112 (1996).
92. McMahon, A. & Sabban, E. L. Regulation of expression of dopamine β-hydroxylase in PC12 cells by glucocorticoids and cyclic AMP analogues. *J. Neurochem.* **59**, 2040–2047 (1992).
93. Rychlik, J. L., Gerbasi, V. & Lewis, E. J. The interaction between dHAND and Arix at the dopamine beta-hydroxylase promoter region is independent of direct dHAND binding to DNA. *J. Biol. Chem.* **278**, 49652–49660 (2003).
94. Wong, D. L., Tai, T. C., Wong-Faull, D. C., Claycomb, R. & Kvetnanský, R. Adrenergic responses to stress: Transcriptional and post-transcriptional changes. *Ann. N. Y. Acad. Sci.* **1148**, 249–256 (2008).
95. Huang, M.-H. *et al.* Neuroendocrine properties of intrinsic cardiac adrenergic cells in fetal rat heart. *Am. J. Physiol. Hear. Circ. Physiol.* **288**, H497–H503 (2005).
96. Kvetnansky, R. *et al.* Localization and regulation of phenylethanolamine N-methyltransferase gene expression in the heart of rats and mice during stress. *Ann. N. Y. Acad. Sci.* **1018**, 405–417 (2004).

97. Pullar, C. E., Rizzo, A. & Isseroff, R. R. β-Adrenergic receptor antagonists accelerate skin wound healing. *J. Biol. Chem.* **281**, 21225–21235 (2006).
98. Kaneda, N. *et al.* Molecular cloning of cDNA and chromosomal assignment of the gene for human phenylethanolamine N-methyltransferase, the enzyme for epinephrine biosynthesis. *J. Biol. Chem.* **263**, 7672–7677 (1988).
99. Knight, J., Munroe, P. B., Pembroke, J. C. & Caulfield, M. J. Human chromosome 17 in essential hypertension. *Ann. Hum. Genet.* **67**, 193–206 (2003).
100. Tai, T. C., Wong-Faull, D. C., Claycomb, R. & Wong, D. L. Hypoxic stress-induced changes in adrenergic function: Role of HIF1α. *J. Neurochem.* **109**, 513–524 (2009).
101. Fuller, R. W. & Hunt, J. M. Inhibition of phenethanolamine N-methyl transferase by its product, epinephrine. *Life Sci.* 1107–1112 (1967).
102. Tai, T. C. *et al.* Stress-induced changes in epinephrine expression in the adrenal medulla in vivo. *J. Neurochem.* **101**, 1108–1118 (2007).
103. Ross, M. E. *et al.* Identification of a functional glucocorticoid response element in the phenylethanolamine N-methyltransferase promoter using fusion genes introduced into chromaffin cells in primary culture. *J. Neurosci.* **10**, 520–530 (1990).
104. Tai, T. C., Morita, K. & Wong, D. Role of Egr-1 in cAMP-dependent protein kinase regulation of the phenylethanolamine N-methyltransferase gene. *J. Neurochem.* **76**, 1851–1859 (2001).
105. Her, S., Claycomb, R., Tai, T. C. & Wong, D. L. Regulation of the rat phenylethanolamine N-methyltransferase gene by transcription factors Sp1 and MAZ. *Mol. Pharmacol.* **64**, 1180–1188 (2003).
106. Tai, T. C., Claycomb, R., Her, S., Bloom, A. K. & Wong, D. L. Glucocorticoid responsiveness of the rat phenylethanolamine N-methyltransferase gene. *Mol. Pharmacol.* **61**, (2002).
107. Tai, T. C. & Wong, D. L. Protein kinase A and protein kinase C signaling pathway interaction in phenylethanolamine N-methyltransferase gene regulation. *J. Neurochem.* **85**, 816–829 (2003).
108. Huang, L. E. & Bunn, H. F. Hypoxia-inducible factor and its biomedical relevance. *J. Biol. Chem.* **278**, 19575–19578 (2003).
109. Semenza, G. L. Regulation of mammalian O2 homeostasis by hypoxia-inducible factor 1. *Annu. Rev. Cell Dev. Biol.* **15**, 551–578 (1999).
110. Wenger, R. H. Cellular adaptation to hypoxia: O2-sensing protein hydroxylases, hypoxia-inducible transcription factors, and O2-regulated gene expression. *FASEB J.* **16**, 1151–1162 (2002).
111. Semenza, G. L. Hydroxylation of HIF-1: Oxygen sensing at the molecular level. *Physiology* **19**, 176–182 (2004).
112. Huang, L. E., Gu, J., Schau, M. & Bunn, H. F. Regulation of hypoxia-inducible factor 1a is mediated by an O2-dependent degradation domain via the ubiquitin-proteasome pathway. *Biochemistry* **95**, 7987–7992 (1998).
113. Kallio, P. J., Wilson, W. J., O'Brien, S., Makino, Y. & Poellinger, L. Regulation of the hypoxia-inducible transcription factor 1a by the ubiquitin-proteasome pathway. *J. Biol. Chem.* **274**, 6519–6525 (1999).
114. Bruick, R. K. & McKnight, S. L. A conserved family of prolyl-4-hydroxylases that modify HIF. *Science (80-.).* **294**, 1337–1340 (2001).
115. Ivan, M. *et al.* HIFα targeted for VHL-mediated destruction by proline hydroxylation:

Implications for O2 sensing. *Science (80-.).* **292**, 464–468 (2001).
116. Masson, N., Willam, C., Maxwell, P. H., Pugh, C. W. & Ratcliffe, P. J. Independent function of two destruction domains in hypoxia-inducible factor-a chains activated by prolyl hydroxylation. *EMBO J.* **20**, 5197–5206 (2001).
117. Ivan, M. & Kaelin, W. G. The von Hippel–Lindau tumor suppressor protein. *Curr. Opin. Genet. Dev.* **11**, 27–34 (2001).
118. Huang, L. E., Pete, E. A., Schau, M., Milligan, J. & Gu, J. Leu-574 of HIF-1a is essential for the von Hippel-Lindau (VHL)-mediated degradation pathway. *J. Biol. Chem.* **277**, 41750–41755 (2002).
119. Huang, L. E., Arany, Z., Livingston, D. M. & Bunn, H. F. Activation of hypoxia-inducible transcription factor depends primarily upon redox-sensitive stabilization of its a subunit. *J. Biol. Chem.* **271**, 32253–32259 (1996).
120. Jaakkola, P. *et al.* Targeting of HIF-α to the von Hippel-Lindau ubiquitylation complex by O2-regulated prolyl hydroxylation. *Science (80-.).* **292**, 468–472 (2001).
121. Elson, D. A. *et al.* Induction of hypervascularity without leakage or inflammation in transgenic mice overexpressing hypoxia-inducible factor-1a. *Genes Dev.* **15**, 2520–2532 (2001).
122. Gu, J., Milligan, J. & Huang, L. E. Molecular mechanism of hypoxia-inducible factor 1a-p300 interaction: A leucine-rich interface regulated by a single cysteine. *J. Biol. Chem.* **276**, 3550–3554 (2001).
123. Lando, D. *et al.* FIH-1 is an asparaginyl hydroxylase enzyme that regulates the transcriptional activity of hypoxia-inducible factor. *Genes Dev.* **16**, 1466–1471 (2002).
124. Dames, S. A., Martinez-Yamout, M., De Guzman, R. N., Dyson, H. J. & Wright, P. E. Structural basis for Hif-1a/CBP recognition in the cellular hypoxic response. *Proc. Natl. Acad. Sci. U. S. A.* **99**, 5271–6276 (2002).
125. Huang, J., Zhao, Q., Mooney, S. M. & Lee, F. S. Sequence determinants in hypoxia-inducible factor-1a for hydroxylation by the prolyl hydroxylases PHD1, PHD2, and PHD3. *J. Biol. Chem.* **277**, 39792–39800 (2002).
126. Gashler, A. L., Swaminathan, S. & Sukhatme, V. P. A novel repression module, an extensive activation domain, and a bipartite nuclear localization signal defined in the immediate-early transcription factor Egr-1. *Mol. Cell. Biol.* **13**, 4556–4571 (1993).
127. Ebert, S. N. *et al.* Egr-1 activation of rat adrenal phenylethanolamine N-methyltransferase gene. *J. Biol. Chem.* **269**, 20885–20898 (1994).
128. Cao, X. M. *et al.* Identification and characterization of the Egr-1 gene product, a DNA-binding zinc finger protein induced by differentiation and growth signals. *Mol. Cell. Biol.* **10**, 1931–1939 (1990).
129. Silverman, E. S. *et al.* cAMP-response-element-binding-protein-binding protein (CBP) and p300 are transcriptional co-activators of early growth response factor-1 (Egr-1). *Biochem. J.* **336 (Pt 1)**, 183–189 (1998).
130. Wong, D. L., Anderson, L. J. & Tai, T.-C. Cholinergic and peptidergic regulation of phenylethanolamine N-methyltransferase gene expression. *Ann. N. Y. Acad. Sci.* **971**, 19–26 (2002).
131. Kriwacki, R. W., Schultz, S. C., Steitz, T. A. & Caradonna, J. P. Sequence-specific recognition of DNA by zinc-finger peptides derived from the transcription factor Sp1. *Proc. Natl. Acad. Sci. U. S. A.* **89**, 9759–9763 (1992).
132. Her, S., Bell, R. A., Bloom, A. K., Siddall, B. J. & Wong, D. L. Phenylethanolamine N-

methyltransferase gene expression: Sp1 and MAZ potential for tissue-specific expression. *J. Biol. Chem.* **274**, 8698–8707 (1999).
133. Ebert, S. N. & Wong, D. L. Differential activation of the rat phenylethanolamine N-methyltransferase gene by Sp1 and Egr-1. *J. Biol. Chem.* **270**, 17299–17305 (1995).
134. Tai, T. C. *et al.* Cellular mechanisms underlying stress-induced changes in adrenergic function. *J. Neurochem.* **101**, 1108–1118 (2007).
135. Kvetnansky, R. *et al.* Gene expression of phenylethanolamine N-methyltransferase in corticotropin-releasing hormone knockout mice during stress exposure. *Cell. Mol. Neurobiol.* **26**, 733–752 (2006).
136. Evinger, M. J. Determinants of phenylethanolamine-N-methyltransferase expression. *Adv. Pharmacol.* **42**, 73–76 (1998).
137. Wurtman, R. J. & Axelrod, J. Adrenaline synthesis: Control by the pituitary gland and adrenal glucocorticoids. *Science (80-.).* **150**, 1464–1465 (1965).
138. Rousseau, G. G. & Baxter, J. D. Glucocorticoid receptors. *Monogr. Endocrinol.* **12**, 49–77 (1979).
139. Strasser, R. Social Accountability and the Supply of Physicians for Remote Rural Canada. *Can. Med. Assoc. J.* **187**, 791–792 (2015).
140. Perlman, R. L. & Chalfie, M. Catecholamine release from the adrenal medulla. *Clin. Endocrinol. Metab.* **6**, 551–576 (1977).
141. Wong, D. L., Lesage, A., White, S. & Siddall, B. Adrenergic expression in the rat adrenal gland: Multiple developmental regulatory mechanisms. *Dev. brain Res.* **67**, 229–236 (1992).
142. Ziegler, M. G., Bao, X., Kennedy, B. P., Joyner, A. & Enns, R. Location, development, control, and function of extraadrenal phenylethanolamine N-methyltransferase. *Ann. N. Y. Acad. Sci.* **971**, 76–82 (2002).
143. Krizanová, O. *et al.* Existence of cardiac PNMT mRNA in adult rats: Elevation by stress in a glucocorticoid-dependent manner. *Am. J. Hear. Circ. Physiol.* **281**, H1372–H1379 (2001).
144. Suh, Y.-H. *et al.* Complete nucleotide sequence and tissue-specific expression of the rat phenylethanolamine N-methyltransferase gene. *J. Neurochem.* **63**, 1603–1608 (2002).
145. Unsworth, B. R., Hayman, G. T., Carroll, A. & Lelkes, P. I. Tissue-specific alternative mRNA splicing of phenylethanolamine N-methyltransferase (PNMT) during development by intron retention. *Int. J. Dev. Neurosci.* **17**, 45–55 (1999).
146. Wong, D. L., Hayashi, R. J. & Ciaranello, R. D. Regulation of biogenic amine methyltransferases by glucocorticoids via s-adenosylmethionine and its metabolizing enzymes, methionine adenosyltransferase and s-adenosylhomocysteine hydrolase. *Brain Res.* **330**, 209–216 (1985).
147. Berenbeim, D., Wong, D., Masover, S. & Ciaranello, R. Regulation of synthesis and degradation of rat adrenal phenylethanolamine N-methyltransferase. *Mol. Pharmacol.* **16**, 482–490 (1979).
148. Yuan, G. *et al.* Role of oxidative stress in intermittent hypoxia-induced immediate early gene activation in rat PC12 cells. *J. Physiol.* **557**, 773–783 (2004).
149. Faeh, D., Gutzwiller, F., Bopp, M. & Swiss National Cohort Study Group. Lower mortality from coronary heart disease and stroke at higher altitudes in Switzerland. *Circulation* **120**, 495–501 (2009).
150. Koehler, U. *et al.* Chronic hypoxia and cardiovascular risk: Clinical significance of different forms of hypoxia. *Herz* **43**, 291–297 (2018).

151. Cherniack, N. S., Shenoy, P. C., Mishra, R., Simonson, M. & Prabhakar, N. R. Induction of immediate early response genes by hypoxia - possible molecular bases for systems adaptation to low pO2. *Adv. Exp. Med. Biol.* **410**, 127–134 (1996).
152. Peng, Y.-J. *et al.* Heterozygous HIF-1alpha deficiency impairs carotid body-mediated systemic responses and reactive oxygen species generation in mice exposed to intermittent hypoxia. *J. Physiol.* **577**, 705–716 (2006).
153. Halliwell, B. & Gutteridge, J. M. Role of free radicals and catalytic metal ions in human disease: An overview. *Methods Enzymol.* **186**, 1–85 (1990).
154. Kroll, S. L. & Czyzyk-Krzeska, M. F. Role of H2O2 and heme-containing O2 sensors in hypoxic regulation of tyrosine hydroxylase gene expression. *Am. J. Physiol.* **274**, C167–C174 (1998).
155. Höhler, B. *et al.* Hypoxic upregulation of tyrosine hydroxylase gene expression is paralleled, but not induced, by increased generation of reactive oxygen species in PC12 cells. *FEBS Lett.* **457**, 53–56 (1999).
156. Hanbauer, I. Regulation of tyrosine hydroxylase in carotid body. *Adv. Biochem. Psychopharmacol.* **16**, 275–280 (1977).
157. Czyzyk-Krzeska, M. F., Bayliss, D. A., Lawson, E. E. & Millhorn, D. E. Regulation of tyrosine hydroxylase gene expression in the rat carotid body by hypoxia. *J. Neurochem.* **58**, 1538–1546 (1992).
158. Czyzyk-Krzeska, M. F., Furnari, B. A., Lawson, E. E. & Millhorn, D. E. Hypoxia increases rate of transcription and stability of tyrosine hydroxylase mRNA in pheochromocytoma (PC12) cells. *J. Biol. Chem.* **269**, 760–764 (1994).
159. Millhorn, D. E. *et al.* Regulation of gene expression for tyrosine hydroxylase in oxygen sensitive cells by hypoxia. *Kidney Int.* **51**, 527–535 (1997).
160. Hui, A. S. *et al.* Regulation of catecholamines by sustained and intermittent hypoxia in neuroendocrine cells and sympathetic neurons. *Hypertension* **42**, 1130–1136 (2003).
161. Schnell, P. O. *et al.* Regulation of tyrosine hydroxylase promoter activity by the von Hippel-Lindau tumor suppressor protein and hypoxia-inducible transcription factors. *J. Neurochem.* **85**, 483–491 (2003).
162. Gozal, E. *et al.* Tyrosine hydroxylase expression and activity in the rat brain: differential regulation after long-term intermittent or sustained hypoxia. *J. Appl. Physiol.* **99**, 642–649 (2005).
163. Kato, K., Yamaguchi-Yamada, M. & Yamamoto, Y. Short-term hypoxia increases tyrosine hydroxylase immunoreactivity in rat carotid body. *J. Histochem. Cytochem.* **58**, 839–846 (2010).
164. Wakai, J., Kizaki, K., Yamaguchi-Yamada, M. & Yamamoto, Y. Differences in tyrosine hydroxylase expression after short-term hypoxia, hypercapnia or hypercapnic hypoxia in rat carotid body. *Respir. Physiol. Neurobiol.* **173**, 95–100 (2010).
165. Kato, K. & Yamamoto, Y. Short-term hypoxia increases phosphorylated tyrosine hydroxylase at Ser31 and Ser40 in rat carotid body. *Respir. Physiol. Neurobiol.* **185**, 543–546 (2013).
166. Kato, K., Yokoyama, T., Yamaguchi-Yamada, M. & Yamamoto, Y. Short-term hypoxia transiently increases dopamine β-hydroxylase immunoreactivity in glomus cells of the rat carotid body. *J. Histochem. Cytochem.* **61**, 55–62 (2013).
167. Evinger, M. J., Cikos, S., Nwafor-Anene, V., Powers, J. F. & Tischler, A. S. Hypoxia activates multiple transcriptional pathways in mouse pheochromocytoma cells. *Ann. N. Y.*

Acad. Sci. **971**, 61–65 (2002).
168. Nieto, F. J. *et al.* Association of sleep-disordered breathing, sleep apnea, and hypertension in a large community-based study - sleep heart health study. *JAMA* **283**, 1829–1836 (2000).
169. Imadojemu, V. A., Gleeson, K., Gray, K. S., Sinoway, L. I. & Leuenberger, U. A. Obstructive apnea during sleep is associated with peripheral vasoconstriction. *Am. J. Respir. Crit. Care Med.* **165**, 61–66 (2002).
170. Souvannakitti, D., Kumar, G. K., Fox, A. & Prabhakar, N. R. Neonatal intermittent hypoxia leads to long-lasting facilitation of acute hypoxia-evoked catecholamine secretion from rat chromaffin cells. *J. Neurophysiol.* **101**, 2837–2846 (2009).
171. Kumar, G. K. *et al.* Chronic intermittent hypoxia induces hypoxia-evoked catecholamine efflux in adult rat adrenal medulla via oxidative stress. *J. Physiol.* **575**, 229–39 (2006).
172. Kuri, B. A., Khan, S. A., Chan, S.-A., Prabhakar, N. R. & Smith, C. B. Increased secretory capacity of mouse adrenal chromaffin cells by chronic intermittent hypoxia: involvement of protein kinase C. *J. Physiol.* **584**, 313–319 (2007).
173. Souvannakitti, D. *et al.* NADPH oxidase-dependent regulation of T-Type Ca2+ channels and ryanodine receptors mediate the augmented exocytosis of catecholamines from intermittent hypoxia-treated neonatal rat chromaffin cells. *J. Neurosci.* **30**, 10763–10772 (2010).
174. Yuan, G., Nanduri, J., Khan, S., Semenza, G. L. & Prabhakar, N. R. Induction of HIF-1alpha expression by intermittent hypoxia: Involvement of NADPH oxidase, Ca2+ signaling, prolyl hydroxylases, and mTOR. *J. Cell. Physiol.* **217**, 674–685 (2008).
175. Nanduri, J. *et al.* Xanthine oxidase mediates hypoxia-inducible factor-2α degradation by intermittent hypoxia. *PLoS One* **8**, e75838 (2013).
176. Nanduri, J. *et al.* Intermittent hypoxia degrades HIF-2alpha via calpains resulting in oxidative stress: Implications for recurrent apnea-induced morbidities. *Proc. Natl. Acad. Sci. U. S. A.* **106**, 1199–1204 (2009).
177. Kim, D.-K., Natarajan, N., Prabhakar, N. R. & Kumar, G. K. Facilitation of dopamine and acetylcholine release by intermittent hypoxia in PC12 cells: Involvement of calcium and reactive oxygen species. *J. Appl. Physiol.* **96**, 1206–1215 (2004).
178. Yuan, G., Nanduri, J., Bhasker, C. R., Semenza, G. L. & Prabhakar, N. R. Ca2+/calmodulin kinase-dependent activation of hypoxia inducible factor 1 transcriptional activity in cells subjected to intermittent hypoxia. *J. Biol. Chem.* **280**, 4321–4328 (2005).
179. Raghuraman, G., Rai, V., Peng, Y.-J., Prabhakar, N. R. & Kumar, G. K. Pattern-specific sustained activation of tyrosine hydroxylase by intermittent hypoxia: Role of reactive oxygen species-dependent downregulation of protein phosphatase 2A and upregulation of protein kinases. *Antioxid. Redox Signal.* **11**, 1777–1789 (2009).
180. Khurana, S. *et al.* Phenylethanolamine N-methyltransferase gene expression in PC12 cells exposed to intermittent hypoxia. *Neurosci. Lett.* **666**, 169–174 (2018).
181. Nanduri, J. *et al.* HIF-1α activation by intermittent hypoxia requires NADPH oxidase stimulation by xanthine oxidase. *PLoS One* **10**, (2015).
182. Jouett, N. P. *et al.* N -Acetylcysteine reduces hyperacute intermittent hypoxia-induced sympathoexcitation in human subjects. *Exp. Physiol.* **101**, 387–396 (2016).
183. Boussif, O. *et al.* A versatile vector for gene and oligonucleotide transfer into cells in culture and in vivo: Polyethylenimine. *Proc. Natl. Acad. Sci. U. S. A.* **92**, 7297–301 (1995).
184. Shahar, E. *et al.* Sleep-disordered breathing and cardiovascular disease. *Am. J. Respir. Crit. Care Med.* **163**, 19–25 (2001).

185. Koike, G. *et al.* Investigation of the phenylethanolamine N-methyltransferase gene as a candidate gene for hypertension. *Hypertension* **26**, 595–601 (1995).
186. Diogo, L. N. & Monteiro, E. C. The efficacy of antihypertensive drugs in chronic intermittent hypoxia conditions. *Front. Physiol.* **5**, 361 (2014).
187. Lewis, E. J., Harrington, C. A. & Chikaraishi, D. M. Transcriptional regulation of the tyrosine hydroxylase gene by glucocorticoid and cyclic AMP. *Proc. Natl. Acad. Sci. U. S. A.* **84**, 3550–3554 (1987).
188. Kim, K.-T., Park, D. H. & Joh, T. H. Parallel up-regulation of catecholamine biosynthetic enzymes by dexamethasone in PC12 cells. *J. Neurochem.* **60**, 946–951 (1993).
189. Berk, M., Malhi, G. S., Gray, L. J. & Dean, O. M. The promise of N-acetylcysteine in neuropsychiatry. *Trends Pharmacol. Sci.* **34**, 167–177 (2013).
190. Byrne, C. J., Khurana, S., Kumar, A. & Tai, T. C. Inflammatory signaling in hypertension: Regulation of adrenal catecholamine biosynthesis. *Front. Endocrinol. (Lausanne).* **9**, 343 (2018).
191. Kitagawa, H. *et al.* A reduction state potentiates the glucocorticoid response through receptor protein stabilization. *Genes to cells* 1281–1287 (2007).
192. Nguyen, P. *et al.* Prenatal glucocorticoid exposure programs adrenal PNMT expression and adult hypertension. *J. Endocrinol.* **227**, 117–127 (2015).
193. Leonard, M. O., Godson, C., Brady, H. R. & Taylor, C. T. Potentiation of glucocorticoid activity in hypoxia through induction of the glucocorticoid receptor. *J. Immunol.* **174**, 2250–2257 (2005).
194. Kodama, T. *et al.* Role of the glucocorticoid receptor for regulation of hypoxia-dependent gene expression. *J. Biol. Chem.* **278**, 33384–33391 (2003).
195. Sasaki, M. *et al.* Quercetin-induced PC12 cell death accompanied by caspase-mediated DNA fragmentation. *Biol. Pharm. Bull.* **30**, 682–686 (2007).
196. Crispo, J. A. G. *et al.* Protective effects of polyphenolic compounds on oxidative stress-induced cytotoxicity in PC12 cells. *Can. J. Physiol. Pharmacol.* **88**, 429–438 (2010).
197. Sgarbi, G., Gorini, G., Liuzzi, F., Solaini, G. & Baracca, A. Hypoxia and IF_1 expression promote ROS decrease in cancer cells. *Cells* **7**, (2018).
198. Birben, E., Sahiner, U. M., Sackesen, C., Erzurum, S. & Kalayci, O. Oxidative stress and antioxidant defense. *world allergy Organ. J.* **5**, 9–19 (2012).
199. Gozal, E., Sachleben, L. R., Rane, M. J., Vega, C. & Gozal, D. Mild sustained and intermittent hypoxia induce apoptosis in PC-12 cells via different mechanisms. *Am. J. Physiol.* **288**, C535–C542 (2005).
200. Burioka, N. *et al.* Clock gene dysfunction in patients with obstructive sleep apnoea syndrome. *Eur. Respir. J.* **32**, 105–112 (2008).
201. Richards, J., Diaz, A. N. & Gumz, M. L. Clock genes in hypertension: Novel insights from rodent models. *Blood Press. Monit.* **19**, 249–254 (2014).

Appendices

Appendix 1: Reagents, equipment, and manufacturers.

Abcam (Cambridge, United Kingdom)	DCFDA Cellular ROS Detection Assay Kit
	DCFDA solution
	HBSS
Beckman Coulter (Brea, California, USA)	Centrifuge for cell culture
	Vi-CELL XR
BioTek (Winooski, Vermont, USA)	Fluorescence plate reader
	KC4 software
	PowerWave XS microplate spectrophotometer
Bio-Rad Laboratories (Hercules, California, USA)	1.5-mm spaced plates
	10-well comb
	Chemidoc XRS
	Protein assay dye reagent concentrate
	Quantity One analysis software
	Tank system
	Thermocycler
	Transfer cassette
BMG LABTECH (Ortenberg, Germany)	FLUOstar Optima microplate luminometer
Corning; Thermo Fisher Scientific (Corning, New York, USA)	0.2 mL PCR tube strip
	0.45 μm filter
	1.5 mL microcentrifuge tube
	6-well, clear, tissue culture-treated plate
	15 mL conical tube
	24-well, clear, tissue culture-treated plate
	96-well, clear bottom, black-sided, tissue culture-treated plate
	96-well, clear plate
	96-well, clear, v-shaped bottom plate
	96-well, white, round-shaped bottom plate
	100-mm, clear, tissue culture-treated dish
	Cell scraper
	Trypan blue
Coy Laboratory Products Inc. (Grass Lake, Michigan, USA)	Hypoxic chamber system
Dr. Daniel O'Connor (University of California; San Diego, California, USA)	PC12 cells
Eppendorf (Hamburg, Germany)	Centrifuge 5415 R
	Innova 42

	Thermomixer
Excel Scientific Inc. (Victorville, California, USA)	AeraSeal
FroggaBio (North York, Ontario, Canada)	1 kbp DNA ladder
	Agarose
	PageRuler prestained protein ladder
Hyclone Laboratories Inc. (South Logan, Utah, USA)	BCS
	DMEM
	ES
	Trypsin
Invitrogen (Carlsbad, California, USA)	DH5α cells
	PureLink HiPure Plasmid DNA Purification Maxipreps Kit
	SOC
Konica (Mississauga, Ontario, Canada)	SRX 101A Konica Film Processor and reagents
Merck Millipore (Billerica, Massachusetts, USA)	PVDF
NanoDrop Technologies (Wilmington, Delaware, USA)	ND-1000
New England Biolabs (Ipswich, Massachusetts, USA)	NEBuffer 3.1
	NEBuffer 4
	Restriction enzymes
Pierce Biotechnology (Waltham, Massachusetts, USA)	PMSF
Promega (Madison, Wisconsin, USA)	dNTP
	GoTaq Flexi DNA polymerase
	Green GoTaq Flexi reaction buffer
	$MgCl_2$
	Mu-MLV RT
	pGL3 basic vector
	Reaction buffer
Roche Diagnostics (Basel, Switzerland)	Random primers
Sigma-Aldrich (St. Louis, Missouri, USA)	1 mL syringe
	22-gauge needle
	Amplification Grade DNase
	ATP sodium salt
	β-mercaptoethanol
	Bromophenol blue
	CDTA
	Charcoal
	$CoCl_2$
	Coenzyme A sodium salt

	DAPI
	D-luciferin potassium salt
	Dex
	DNase reaction buffer
	Forward primer
	H_2O_2
	HEPES-KOH
	IgG antibody
	Linear PEI
	Luminol
	Methanol
	MG
	$MgCl_2$
	$MgCO_3 \cdot 5H_2O$
	$MgSO_4$
	NAC
	Paraformaldehyde
	p-coumaric acid
	Ponceau S
	Reverse primer
	TAE
	TBS-T
	TP
	Tricine
	Triton X-100
	TRIzol reagent
	Stop solution
Simport Scientific (Saint-Mathieu-de-Beloeil, Quebec, Canada)	Round bottom tube
Stovall Life Science (Thermo Fisher Scientific; ON, Canada)	Belly Dancer
Thermo Fisher Scientific (ON, Canada)	0.2 mL PCR tubes
	37°C incubator
	Acrylamide/bis-acrylamide
	Adenosine monophosphate (AMP)
	Anhydrous ethanol
	APS
	Chloroform
	CL-XPosure film
	DEPC
	DTT
	Ethidium bromide

	EVOS XL Core Cell Imaging System
	Film
	Forma Series I Water Jacketed CO_2 Incubator
	GS
	Glycerol
	Glycine
	Isopropanol
	Isotemp 202
	KCl
	LB
	NaCl
	PermaFluor aqueous mounting medium
	Petri dish
	Protease inhibitor
	pTracer-CMV2 mammalian expression vector
	SDS
	Shaking water bath
	TBE
	TEMED
Toronto Research Chemicals (North York, Ontario, Canada)	EGCG
VWR International (Radnor, Pennsylvania, USA)	Analog vortex mixer
Zeiss Microscopy (Jena, Germany)	Zeiss Axioplan 2 Imaging Microscope